Technical Report Documentation Page

1. Report No.	2. Government Accession No.	3. Recipient's Catalog No.
FHWA/TX-92+1239-1		

4. Title and Subtitle	5. Report Date
BRACING REQUIREMENTS FOR ELASTIC STEEL BEAMS	May 1992
	6. Performing Organization Code
7. Author(s)	8. Performing Organization Report No.
Joseph A. Yura and Brett A. Phillips	Research Report 1239-1
9. Performing Organization Name and Address	10. Work Unit No. (TRAIS)
Center for Transportation Research The University of Texas at Austin Austin, Texas 78712-1075	11. Contract or Grant No. Research Study 3-5-90/1-1239
12. Sponsoring Agency Name and Address	13. Type of Report and Period Covered
Texas Department of Transportation Transportation Planning Division P. O. Box 5051 Austin, Texas 78763-5051	Interim
	14. Sponsoring Agency Code

15. Supplementary Notes

Study conducted in cooperation with the U. S. Department of Transportation, Federal Highway Administration

Research Study Title: "Bracing Effects of Bridge Decks"

16. Abstract

Two types of bracing are studied to control the lateral-torsional buckling of steel beams; namely, lateral bracing at the compression flange and torsional bracing. A computer program, BASP, was used to study the effects of brace type, size and number of braces on the buckling strength of beams subject to different loading conditions. It was found that cross section distortion at the brace point significantly affects the efficiency of torsional bracing. Properly attached web stiffness can minimize the distortion.

Based on the analytical solution two bracing equations are developed; one for lateral bracing and one for torsional bracing. The torsional bracing formula accounts for cross section distortion and the presence of web stiffness. Top flange loading requires larger bracing members and the equations consider the effect as well as the variation of moments along the span.

Seventy-six lateral buckling tests were conducted on twin W12X14 beams with a 24-ft. span with a top flange concentrated load at midspan to compare with the analytical solution and the bracing equations. Lateral bracing or torsional bracing of different magnitudes were attached to the beams to determine the required bracing to force the buckle between the end and the midspan. Different beam initial out-of-straightness and web stiffeners were considered. It was found that the bracing equations and buckling program, BASP, compare very well with the test results.

17. Key Words	18. Distribution Statement
bracing, lateral-torsional buckling, steel beams, compression flange, buckling strength, loading, distortion, web stiffness, cross section, moments	No restrictions. This document is available to the public through the National Technical Information Service, Springfield, Virginia 22161.

19. Security Classif. (of this report)	20. Security Classif. (of this page)	21. No. of Pages	22. Price
Unclassified	Unclassified	88	

BRACING REQUIREMENTS FOR ELASTIC STEEL BEAMS

by

Joseph A. Yura and Brett A. Phillips

Research Report No. 1239-1

Research Project 3-5-90/1-1239
"Bracing Effects of Bridge Decks"

Conducted for

Texas Department of Transportation

In Cooperation with the
U.S. Department of Transportation
Federal Highway Administration

by

CENTER FOR TRANSPORTATION RESEARCH
BUREAU OF ENGINEERING RESEARCH
THE UNIVERSITY OF TEXAS AT AUSTIN

May 1992

NO INTENDED FOR CONSTRUCTION,
PERMIT, OR BIDDING PURPOSES

Joseph A. Yura, P.E.
(Texas No. 29859),
Research Supervisor

PREFACE

This report documents the results of an analytical and experimental study on bracing of steel beams. The purpose was to develop an understanding of the varioius factors that influence brace design and to develop bracing equations suitable for design which are verified by experiments. The equations can be used to determine the required size of bracing to prevent lateral instability.

SUMMARY

Two types of bracing are studied to control the lateral-torsional buckling of steel beams; namely, lateral bracing at the compression flange and torsional bracing. A computer program, BASP, was used to study the effects of brace type, size, and number of braces on the buckling strength of beams subject to different loading conditions. It was found that cross section distortion at the brace point significantly affects the efficiency of torsional bracing. Properly attached web stiffeners can minimize the distortion.

Based on the analytical solution two bracing equations are developed; one for lateral bracing and one for torsional bracing. The torsional bracing formula accounts for cross section distortion and the presence of web stiffness. Top flange loading requires larger bracing members and the equations consider the effect as well as the variation of moments along the span.

Seventy-six lateral buckling tests were conducted on twin W12X14 beams with a 24-ft. span with a top flange concentrated load at midspan to compare with the analytical solution and the bracing equations. Lateral bracing or torsional bracing of different magnitudes were attached to the beams to determine the required bracing to force the buckle between the end and the midspan. Different beam initial out-of-straightness and web stiffeners were considered. It was found that the bracing equations and buckling program, BASP, compare very well with the test results.

IMPLEMENTATION

The bracing equations presented in Appendix B can be used to determine the effect of lateral and torsional bracing on the buckling strength. These formulas are fairly accurate, but may be too complicated for general design use. The equations in a simpler form are illustrated in Interim Report No. 3. These formulas were ultimate strength and factors of safety and need to be implemented for use in service load design.

TABLE OF CONTENTS

LIST OF FIGURES

LIST OF TABLES

CHAPTER ONE
INTRODUCTION

1.1 Beam Buckling Strength

The flexural capacity of beams with large unbraced lengths is often limited by a mode of failure known as lateral torsional buckling. Lateral torsional buckling generally involves both an out-of-plane displacement and a twist of the beam cross section as shown in Figure 1.1. Timoshenko (1961) presented the following equation for elastic critical buckling moment of a doubly-symmetric beam failing by lateral torsional buckling,

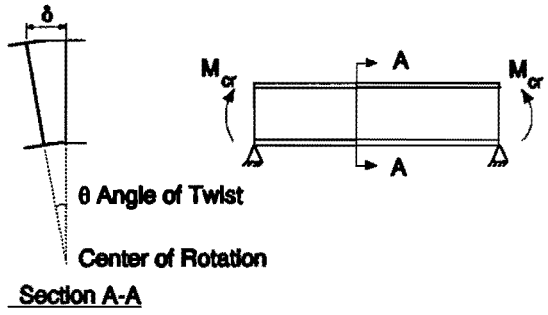

Figure 1.1 Geometry of buckled beam.

$$M_{cr} = \frac{\pi}{L_b}\sqrt{EI_yGJ + \frac{\pi^2E^2I_y^2h^2}{4L_b^2}} \tag{1.1}$$

where L_b = unbraced length, E = modulus of elasticity, I_y = weak axis moment of inertia, G = shear modulus, J = St. Venant's torsional constant, and h = distance between flange centroids. Equation 1.1 is applicable to beams where the twist at the ends of the unbraced length is prevented. The first term under the radical denotes St. Venant torsional resistance of the cross section while the second term is related to the warping torsional resistance. The unbraced length used in this equation should be the distance between points of full lateral support (no twist). The design bending stresses for laterally unsupported beams in the 1990 AASHTO Interim Specification for Highway Bridges for both Allowable Stress Design (ASD) and Load Factor Design (LFD) are based on the Timoshenko formula. The LFD method defines the moment capacity, M_r, as (AASHTO formula 10-102c),

$$M_r = 91 \times 10^6\, C_b\left(\frac{I_{yc}}{L_b}\right)\sqrt{0.772\,\frac{J}{I_{yc}} + 9.87\left(\frac{d}{L_b}\right)^2} \quad \le M_y \tag{1.2}$$

where M_r is given in lb-in. units, M_y is the yield moment, I_{yc} = moment of inertia of the compression flange about the vertical axis in the plane of the web (in^4) = $I_y/2$ for rolled sections, d = depth of the beam and C_b is a modifying factor to account for non-uniform moment within the unbraced length. Equation 1.2 is more general than Eq. 1.1 because it is applicable to unsymmetric girders. For cross sections with equal flanges, Eqs. 1.1 and 1.2

give almost identical results. In ASD (AASHTO Table 10.32.17) the allowable bending stress $F_b = M_r / (1.82\ S_{xc}) \leq 0.55\ F_y$ where S_{xc} = section modulus with respect to the compression flange and 1.82 is the safety factor.

When a beam is subject to a loading other than uniform moment, the lateral buckling capacity may be significantly greater than that given by Equation 1.1. For this reason, a modifying factor, C_b, is used to account for portions of the beam that are subject to a lower moment. The 1990 AASHTO Specification gives $C_b = 1.75 + 1.05\ (M_1 / M_2) + 0.3\ (M_1 / M_2)^2 \leq 2.3$ for the case of a linear variation of moment between the braces, where the maximum moment M_2 occurs at one of the braces. When the maximum moment occurs between the braces, $C_b = 1.0$. The Load and Resistance Factor Design Specification of AISC, 2nd Edition to be published, gives the following formula for C_b which is applicable to all moment diagrams,

$$C_b = \frac{12.5\ M_{max}}{2.5\ M_{max} + 3\ M_2 + 4\ M_{cl} + 3\ M_4} \tag{1.3}$$

where M_{max} = maximum moment on unbraced segment, M_2 = moment at 1/4 segment, M_4 = moment at 3/4 segment, M_{cl} = moment at mid-segment (all moments are taken as positive). This equation is a modification of a formula which first appeared in a text by Kirby and Nethercot (1979).

In most cases, load points are also brace points and in such cases, the point of load attachment (top flange, centroid, etc.) has no effect on the lateral buckling load. When the load point is not a brace point, then load applied to the top flange is more critical than centroid loading (Timoshenko, 1961). The top flange loading causes an extra twist during buckling, whereas bottom flange loading restrains the twist, thus increasing the buckling capacity. Adjustments to account for the effects of load height can be found in Bleich (1978) and the SSRC Guide (Galambos, 1988).

1.2 Beam Bracing

In practice, beams are braced in a variety of ways in order to increase their buckling strength. Braces can be placed continuously along the length of a beam, as in the case of a floor system, or they can be placed at discrete intervals. In some cases, bracing of beams may be provided by another part of the load-carrying system such as a slab, secondary stringer, or purlin.

The effectiveness of a brace is determined by its ability to prevent twist of the cross section. For this reason a brace should be placed at the point where it will best counteract the twisting of the cross section. For the brace to be effective in preventing twist, it must possess not only the required strength but also a definite minimum stiffness. Designing a brace to support some percentage (say 2%) of the compressive bending force in the beam

usually provides sufficient strength in the brace, but it does not guarantee that the brace will provide sufficient stiffness to raise the buckling load of the critical member to the desired level.

Bracing can be categorized into two main types, lateral bracing and torsional bracing. Lateral bracing increases the buckling strength of a member by restraining the lateral movement of the beam. Since most buckling problems involve twisting about a point near or below the tension flange as shown in Figure 1.1, lateral bracing is most efficient when placed at the top compression flange of the member. Figure 1.2 shows the relationship between M_{cr} and brace stiffness for a lateral brace at midspan placed at either the centroid or the top flange. For full or complete bracing, a top flange brace stiffness of 10 k/in. is required to reach the maximum moment associated with buckling between the braces, $M_{cr} / M_o = 3.6$ where M_o is the buckling capacity with no brace. If the lateral brace is at the centroid instead of the top flange, an eighteen fold increase in brace stiffness is required to reach the same moment. Figure 1.2 also shows the effect of cross-section distortion on the stiffness requirements for braces placed at the centroid. While distortion does not significantly effect the stiffness requirements of braces placed at the compression flange, it will significantly increase the required stiffness for braces placed at the centroid. When the brace is placed at a distance below the top flange, the compression flange can move laterally by distorting the web as shown in Figure 1.3.

Historically, requirements for full lateral bracing have been determined using

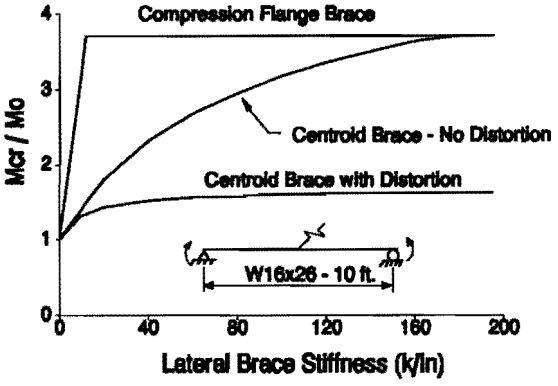

Figure 1.2 Lateral brace location.

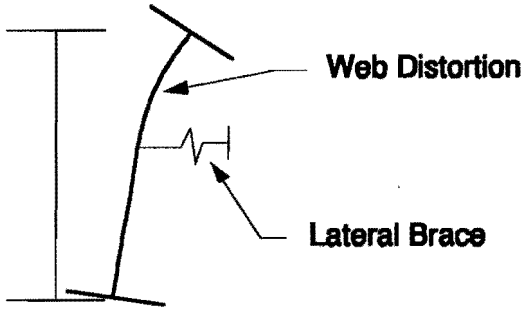

Figure 1.3 Cross-section distortion.

Table 1.1 Lateral Bracing Stiffness Requirements.

Number of Evenly Spaced Braces	Required Stiffness for Ideal Bracing
1	$2 P_e / \ell$
2	$3P_e / \ell$
3	$3.41 P_e / \ell$
4	$3.63 P_e / \ell$
Continuous Bracing	$4.0 P_e / \ell$

a simple model presented by Winter (1960). His model was developed for elastic column buckling and therefore can only be used to determine the required strength and stiffness of an ideal lateral brace attached at the compression flange. The ideal stiffness is defined as the stiffness required to force the member to buckle between the brace points. Table 1.1 shows a summary of Winter's ideal stiffness requirements where P_e is the Euler buckling load of the compression flange between brace points and ℓ is the distance between brace points.

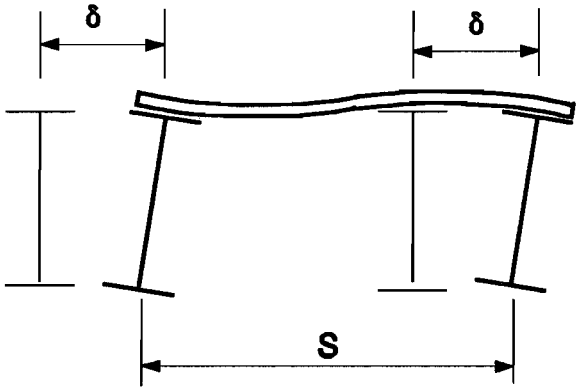

Figure 1.4 Buckled shape of bridge girders.

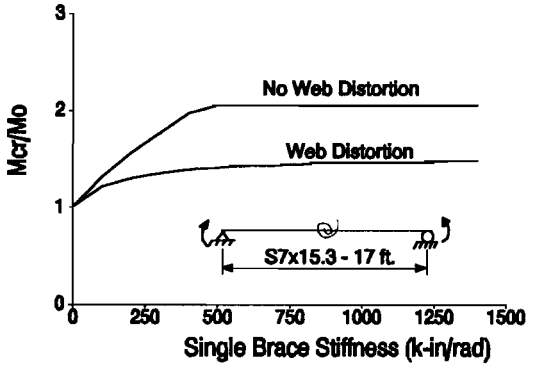

Figure 1.5 Effects of cross-section distortion.

Winter has shown that initial imperfections increase the ideal brace stiffness of a column by a factor of $(1 + \Delta_o / \Delta)$ where Δ_o is the magnitude of the initial imperfection and Δ is the additional deflection permitted before the column fails. Typical values for the deflections are $\Delta = \Delta_o = L / 500$ which gives a brace stiffness requirement of twice the ideal stiffness. The required brace strength is $2P_e (\Delta + \Delta_o) / L$, which reduces to $0.008\ P_e$ for the assumed values of Δ and Δ_o as shown by Yura (1971).

When two or more adjacent beams are loaded simultaneously, they may buckle in such a way that the lateral restraint provided by the connection member is nearly zero (Figure 1.4). The presence of a connection member such as a diaphragm or bridge deck may, however, provide adequate torsional bracing to stabilize the beams. Bridge decking in the form of a concrete slab or wood planks can provide torsional bracing with a stiffness of 6EI/S where E and I are deck properties and S is the spacing of the girders.

Figure 1.5 shows the behavior of a beam braced torsionally at midspan. For a beam with no web distortion, the buckling strength increases with brace stiffness until it reaches the load associated with buckling between the bracing. The value of ideal stiffness required to produce this load is not as sharply defined for torsional bracing as it is with lateral bracing. The lower curve in this figure show the behavior for a torsionally braced beam with the web thickness reduced and no stiffeners. Note that the beam is limited to a much smaller load even at high values of

brace stiffness. Figure 1.6 shows schematically the web distortion of a slender web beam with a torsional brace placed at the compression flange. Since many beams do not possess the required web stiffness to prevent distortion, it is often necessary to either attach a stiffener at locations of torsional bracing or reduce the allowable load of the member to account for web distortion.

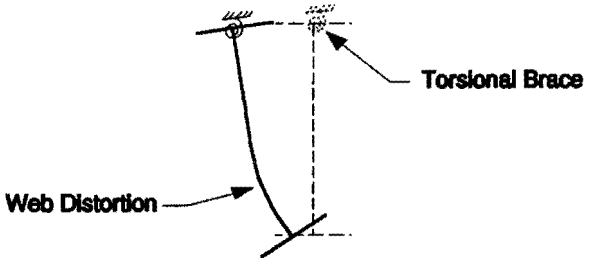

Figure 1.6 Cross-section distortion.

Figure 1.7 shows the relationship between brace stiffness and critical load for one discrete torsional brace at midspan and continuous torsional bracing along the entire span. With continuous bracing, the critical moment of the member will increase without limit, until yielding occurs, as the brace stiffness is increased whereas a beam that is braced at discrete intervals will be limited to the critical moment corresponding to buckling between the brace points. For a single brace at midspan, the maximum moment is reached when the beam reaches the load corresponding to the second mode of buckling. The second mode can be identified by the "S"-shaped curve of the compression flange. The relationship in Figure 1.7 indicates that a design formula for continuous bracing can be used for discrete bracing if the maximum moment is limited to the buckling load between braces.

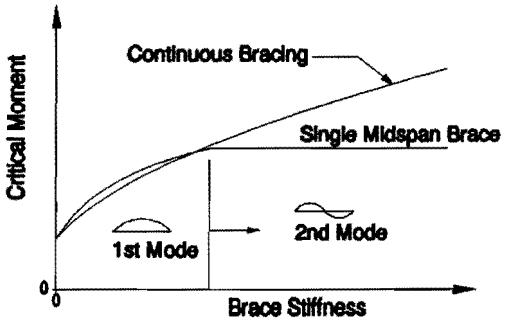

Figure 1.7 Continuous vs. discrete bracing.

1.3 Previous Approaches to Beam Bracing

Many authors have studied beam bracing requirements and some texts have given a brief review of bracing requirements. A partial list of these texts include Salmon and Johnson (1990), Rhodes and Walker (1982), Kirby and Nethercot (1979), and the SSRC Guide (Galambos, 1988). To provide a brief historical review of the developments in beam bracing, only a few selected papers are presented.

Flint (1951a) presented experimental data for the buckling of a beam with a lateral brace located at midspan on the top flange, bottom flange, or at the shear center. He also presented graphical solutions for a torsional brace at midspan. In his theoretical solution,

the critical moment increased to a maximum moment of twice the unbraced beam moment at a brace stiffness of infinity. The inaccuracy of this solution can be seen by observing that the critical moment will increase nearly linearly with brace stiffness until the second mode "S" shape is reached at a finite brace stiffness, as shown in Figure 1.5. Flint also indicated that a brace can be effective by only preventing twist of the cross section while allowing lateral movement to occur.

Flint (1951b) studied the stability of beams loaded through secondary members. He examined the restoring effect of a load that is applied through a relatively stiff secondary member resting on the top flange of the critical beam. Ignoring the effects of cross-section distortion, Flint found that no lateral buckling can occur in the first mode unless the beam has an initial bow greater than half the flange width. This conclusion has not been verified by experiments.

Winter (1960) has shown that an effective column brace must possess not only the required strength, but also a minimum stiffness (Table 1.1). He examined discrete column bracing both experimentally and analytically, and concluded that an initial imperfection has the effect of increasing the required brace stiffness by a factor of $(1 + \Delta_o / \Delta)$.

Taylor and Ojalvo (1966) presented solution for the buckling capacity of a beam with continuous torsional bracing or a discrete torsional brace at midspan. The beam can be loaded with uniform moment, point loading at midspan, or uniform load. The analysis used to determine the critical load was an improvement over previous approaches since it included both St. Venant and warping resistance. The buckling moment is

$$M_{cr} = \frac{m}{L}\sqrt{EI_y GJ} \tag{1.4}$$

The main drawback to this equation is that the constant m must be obtained from a set of graphs corresponding to unique bracing cases. In addition to graphical solutions, Taylor and Ojalvo indicated that the critical moment of a beam with continuous torsional bracing under uniform moment can be determined from the following equation:

$$M_{cr} = \frac{\pi}{L}\sqrt{EI_y GJ + \frac{\pi^2 E^2 I_y^2 h^2}{4L^2} + \frac{\beta_T L^2 EI_y}{\pi^2}} \tag{1.5}$$

where β_T = continuous torsional brace stiffness (k-in/rad per in. length).

Mutton and Trahair (1973) presented equations for the interaction of lateral and torsional bracing for beams subject to equal end moments or central concentrated loads. Their paper gave close-form equations to find the amount of additional torsional bracing needed when a lateral brace is placed at the centroid of the beam cross section. The effects of cross-section distortion were not considered.

Trahair and Nethercot (1982) presented an overview of bracing requirements for beams. Graphical solutions were given for beams loaded with uniform moment, point loads, or uniform load braced by continuous or discrete braces. Their evaluations of lateral brace attachment heights indicated that a lateral brace is most effective when placed at the compression flange. The influence of load height on brace stiffness was examined and presented in graphical form. A method for estimating the torsional restraint with flexible brace connections was given as follows,

$$\frac{1}{\alpha_{kr}} = \frac{1}{\alpha_p} + \frac{1}{\alpha_{web}} + \frac{1}{\alpha_j} \tag{1.6}$$

where $\alpha_{web} = 0.5Et^3$, t = web thickness, α_{kr} = reduced torsional brace stiffness, α_p = brace stiffness, and α_j = stiffness of connection.

Tong and Chen (1988) have studied the buckling behavior of a simply supported beam under uniform moment. Their equations are applicable to doubly-symmetric or mono-symmetric beams braced laterally or torsionally at the midspan. Closed-form solutions for the required stiffness of ideal bracing for these cases were obtained. For torsional bracing, the ideal brace stiffness is given by the following equations:

$$K_{ideal} = \frac{2\pi\left(8 + \alpha_c^2\right)\sqrt{\left(4 + \alpha_c^2\right)}}{\alpha_c^2} \tag{1.7}$$

where

$$\alpha_c^2 = \frac{GJL^2}{\pi^2 EC_w} \tag{1.8}$$

The Tong and Chen solutions do not consider web distortion which often has a significant effect on the bracing requirements as shown in Figure 1.5.

1.4 Limitations of Current Approaches

While the approaches mentioned above provide useful information on the behavior of bracing, they do not provide practical design guidelines for the determination of brace requirements under normal design situations. Few authors have considered the effects of cross-section distortion, initial imperfections, or inelastic behavior. Little work has been done to verify the behavior of partially effective braces or to determine the effects of cross-section distortion, initial imperfections and moment gradients experimentally.

1.5 Objectives of Research Program

A testing program was undertaken to study experimentally the lateral torsional buckling of beams with lateral and torsional bracing. The objective of the program was to develop general design equations and to provide experimental evidence of their validity. The program involved the testing of two 24-foot-long W12x14 steel beams with point loads at midspan. Both lateral braces and torsional braces were applied at the midspan of the beams. Varying levels of initial imperfection and stiffener sizes were studied. Design recommendations are developed based on previous literature, finite element computer studies, and the current experimental work.

CHAPTER TWO
ANALYTICAL PROGRAM

2.1 General

The analytical portion of the research program consisted of two key components: finite element buckling analysis of rolled steel beams and development of design equations for beam bracing. The finite element analysis was conducted to study the effects of brace type, location, number and size on the buckling strength of beams subjected to a variety of loading conditions. Bracing design equations for initially straight beams are presented and compared to results from finite element studies.

2.2 Description of BASP Computer Program

The finite element program, BASP, an acronym for Buckling Analysis of Stiffened Plates, was developed at The University of Texas by Akay (1977) and extended for use on a personal computer by Choo (1987). The BASP program will handle many types of restraints including lateral and torsional braces at any node point along the span. It is limited, however, to elastic modeling of initially straight beams with loads acting only in the plane of the web. Due to these limitation, the effects of initial imperfections were not studied using the program. However, BASP does account for web distortion and was used extensively in the development of basic design equations for straight beams.

One of the beams modeled by BASP was the W12x14 test beam using the boundary conditions shown in Figure 2.1. The in-plane supports were modeled as a pin and roller and out-of-plane displacements at the ends were prevented. In order to more accurately analyze web distortion that may occur near the brace point, the finite element mesh was broken into finer elements near the brace locations at midspan (Figure 2.2). This change also provided the proper node location for attachment of the torsional bracing at 5 in. on either side of the test beam at midspan.

The output of the BASP program is the buckling load and the buckled shape. Figure 2.3 shows the buckled shape of a W12x14 beam with no bracing at P_{cr} = 1.28 kips and Figure 2.4 shows the buckled shape at P_{cr} = 6.50 kips of the same beam with a relatively stiff brace at midspan. The curves in these plots show the lateral displacement of each longitudinal line of

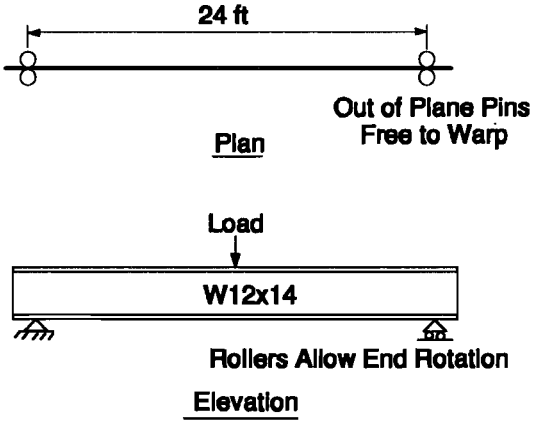

Figure 2.1 Boundary conditions used in BASP program.

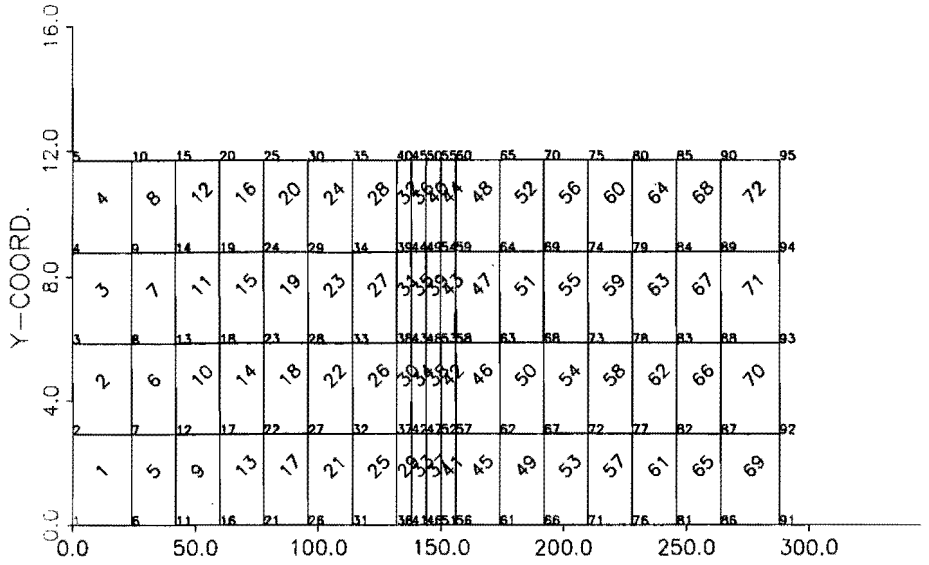

Figure 2.2 Finite element mesh used in BASP.

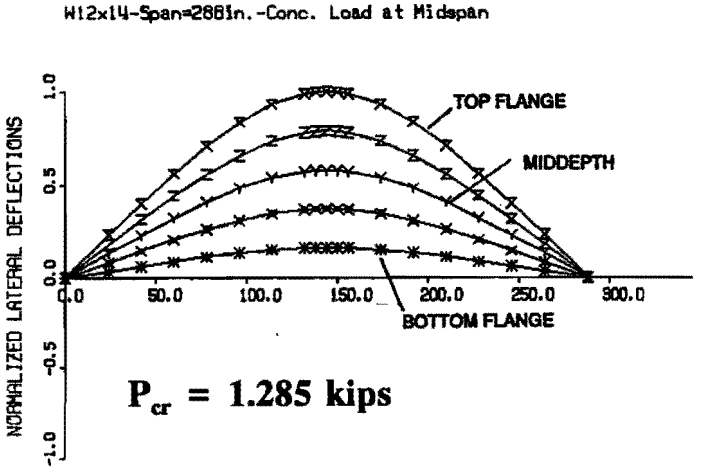

Figure 2.3 First mode buckled shape.

nodes on the beam mesh. The outer curve corresponds to the nodal line on the top flange while the inner-most curve corresponds to the bottom flange of the beam. Both the center of twist and the amount of cross-section distortion can be estimated and compared by careful observation of these plots.

2.3 Design Equations for Intermediate Lateral Bracing

A general design equation has been developed by Yura (1990) for discrete or continuous lateral bracing of beams as follows,

$$M_{cr} = \sqrt{\left(M_o^2 + \frac{P_y^2 h^2 A}{4}\right)\left(1 + A\right)} \quad \leq M_s \text{ or } M_y \tag{2.1}$$

where

$$A = \frac{L^2}{\pi}\sqrt{\frac{.67\bar{\beta}_L}{EI_y}} \tag{2.2}$$

$$P_y = \frac{\pi^2 E I_y}{L^2} \qquad (2.3)$$

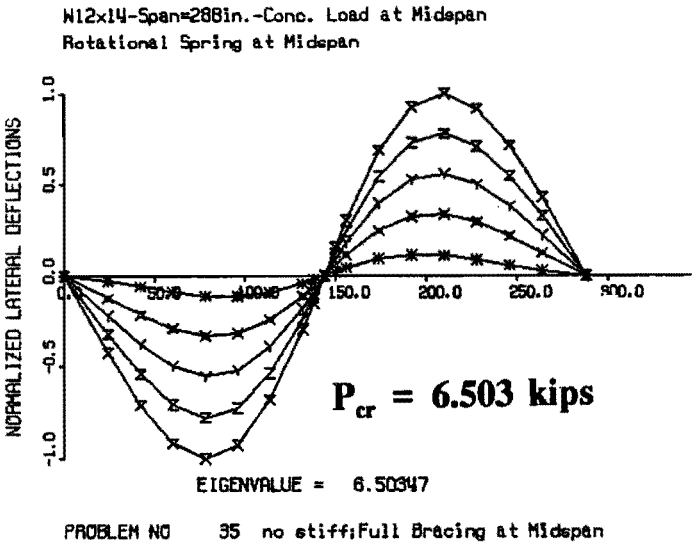

Figure 2.4 Second mode buckled shape.

where M_o is given by Equation 1.1, assuming the beam is unbraced, M_s = buckling strength assuming the unbraced length is the bracing spacing, M_y = yield moment, L = span length, and β_L = equivalent continuous lateral brace stiffness in k/in./in. Since lateral bracing becomes ineffective when placed at a distance below the compression flange, Equation 2.1 applies only to compression flange bracing. Analytical studies using BASP have shown that the effect of cross-section distortion on the effective stiffness of lateral bracing placed at the compression flange is minimal and can be neglected.

When using Equation 2.1, a finite number of discrete lateral braces along a beam should be converted to an effective continuous lateral brace. In general, multiple braces can be represented by summing the stiffness of each brace and dividing by the beam length. This approach is accurate for two or more intermediate braces; it is conservative for one brace at midspan. A single discrete brace at midspan can be more accurately represented as a continuous brace by dividing the brace stiffness by 75 percent of the beam length.

Equation 2.1 has no limit as the stiffness of continuous bracing is increased. When Equation 2.1 is used with discrete braces, the critical moment must be limited to the value corresponding to buckling between the braces, M_s. Also M_{cr} is not valid beyond the yield moment. Figure 2.5 shows the maximum moment level that can be reached for various numbers of equally spaced braces. The solid line represents Equation 2.1; the dashed line, M_s for three different bracing spacings. Figure 2.6 shows a comparison of Equation 2.1 and solutions given by the BASP program for a W16x26 beam under uniform moment with three equally spaced braces. Equation 2.1 shows good agreement with the theoretical solutions.

2.4 Design Equations for Intermediate Torsional Bracing

Taylor and Ojalvo (1973) derived an equation for the critical moment of a beam under uniform moment with continuous torsional bracing along the compression flange as follows,

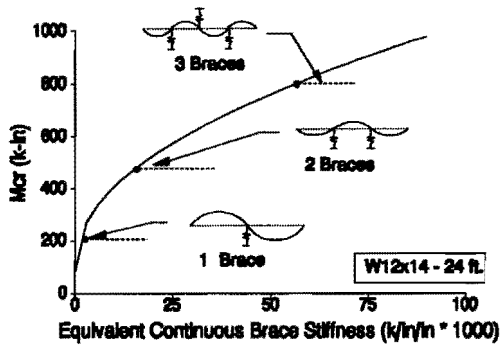

Figure 2.5 Limiting values of critical moment.

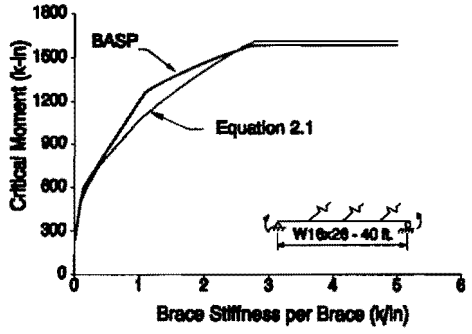

Figure 2.6 Comparison of lateral bracing under uniform moment.

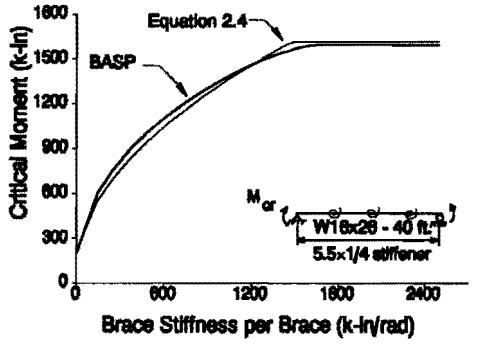

Figure 2.7 Comparison of torsional bracing under uniform moment.

$$M_{cr} = \sqrt{M_o^2 + \overline{\beta}_T EI_y} \qquad (2.4)$$

where M_o is given by Equation 1.1, and $\overline{\beta}_T$ = effective continuous torsional brace (k-in/rad per in. length). Yura (1990) showed that this equation can be used to represent multiple discrete torsional braces by summing the stiffness of each brace and dividing by the beam length provided cross-section distortion is controlled. For a single brace at midspan, the equivalent continuous brace stiffness can be found by dividing the brace stiffness of the single brace by 75 percent of the beam length; this is the same procedure that was suggested for a single lateral brace at midspan. Figure 2.7 shows a comparison of Equation 2.4 and solutions predicted by the BASP program for a beam under uniform moment with three equally spaced braces and stiffeners at the brace points. The excellent agreement between the BASP solutions and Equation 2.4 indicates that discrete braces can be represented by equivalent continuous bracing.

Analytical studies using BASP and earlier research by Milner and Rao (1978) have shown that the effective stiffness provided by a torsional brace is greatly reduced by web distortion that may occur at the brace location. Since many beams do not possess the required web stiffness, a stiffener must often be attached at locations of torsional bracing to increase the brace effectiveness. Equation 2.5 was developed to account for the effect of web distortion on the effective brace stiffness or to determine the required stiffener size to develop the desired effective torsional stiffness of the beam cross section.

$$\frac{1}{\beta_T} = \frac{1}{\beta_b} + \frac{1}{\beta_{sec}} \tag{2.5}$$

and

$$\beta_{sec} = 3.3\,\frac{E}{h}\left(\frac{1.5ht_w^3}{12} + \frac{t_s b_s^3}{12}\right) \tag{2.6}$$

where β_b = attached brace stiffness, β_{sec} = cross section stiffness, t_w = thickness of web, h = depth of web, t_s = thickness of stiffener, b_s = width of stiffener, and $\overline{\beta}$ = β_T × number of braces/span length. For continuous bracing use 1 in. in place of *1.5h* in Equation 2.6.

When a beam is braced with both lateral and torsional bracing, Equations 2.1 and 2.4 can be combined as follows,

$$M_{cr} = \sqrt{\left(M_o^2 + \frac{P_y^2 h^2 A}{4}\right)\left(1 + A\right) + \overline{\beta}_T EI_y} \le M_s \text{ or } M_y \tag{2.7}$$

A typical interaction solution is shown in Figure 2.8 for a 24-ft. W12x14 section braced at midspan. The theoretical bracing required to enable the section to support a moment of 212 k-ft is given by the BASP solution. The exact relationship is non-linear indicating that combined lateral and torsional bracing is more effective than torsional or lateral bracing alone. The BASP solution shown in Figure 2.8 agrees with the solution of combined bracing given by Tong and Chen (1988). Equation 2.7 is a conservative approximation of the interaction between lateral and torsional bracing. The line labeled "Linear Interaction" corresponds to the levels of bracing that would be required if Equation 2.1 and Equation 2.4 were applied independently.

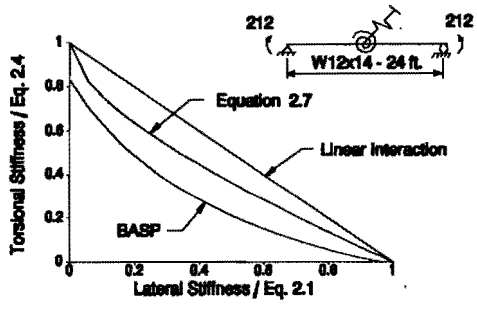

Figure 2.8 Interaction of lateral and torsional bracing.

2.5 Bracing Modifications for Moment Diagram Effects and Load Height

The bracing equations given in Sections 2.3 and 2.4 were derived for the case of uniform moment. Beams are usually subjected to concentrated loads from wheel loads or uniform loads due to dead weight and lane loads which cause nonuniform moment diagrams. The buckling capacity of such beams is increased by the C_b factors discussed in Chapter 1. This increased buckling capacity will also require larger braces. In addition the position of the load also affects the brace requirements as will be shown subsequently.

Numerous braced beams were analyzed using BASP. Variables studied included number of braces along the span, beam length, beam section, load type, continuous beams, load position (top flange, centroid) and bracing type (lateral, torsional). For the case of simply supported beams, the following modification to Eqs. 2.1 and 2.4 give reasonable correlation to the exact BASP solutions for lateral and torsional bracing:

Lateral Bracing

$$M_{cr} = \sqrt{\left(C_{bu}^2 M_o^2 + .25\, C_{bb}^2 P_y^2 h^2 A\right)\left(1 + A\right)} \le M_y \text{ or } M_s \tag{2.8}$$

where

$$A = \frac{L^2}{\pi}\sqrt{\frac{.67\,\bar{\beta}_L}{C_L EI_y}} \quad \text{and} \quad C_L = 1 + \frac{1.2}{\text{No. of braces}}$$

Torsional Bracing

$$M_{cr} = \sqrt{C_{bu}^2 M_o^2 + \left(C_{bb}^2\, \bar{\beta}_T EI_y\right) \Big/ C_t} \le M_y \text{ or } M_s \tag{2.9}$$

where $C_T = 1.2$ and C_{bu} and C_{bb} are the two limiting C_b factors corresponding to an unbraced beam (very weak braces) and an effectively braced beam (buckling between the braces). C_L and C_T are top flange loading modification factors; $C_L = C_T = 1.0$ for centroid loading.

In Figure 2.9, the approximate bracing Equation 2.8 is compared to the exact theory for a simple span beam with three lateral braces on the top flange and a midspan concentrated load at the centroid. As the brace stiffness increases, the lateral buckling load increases rapidly from 1.7 kips to 14.5 kips for small values of bracing. In this region the buckled shape resembles a half sine curve. At a brace stiffness of 2.0 k/in., the buckled

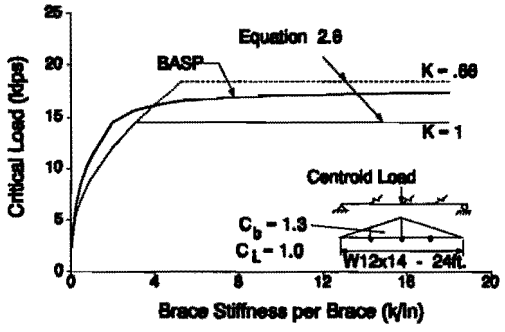

Figure 2.9 Three lateral braces with centroid midspan loading.

shape becomes a full sine curve with no lateral movement at midspan. Additional brace stiffness becomes less effective at this stage but the moment corresponding to buckling between all three braces has been reached as denoted by the k = 1 curve. The limiting moment, M_s, was calculated by Equation 1.1 with the AASHTO C_b factor of 1.3 corresponding to $M_1 / M_s = -0.5$.

In this example, C_{bu} = 1.32 from Eq. 1.2, the C_b factor for an unbraced beam with a concentrated load at midspan. AASHTO conservatively recommends 1.0 for this case. C_{bb} = 1.3 for the critical braced span. In this example the two C_b values are similar. For centroid loading, C_L = 1.0. The conservatism of the design equation at high load level is due to the method used to determine the buckling moment between brace points. Each unbraced length was treated independently and for equal brace spacing, the interior unbraced lengths are critical. The moment levels are much higher between the midspan brace and the 1/4-span brace and the interior sections also has the lowest C_b factor. The exterior spans are not critical so they provide additional lateral restraint to the interior spans. The out-of-plane restraint provided to the most critical portions of the beam can be accounted for through the use of an effective length factor KL_b as outlined in the SSRC Guide (Galambos, 1988). For the example shown, K = 0.88 was determined. The buckling solution given by Equation 2.8 is unconservative at the high load levels associated with K < 1.0, therefore the use of effective length factors for lateral buckling of beams is not recommended. It takes very little bracing for the beam to reach load levels corresponding to K = 1.0; conversely, a large brace is required to force buckling between the braces when the load in each unbraced length is not uniform. In the example problem, a brace stiffness = 1000 k/in. was still not sufficient to reach a K = 0.88. The AASHTO Specification does not use effective length factors for beams.

Figure 2.10 shows good correlation between Equation 2.9 and the exact solution for three torsional braces and centroid loading. The C_b factors are the same as in Figure 2.9 and C_T = 1.0.

The effect of top flange loading on the buckling capacity of laterally braced beams and torsionally braced beams is illustrated in Figures 2.11 and 2.12, respectively. For lateral

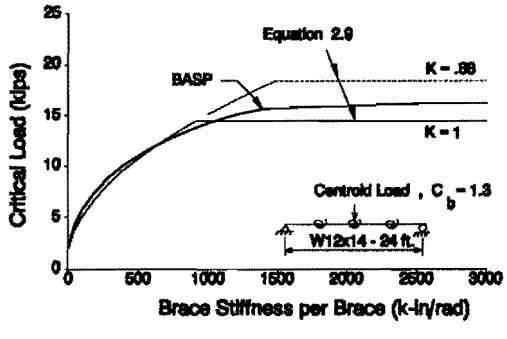

Figure 2.10 Three torsional braces with centroid midspan loading.

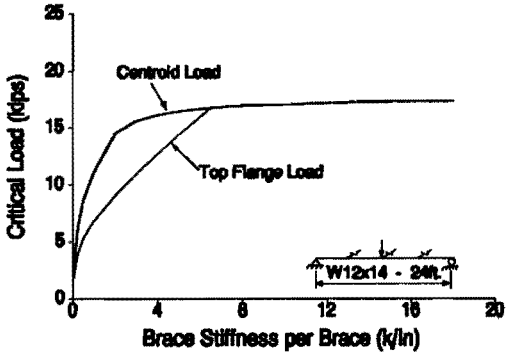

Figure 2.11 Load position effect for lateral braces.

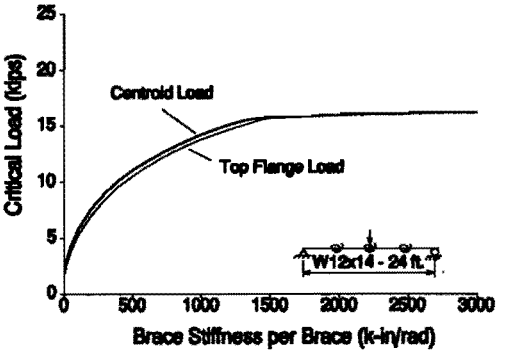

Figure 2.12 Load position effect for torsional braces.

bracing at the top flange, the required brace stiffness for a given load level is significantly greater for top flange loading compared to centroid loading. At a load level of 10 kips, the brace stiffness for top flange loading is double that required for centroid loading. It was also found that the difference in required stiffness of lateral braces due to load position decreased as the number of braces increased. The C_L factor in Equation 2.8 varies with the number of braces. For one brace C_L = 2.2; for three braces, C_L = 1.4. The top flange loading effect is not as significant for torsional bracing as illustrated in Figure 2.12. A constant C_T = 1.2 was satisfactory for all torsionally braced beams with top flange loading. Figures 2.13 and 2.14 show good correlation between the bracing equations and the exact solution. M_o in Eqs. 2.8 and 2.9 is the beam capacity assuming no bracing which should consider the effect of top flange loading. The SSRC Guide recommendations give load position effects. The top flange loading effect can also be approximated by neglecting the warping term in Eq. 1.1. This approach was used in Figures 2.13 through 2.16.

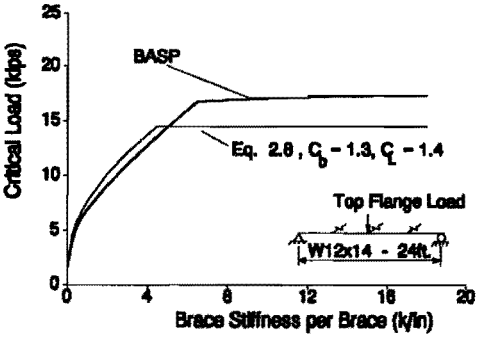

Figure 2.13 Lateral bracing under top flange loading.

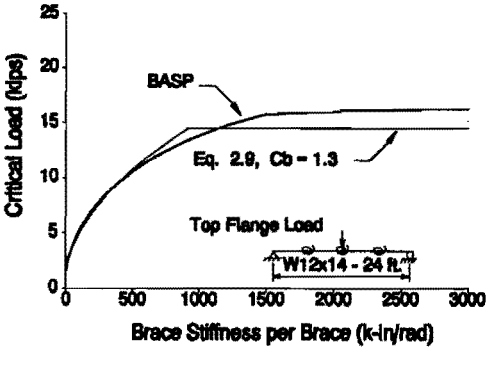

Figure 2.14 Torsional bracing under top flange loading

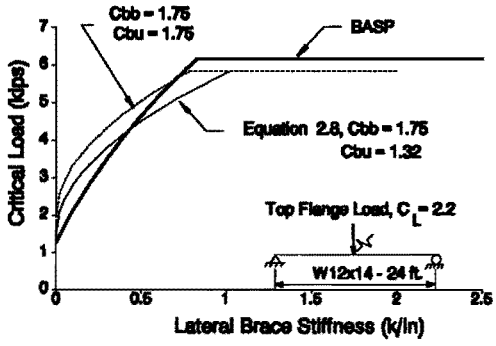

Figure 2.15 Midspan lateral brace and top flange loading.

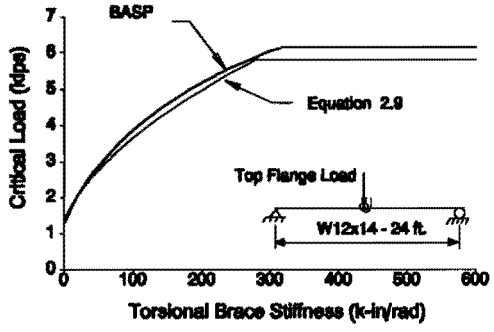

Figure 2.16 Midspan torsional brace and top flange loading.

For the case of one lateral brace and top flange loading at midspan in Figure 2.15, the comparison between Equation 2.8 and the exact theory is not as good as the previous cases. The buckling equation is conservative as the load approaches the limit of buckling between the braces. The equation indicates that a brace stiffness of about 1 k/in. is required to force the beam to buckle between braces (ideal brace). The theory indicates 0.8 k/in. would be sufficient. Since this amount of bracing is still extremely small, the difference has little practical significance. At low loads the bracing equation is unconservative. The difficulty of developing a simple expression that accurately predicts the buckling load for any brace stiffness is illustrated in this figure. At low load C_b = 1.32; at M_s, C_b = 1.75. The effect of top flange loading on bracing increases as the load increases. Once the beam buckles between the braces, top flange loading then has no effect. In addition, it is more approximate to convert a single brace into an equivalent continuous brace than the multiple brace examples given earlier. In Fig. 2.15, C_L = 2.2 and the equivalent continuous brace stiffness was obtained by dividing the single brace stiffness (k/in) by 0.75 times the span as discussed earlier. If C_{bu} = C_{bb} = 1.75 is used as shown by dashed curves, the ideal stiffness is predicted accurately but the results are unconservative for less than ideal bracing.

The case of a single torsional brace at midspan shown in Figure 2.16 shows good agreement with Equation 2.9. For the combination of one torsional brace plus top flange loading, it was found that $\overline{\beta}_T = \beta_T / L$, not 0.75L. For centroid loading, 0.75L can be used.

Equations 2.8 and 2.9 will form the basis for the development of practical bracing design formulas in the final report. Factors of safety must be incorporated and adjustments made for initial beam out-of-straightness. At this stage, the bracing equations illustrate the significance of the moment diagram and load position and that a single formulation can handle both discrete and continuous bracing. In the following chapters an experimental program is described which was used to check the validity of the theoretical results.

CHAPTER THREE
EXPERIMENTAL PROGRAM

3.1 General

The experimental program consisted of 76 tests designed to evaluate the effects of lateral and torsional brace stiffness, brace location, stiffener size, and initial imperfections on the lateral torsional buckling of steel beams. Two identical simply supported beams were loaded at midspan, as shown in Figure 3.1, until buckling occurred. The buckling load determined from this beam arrangement was an average buckling load for the two beams. Figure 3.2 shows the overall test setup.

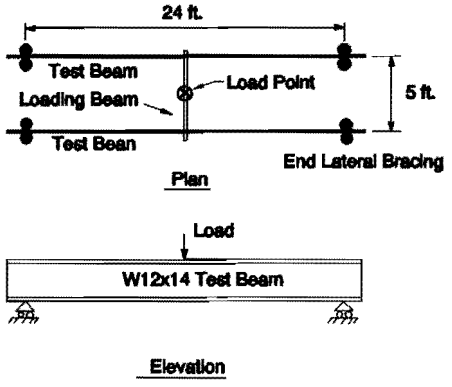

Figure 3.1 Schematic of test setup.

Both test beams were taken from the same mill batch of high-strength steel so that all buckling would occur in the elastic range. The measured yield strengths of the flange and web were 65 ksi and 69 ksi, respectively. Figure 3.3 shows the average measured cross-section properties of the two beams.

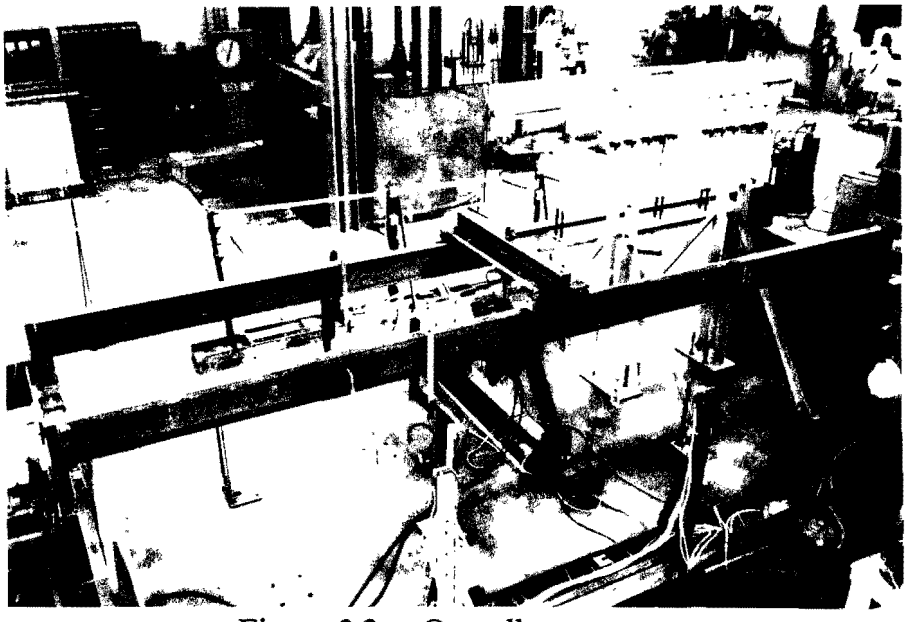

Figure 3.2 Overall test setup.

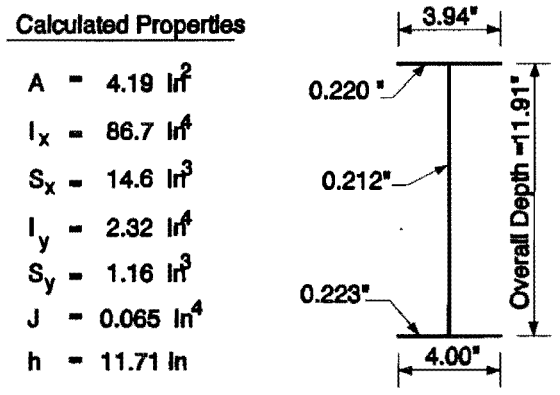

Figure 3.3 Average cross-section properties of test beam.

3.2 Loading and Support System

In the laboratory, gravity type loads are usually applied by using a testing machine or a firmly supported jack. This technique works well for structures that displace following the line of action for the loading device. For structures that are allowed to sway or buckle, the line of action of the load will no longer be vertical and care must be taken so that the loading device will not restrain the lateral movement of the test specimen. When a structure sways, the vertical nature of true gravity load must be approximated.

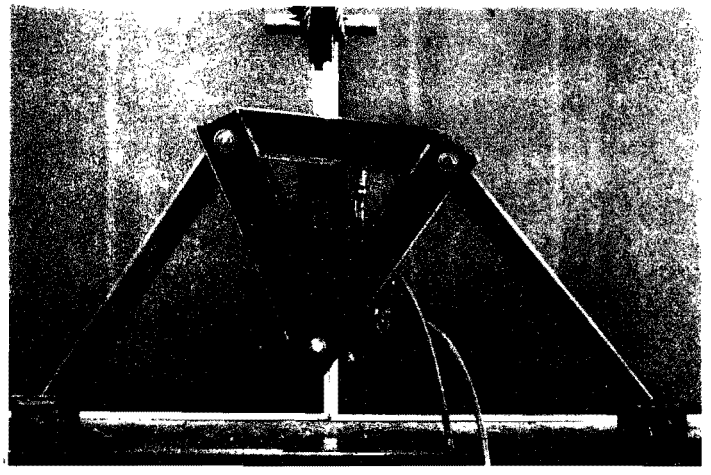

Figure 3.4 Gravity load simulator.

In the twin beam setup, the midspan load was maintained vertical by the use of a gravity load simulator mechanism shown in Figure 3.4. This mechanism has been used extensively in the testing of structures permitted to sway. The design concept of the simulator is given by Yarimci, Yura, and Lu (1966) and will not be discussed here. The simulator used in the test setup could safely maintain a load of 44 kips with a sway of six inches.

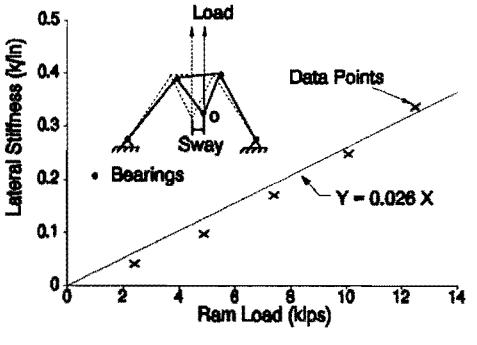

Figure 3.5 Lateral stiffness of gravity load simulator due to friction.

While the mechanism does a very good job of simulating gravity load, it is not perfect. The friction in the bearings produce a slight "lag" in the realignment of the ram to the vertical position during sway. This effect was determined experimentally by applying a lateral load to the base of the loading ram at point o (Figure 3.5) and measuring the corresponding lateral movement. The value of this restraint was determined at six different load levels. During the first test it was found that the friction in the gravity load simulator produced a sawtooth-type load-deflection curve. In order to minimize this effect, a small vibration motor

was attached to the frame of the load simulator that served to increase the rate at which the ram was realigned to the vertical position. It was not possible to perform a calibration of the gravity load simulator with the vibration motors running due to the sensitivity of the instrumentation.

The effects of non-ideal behavior, such as restraints at the ends of the beam, were studied using BASP and found to have a significant effect on the buckling load. In light of this, the friction at the end supports was minimized by using ball-bearing fixtures that would allow axial lengthening of the beam as well as out-of-plane rotations at the supports (Figure 3.6). Load was transferred to the test beams through knife-edges placed between the loading beam and the test beam (Figure 3.7). The knife edges were placed at the center of the flange, parallel to the beam span, so that they would not affect the twist of the test beam. The knife edges were connected to the loading tube with roller bearings to prevent the addition of significant warping restraint to the test beams from the applied loading.

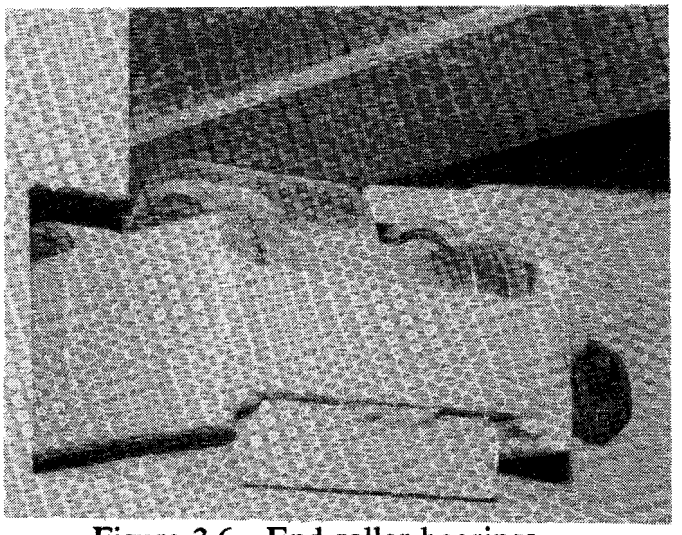

Figure 3.6 End roller bearings.

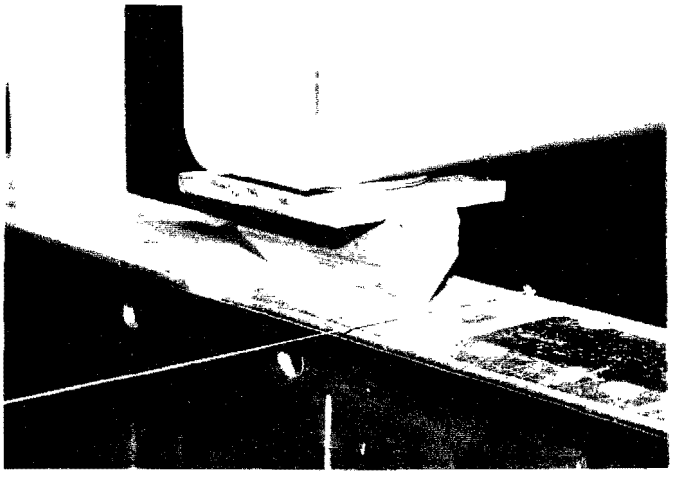

Figure 3.7 Knife edges.

3.3 Instrumentation

Lateral deflections, vertical deflections, flange rotation, and load were recorded during testing. Lateral deflection measurements were recorded on both the top and bottom flange at the midspan and quarter points of each beam. Vertical deflections were recorded at the midspan of each beam. Load was recorded using a load cell located between the ram and loading tube. The load cell had a capacity of 50 kips and a precision of 50 pounds. A pressure transducer measured the hydraulic pressure in the ram to provide another measure of load. There was no significant difference between load levels reported by the load cell and those calculated from the pressure readings.

All deflections were recorded using electronic linear displacement gauges. To obtain an accurate measure of lateral deflection directly from the gauge readings, the lateral displacement gauges were placed four feet from the test beam in order to minimize the error due to the vertical component of the gauge displacement. This resulted in an accuracy of 0.05 inches at the maximum vertical deflection experienced during testing. Displacement gauges were connected to the top and bottom flanges of each beam at the quarter-span, midspan, and three-quarter span, giving a total of 12 lateral displacement readings at each load level. By placing gauges at both the top and bottom flanges, the average twist of the cross section could be calculated at each gauge location.

Additional measurements of twist were recorded using two electronic tilt meters. These meters were located at the midspan of one beam, one on the top flange and one on the bottom flange. Since these meters recorded the tilt of each flange near the brace point, an estimate of the cross section distortion was obtained for each test. All displacement and load readings were recorded using a computer controlled data acquisition unit in which all data during a load cycle could be recorded within a few seconds.

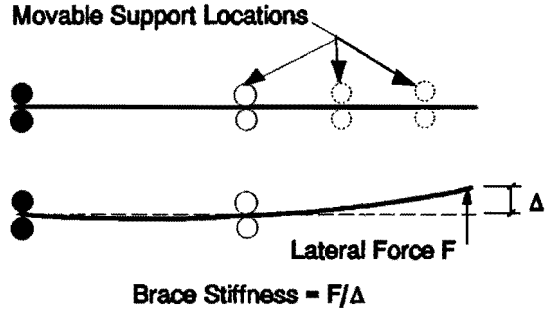

Figure 3.8 Schematic of lateral brace.

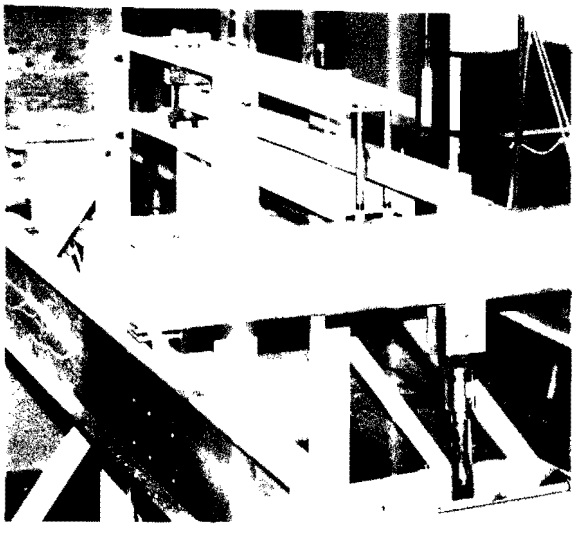

Figure 3.9 Lateral bracing system.

3.4 Lateral Bracing System

The lateral bracing was provided by a simply supported aluminum bar with an adjustable overhang (Figure 3.8). Six different levels of stiffness were provided in this fashion by simply changing the size of the aluminum bar or the location of the adjustable support. Figure 3.9 shows the lateral bracing system used in the test setup. The stiffness of the lateral bracing system was significantly affected by the stiffness of the accompanying supports, so it was necessary to obtain the effective stiffness of the bar-support system experimentally. The measured value of stiffness for each lateral brace configuration is shown in Table 3.1.

3.5 Torsional Bracing

Torsional bracing was provided by connecting a flexible aluminum bar to each test beam spanning between the two beams. During testing, the lateral deflection of the test beams

forced the aluminum brace into double curvature as shown in Figure 1.4. Since the brace is bent in double curvature, the brace stiffness is equal to $6EI/L$ of the aluminum brace. The torsional braces were attached six inches on each side of the midspan of the test beam to avoid interfering with the loading beam and to provide symmetry. Figure 3.10 shows a typical torsional brace used in the test.

The torsional brace attachment fixtures were designed to prevent the addition of any significant warping restraint to the test beams, especially as they buckled into the second mode shape. This required the brace and fixtures to provide a high stiffness in the vertical plane while simultaneously providing little or no restraint in the horizontal plane. Figure 3.11 shows a photo of the overall fixture assembly and Figure 3.12 shows the individual fixture components. Item 1 in Figure 3.12 is the base of the fixture. This was rigidly attached to the test beam and contained a two-inch fixed dowel at the center. Item 2 was placed over the dowel on Item 1 and was secured with the use of a bearing nut. Roller thrust bearings were placed between both contact surfaces formed by the attachment of 1 and 2. The aluminum bracing, Item 3, was rigidly connected to the fixture by the use of a cover plate (Item 4). All rotation in the horizontal plane occurred between Items 1 and 2. Each of the eight brace end fixtures was calibrated and found to vary from 1600 to 3700 k-in/rad with an average stiffness of 2900 kip-in/rad. By repeated trials, it was found that a large variation in stiffness would occur depending on the tension that was applied to the bearings in the fixture assembly. Since measuring the brace fixture stiffness between each test would have been prohibitive, the average stiffness of 2900 kip-in/rad was used for all fixtures. The total stiffness of the brace-fixture combination was determined from the use of the fixture

Table 3.1 Measured Lateral Brace Stiffness

Lateral Brace Configuration	Stiffness kips/in
1	0.22
2	0.36
3	0.65
4	0.75
5	1.20
6	1.90

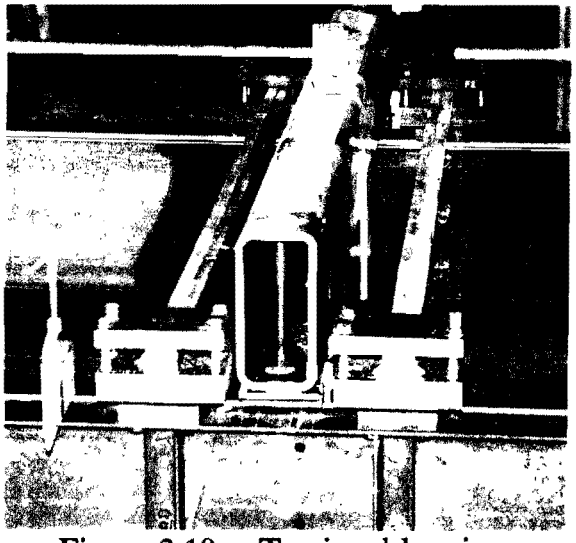

Figure 3.10 Torsional bracing.

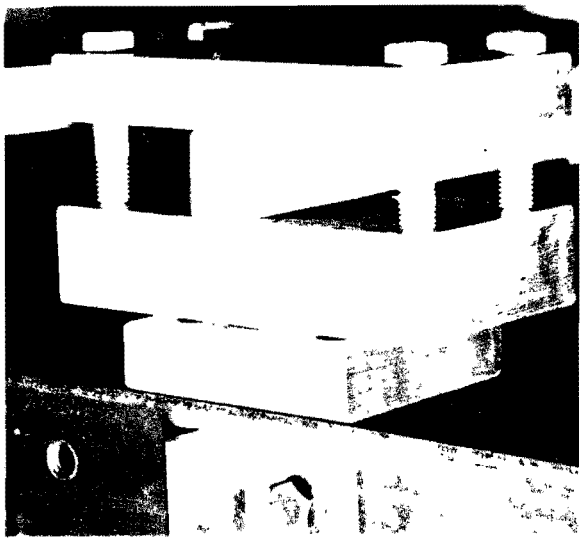

Figure 3.11 Torsional brace fixtures.

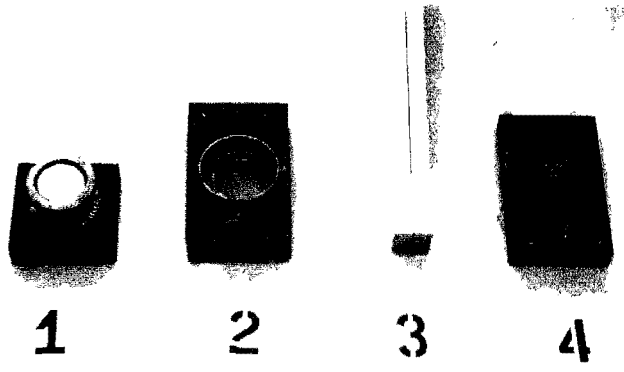

Figure 3.12 Brace fixture components.

No.	DESCRIPTION	Inertia in^4	Bar Stiffness in-k/rad	Fixture Stiffness in-k/rad	Total Brace Stiffness in-k/rad
1	3/4" x 3/4" Bar	0.026	27.1	2900	53.7
2	1-1/4" x 3/4" Bar	0.044	45.0	2900	88.6
3		0.088	90.3	2900	175
4	3/4" x 1-1/4" Bars	0.244	250	2900	462
5		0.366	375	2900	666
6		0.488	501	2900	855
7		0.610	626	2900	1030
8		0.732	752	2900	1190

Figure 3.13 Adjusted torsional brace stiffness.

flexibility and the brace flexibility as shown in Equation 3.1. Based on the original stiffness measurements, the use of the average fixture stiffness could result in an error of 3 percent for the lowest level of brace stiffness and an error of 17 percent for the highest level of brace stiffness. Thus, the total stiffness of each brace-fixture combination was calculated using an average value of 2900 k-in/rad for the fixture stiffness. The total brace stiffness given in Figure 3.13 was calculated for the bar configuration shown and then doubled to account for the bracing on each side of the loading tube.

$$\frac{1}{\beta_T} = \frac{1}{\beta_{brace}} + \frac{1}{\beta_{fixture}} \qquad (3.1)$$

where β_T = torsional brace stiffness, β_{brace} = stiffness of brace alone, $\beta_{fixture}$ = stiffness of brace fixture alone.

Many tests were performed with stiffeners placed directly beneath the brace attachment points. They were made of 11-inch-long steel angles bolted to the web of the test beam. This permitted both the stiffener size and vertical location of the stiffener to be easily adjusted.

CHAPTER FOUR
TEST RESULTS

4.1 Test Procedure

The experimental program of 76 tests was divided into six groups. Group A is composed of tests that contained no bracing. Group B is composed of tests with lateral bracing located at midspan attached to the compression flange. Group C contains tests with compression flange torsional bracing located at midspan as discussed in Chapter 3. Group D contains results from tests with forced imperfections. Group E contains tension flange torsional bracing and Group F contains a combination of tension flange and compression flange torsional bracing.

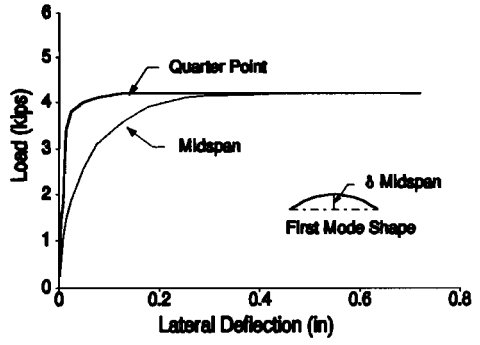

Figure 4.1 Typical load - deflection curves for first mode test.

The test procedure for each test started with an initial reading of all gauges. A load of approximately one kip was applied to the beams before the vibration equipment was activated so that the knife edges would seat in the grooves on the top flanges of the test beams. Readings were then taken at a constant increment of about 500 pounds until the load on the beams was near the buckling load; the frequency of the readings were then increased. The number of readings taken at or near the buckling load varied greatly between tests and can be seen in the load-deflection curves located in Appendix A. During each test, the inclinations of the compression and tension flanges were measured near the brace point. These readings were not taken as frequently since the data were recorded manually.

4.2 Determination of Critical Load

The lateral torsional buckling load of a beam can be defined as the load at which the member has zero lateral stiffness. Figure 4.1 shows a typical load-deflection curve from a test where the beam buckled in the first mode and Figure 4.2 shows a typical load-deflection curve from a test where the beam buckled in the second mode. The critical load for these

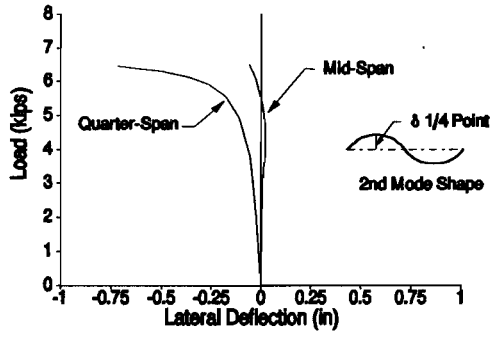

Figure 4.2 Typical load - deflection curve for second mode test.

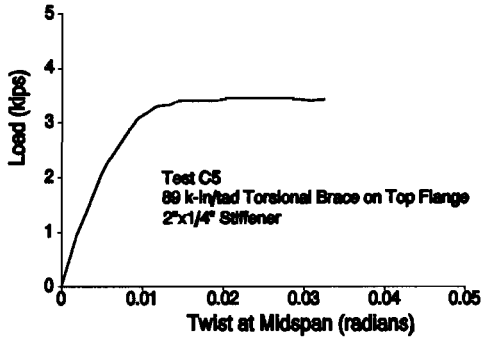

Figure 4.3 Typical load - twist curve for first mode test.

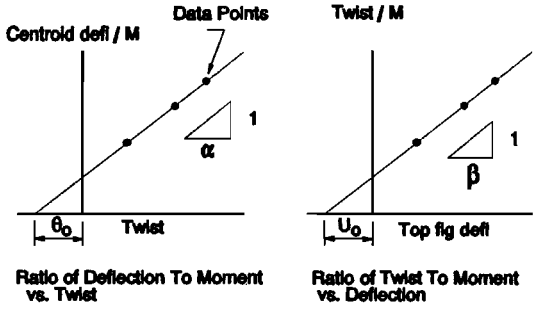

Figure 4.4 Meck plotting technique.

tests is characterized by a horizontal or near horizontal line on the load-deflection curve. Since the beams buckled in an "S" shape for all second mode tests, the midspan deflection was small or zero for all values of load. The critical load can also be found from the horizontal line on the load-twist curve as shown in Figure 4.3. Due to the high yield strength of the W12x14 beam material (approximately 65 ksi), the large deflections needed to reach the critical load of the test beam were achieved without yielding.

Alternative methods have been developed to determine the experimental buckling strength of beams that cannot be loaded to the actual buckling load. For example, in Figure 4.2, the test was stopped before a flat plateau was reached. Some of the better known procedures for this type of analysis include techniques presented by Southwell (1932) and Meck (1977). The Meck Plotting Technique is applied specifically to beams by using two equations which involve linear relations between functions of the measured lateral deflection and measured twist. The applied moment is plotted against the experimental twist and lateral deflection as shown in Figure 4.4. For beams loaded on the top flange, the inverse slopes of the lines of best fit through the data points for these plots are defined as α and β where the critical moment is given by

$$P_{cr}^2 + \beta \frac{d}{2} P_{cr} - \alpha\beta = 0 \qquad (4.1)$$

The initial lateral twist, θ_o, and deflection, U_o, are found from negative horizontal intercepts of the plots shown in Figure 4.4

The Meck Plotting Technique for the determination of M_{cr} gives results practically identical to the load level corresponding to a horizontal line on the load-deflection curve for all tests without bracing. However, the Meck Plotting Technique did not work for tests in which there was local distortion such as when the load was applied through a flexible

member or for torsionally braced beams without stiffneners. For these cases, usually a peak load was reached which was taken as the buckling load. The critical load for all tests was obtained from the horizontal portion of the load-deflection curve. The Meck Technique also established the initial imperfection of each beam which was checked independently. In general the critical load given in the subsequent tables were obtained by the Meck Plotting Technique unless a peak load was reached.

4.3 Determination of Initial Imperfections

Two types of initial imperfections were studied during the testing program. The first type of imperfection will be referred to as natural imperfections. All tests, except group D, were performed with permanent out-of-straightness. Tests A1, A5 and A6 in Table 4.1 give values of initial top flange displacement and initial twist at midspan for the three levels of imperfections used during testing. The second type of imperfection will be referred to as forced imperfections. These were applied at the quarter point of the beam by displacing the compression flange of the test beam laterally with a rigid stop and then securing the stop in the displaced position. Tests D1 through D4 give measured values of initial deflection and initial twist at the midspan of the test beams for tests with forced imperfections. All forced imperfections listed are in addition to the 0.04-inch natural out-of-plane sweep of test beam A1.

Table 4.1 Measured Initial Top Flange Deflection and Twist

Test Number	Initial Deflection (in.)	Initial Twist (degrees)
A1	0.04	0.26
A2	0.45	0.95
A5	0.16	0.01
A6	0.22	0.13
D1	0.26	0.17
D2	0.15	0.07
D3	0.12	0.05
D4	0.31	0.12

4.4 Test Series A - No Bracing

The first test series consisted of six tests with different loading beams. Test A1 was loaded with knife edges between the loading member and the test beam, and can be considered a basically straight beam with no bracing other than the friction in the gravity load simulator. Test A2 had the same configuration as A1 with a forced imperfection imposed at the quarter point of one beam.

The term "tipping effects" describes tests in which the loading beam was placed directly on the compression flanges of the test beams without the use of the knife edges. Tests A3 and A4 were performed to study the effects of the externally applied flange rotation which occurs when the loading member is placed directly on the compression

Table 4.2 Test Series A, No Bracing

Test No.	Description	Stiffener Size	Initial Imperfection (inches)	Critical Load (kips)	"S" Shape
+A1	Knife edge loading	None	0.04	1.55	No
A2	Knife edge loading	None	0.45	1.59	No
+A3	Tipping effects	None	0.04	3.91	No
A4	Tipping effects	2" x1/4"	0.04	6.2	Yes
+A5	Knife edge loading	None	0.16	1.56	No
+A6	Knife edge loading	None	0.22	1.67	No

+ Test was repeated

flanges of the test beams. Tests A5 and A6 were loaded with the original knife edge loading and are similar to test A1 except for the level of initial imperfection present. Table 4.2 gives a summary of these tests and the corresponding experimental buckling loads. The reported buckling load is an average of the two test beams. Tests marked with a plus sign were reproduced to check for repeatability. With the exception of tests C4 and C29 presented in Section 4.6, all duplicate tests gave a critical load within 6 percent of the original test. Test C4 had a variation of 20 percent and test C29 had a variation of 8 percent.

4.5 Test Series B - Lateral Bracing

The second series of tests, as well as subsequent tests, were loaded using the steel loading beam and knife edges as shown in Figure 3.7. All boundary conditions were the same as Test Series A except that a lateral brace was added as shown in Figures 3.8 and 3.9. Six levels of lateral bracing and two levels of initial imperfections were tested. Table 4.3 shows the amount of lateral bracing attached to the test beams through the bracing device and the corresponding critical load per beam.

4.6 Test Series C - Compression Flange Torsional Bracing

Test Series C consisted of 40 tests with varying levels of torsional brace stiffness, initial imperfection and stiffener size. A total of eight levels of brace stiffness, three levels of initial imperfection, and two stiffener sizes were tested. Tests were also performed with no stiffener and with the 4"x1/4" stiffener touching the compression flange at both brace locations. Tests performed with the stiffeners touching the compression flange are marked with an asterisk in the table.

Table 4.3 Test Series B, Lateral Bracing

Test Number	Brace Stiffness (kips/in)	Stiffener Size	Initial Imperfection (inches)	Critical Load (kips)	"S" Shape
B1	0.22	4" x 1/4"	.19	3.17	No
B2	0.75	4" x 1/4"	.24	6.02	No
B3	0.36	4" x 1/4"	.36	4.11	No
B4	1.20	4" x 1/4"	.35	6.54	No
B5	0.36	4" x 1/4"	.15	3.97	No
B6	1.20	4" x 1/4"	.16	6.73	Yes
B7	1.90	4" x 1/4"	.15	6.62	Yes
B8	0.65	4" x 1/4"	.15	5.39	No
B9	0.65	None	.15	5.47	No
B10	1.90	None	.16	6.75	Yes

As described in Chapter 3, the torsional bracing was attached to the compression flange of each test beam with half the indicated amount being placed six inches on either side of the mid-span. Table 4.4 contains a summary of these tests and the corresponding experimental buckling loads.

4.7 Test Series D, E and F

Test Series D consists of six tests where the initial imperfection was applied to the beam by a forced displacement at the quarter span of one beam. The forced displacement was transferred to the other beam through the loading tube. As mentioned in the previous sections, the initial imperfection reported for all other test series was the natural state of the test beams due to a previous yielding or manufacturing process. Test Series E consisted of ten tests similar to those in Series C except the torsional bracing was attached to the tension flange instead of the compression flange. Test Series F consisted of 6 tests similar to those in series C except half the indicated value of torsional bracing was attached to the compression flange and half was attached to the tension flange. Table 4.5 contains a summary of these tests and the corresponding experimental buckling loads.

Table 4.4 Test Series C, Compression Flange Torsional Bracing.

Test Number	Brace Stiffness (k-in/rad)	Stiffener Size	Initial Imperfection (inches)	Critical Load (kips)	"S" Shape
C1	55	NONE	0.22	2.87	NO
C2	55	2"X1/4"	0.22	3.13	NO
C3	55	4"X1/4"	0.22	3.17	NO
+ C4	89	NON	0.22	3.44	NO
+ C5	89	2"X1/4"	0.22	3.49	NO
+ C6	89	4"X1/4"	0.22	3.55	NO
C7	175	NONE	0.22	4.37	NO
+ C8	175	2"X1/4"	0.22	4.40	NO
C9	175	4"X1/4"	0.22	4.54	NO
C10	462	NONE	0.22	4.83	NO
C11	462	2"X1/4"	0.22	5.17	NO
C12	462	4"X1/4"	0.22	5.31	NO
C13	666	NONE	0.22	5.05	NO
C14	666	2"X1/4"	0.22	5.45	NO
C15	666	4"X1/4"	0.22	5.73	NO
C16	855	4"X1/4"	0.22	5.80	NO
+ C17	1030	4"X1/4"	0.22	5.72	NO
C18	1190	4"X1/4"	0.22	5.98	NO
C19	1190	* 4"X1/4"	0.22	6.83	YES
C20	1030	* 4"X1/4"	0.22	6.82	YES
C21	666	* 4"X1/4"	0.22	6.81	YES
C22	462	* 4"X1/4"	0.22	6.87	YES
C23	175	* 4"X1/4"	0.22	5.45	NO
C24	89	* 4"X1/4"	0.22	3.38	NO
C25	55	NONE	0.16	2.89	NO
C26	55	2"X1/4"	0.16	3.03	NO
C27	55	4"X1/4"	0.16	2.96	NO
C28	89	NONE	0.04	4.48	NO
+ C29	89	2"X1/4"	0.04	4.33	NO
C30	89	4"X1/4"	0.04	5.14	NO
C31	175	NONE	0.04	5.55	NO
+ C32	175	2"X1/4"	0.04	6.38	YES
+ C33	175	4"X1/4"	0.04	6.54	YES
C34	175	* 4"X1/4"	0.16	4.83	NO
C35	462	* 4"X1/4"	0.16	6.58	YES
+ C36	462	4"X1/4"	0.16	5.71	NO
+ C37	666	4"X1/4"	0.16	5.92	NO
C38	855	4"X1/4"	0.16	6.33	NO
C39	1030	4"X1/4"	0.16	6.50	YES
C40	1190	4"X1/4"	0.16	6.41	YES

* Stiffener touching tension flange + Test was repeated

Table 4.5 Test Series D, E, and F

Test Number	Brace Stiffness (k-in/rad)	Stiffener Size	Initial Imperfection (inches)	Critical Load (kips)	"S" Shape
Forced Imperfections					
D1	89	NONE	0.26	3.59	NO
D2	175	NONE	0.15	4.13	NO
D3	175	4"X1/4"	0.12	5.8	NO
D4	175	4"X1/4"	0.31	5.27	NO
Tension Flange Torsional Bracing					
E1	175	NONE	0.22	4.25	NO
E2	175	* 4"X1/4"	0.22	6.53	YES
E3	666	* 4"X1/4"	0.22	6.69	YES
E4	666	4"X1/4"	0.22	6.79	YES
E5	666	NONE	0.22	4.72	NO
E6	175	NONE	0.16	3.83	NO
+ E7	175	* 4" X 1/4"	0.16	5.15	NO
E8	666	* 4"X1/4"	0.16	6.99	YES
E9	666	4"X1/4"	0.16	7.03	YES
E10	666	NONE	0.16	4.78	NO
Combined Compression and Tension Flange Torsional Bracing					
F1	462	NONE	0.22	6.53	YES
F2	175	NONE	0.22	4.89	NO
F3	175	4"X1/4"	0.22	4.99	NO
F4	462	NONE	0.16	6.94	YES
F5	175	NONE	0.16	4.87	NO
F6	175	4"X1/4"	0.16	4.86	NO

* Stiffener Touching Tension Flange
+ Test was repeated

CHAPTER FIVE
COMPARISON AND DISCUSSION OF TEST RESULTS

The experimental buckling loads of unbraced beams is presented first, followed by a discussion of the importance in over-designing the brace stiffness in order to keep brace forces low. Then, using the test results presented in Chapter 4, the effects of brace stiffness, brace location, stiffener size, and initial imperfections on the lateral buckling of beams will be evaluated. Test results will be compared with the theoretical solutions developed by BASP and the bracing equations presented in Chapter 2.

5.1 Unbraced Beams

Series A had no apparent lateral or torsional bracing other than the lateral restraint provided by the friction in the loading device (gravity load simulator). The seven tests with knife-edge loading on the top flange varied between 1.53 and 1.69 kips, with an average of 1.60 kips. All test loads reported herein include the weight of the loading beam. With no bracing, BASP gives a predicted buckling load of 1.29 kips which indicates that some lateral restraint is present. At a ram load of 3.2 kips corresponding to the average unbraced beam test load, the lateral stiffness of the loading device given in Figure 3.5 is 0.083 k/in. For one beam with a lateral restraint of 0.042 k/in., the BASP buckling load is 1.65 kips which is within three percent of the average test load. The small vibration motor probably reduced the restraint below that given in Figure 3.5.

When the loading beam without knife edges was placed directly on the top flange of the twin test beams, the buckling load increased from 1.60 kips to 3.91 kips when no web stiffener was used. The 244 percent increase was due to the tipping effect. When the beam tried to twist at 1.6 kips, the top flange load was then applied at the flange tip and a restoring torque (shown in Figure 5.1(a)) kept the beam in the straight position. This tipping effect phenomenon has been studied by Flint (1951a) and Fischer (1970) assuming no cross section distortion. Under this condition, they found that no twist could occur at the load point, so this position would be a brace point. Buckling could only occur between supports. The test beam A3, however, did twist at the load point at 3.91 kips because of cross-section distortion, as illustrated in Figure 5.1(b). When a 2-x-1/4 web stiffener was attached at the load point (to control distortion), the

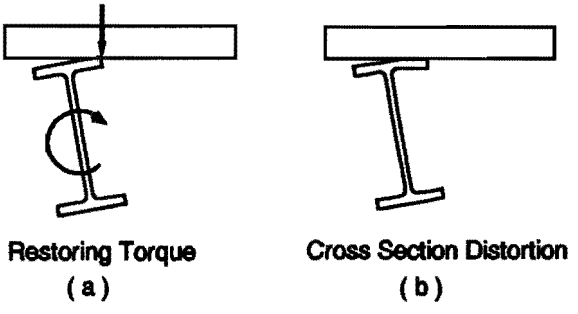

Figure 5.1 Tipping effect.

beam load (Test A4) reached 6.2 kips corresponding to buckling between the midspan and the end support (S shape).

The program BASP cannot determine the tipping buckling load because it assumes that the load is in the plane of the web. Linder (1982, in German) has developed a solution for the tipping effect which considers the flange-web distortion. The test data indicates that a cross member merely resting (not positively attached) on the top flange can significantly increase the lateral buckling capacity. The tipping solution is sensitive to the initial shape of the cross section and location of the load point on the flange. Because of these difficulties, it is recommended that the tipping effect be considered in design only when cross section distortion is prevented by stiffeners. In this case, the load point can be considered a brace point. Unfortunately, in a bridge structure subjected to moving concentrated loads, stiffening the web at the load point is impractical.

5.2 Effect of Imperfections on Lateral Bracing Requirements

In a column braced at midspan, the ideal brace stiffness, $\beta_i = 2P / L_b$ from Table 1.1 This stiffness requirement is applicable to columns that are straight. For a column with an initial out-of-straightness Δ_0 in Figure 5.2, the brace requirements can be derived by taking moments about point n,

$$P\left(\Delta_0 + \Delta\right) = \beta_L \Delta L_b / 2 \qquad (5.1)$$

Solving Eq. 5.1 for brace stiffness

$$\beta_L = \frac{2P}{L_b}\left(1 + \frac{\Delta_0}{\Delta}\right) = \beta_i\left(1 + \frac{\Delta_0}{\Delta}\right) \qquad (5.2)$$

and for brace strength

$$F_{br} = \beta_L \Delta = \frac{2P}{L_b}\left(\Delta + \Delta_0\right) \qquad (5.3)$$

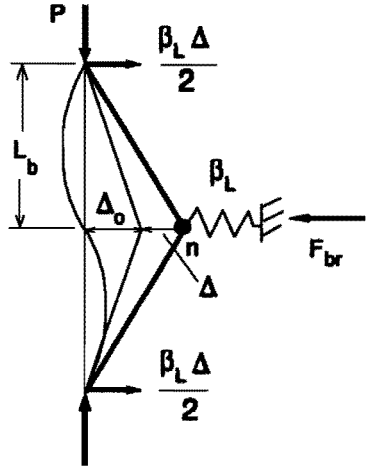

Figure 5.2 Imperfect column.

If $\Delta_o = 0$, then $\beta_L = 2P / L_b$, the ideal stiffness given in Table 1.1. However, for any out-of-straightness, the design stiffness must be greater than the ideal stiffness. In general, the relationship between initial displacement Δ_o and deflection under compressive load, P, is given by

$$\Delta_T = \frac{\Delta_0}{1 - \frac{P}{P_{cr}}} \tag{5.4}$$

Substituting $\Delta_T = \Delta + \Delta_o$ in Eq. 5.4 gives:

$$\Delta = \frac{\Delta_0}{\frac{P_{cr}}{P} - 1} \tag{5.5}$$

Equation 5.5 shows that when P approaches the buckling load P_{cr}, Δ gets very large. This reduces the stiffness requirement, Equation 5.2, to the ideal value, but unfortunately the brace force given by Equation 5.3 gets very large. In order to develop a reasonable solution for brace force, it is necessary to choose a design brace stiffness greater than the ideal value so that Δ at the brace will be small when the desired load P for buckling between braces is reached. For example, if a brace stiffness of twice the ideal stiffness is chosen, then from Eq. 5.5 $\Delta = \Delta_o$ since $P_{cr} = 2P$ and the brace force, Eq. 5.3, gives $F_{br} = 4P\Delta_o / L_b$. For an initial out-of-straightness $\Delta_o = L_b / 500$, F_{br} becomes 0.008P or only 0.8% of the column load. In general, substituting Eq. 5.5 into 5.3 gives the brace strength formulation in terms of brace stiffness

$$F_{br} = \frac{\beta_L \Delta_0}{\frac{\beta_L}{\beta_i} - 1} \tag{5.6}$$

where β_L is the brace stiffness provided and β_i is the ideal brace stiffness for a perfectly straight system. The brace force is a linear function of Δ_o. If a brace stiffness ten times the ideal value is available and the initial out-of-straightness is $L_b / 500$, Eq. 5.6 gives a brace force of 0.44 percent of P. For this same Δ_o, a brace stiffness of 1.67 β_i will require a one percent brace force. For a brace force of two percent, a stiffness of 1.25 β_i is required. For simplicity a brace stiffness of $2\beta_i$ and a brace force = 0.008P is recommended.

The effect of initial out-of-straightness on bracing requirements for beams follows a similar trend. Figure 5.3 shows the theoretical response of Test B9: 24-ft. span, W12X14

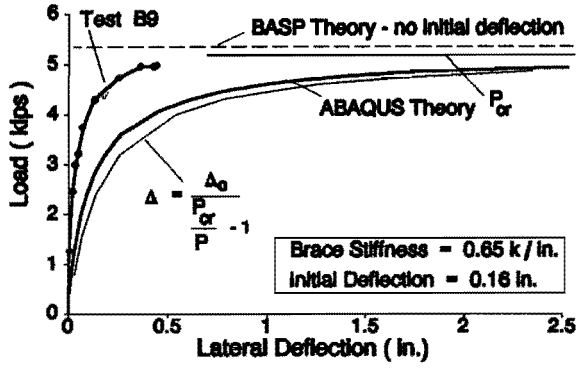

Figure 5.3 Beam with initial out - of - straightness.

section midspan load at the top flange, lateral brace stiffness = 0.65 k/in which is less than ideal, top and bottom flange out-of-straightness = 0.16 in. and 0.13 in. respectively. The finite element computer program, ABAQUS, was used to develop the load-deflection response and P_{cr} = 5.18 kips at very large deflections. The BASP buckling program gave P_{cr} = 5.34 kips. These two P_{cr} estimates are within three percent of each other. The experimental P_{cr} from a Meck plot of test data gave P_{cr} = 5.47 kips as listed in Table 4.3. The experimental lateral deflections are much less than the theoretical values. This is probably due to the fact that the experimental midspan lateral deflection is for two beams with some difference in out-of-straightness. The test result is an average of two beams. Even though the measured lateral displacements are one-third of the expected, the buckling loads are very similar. Equation 5.5 developed for columns gave results very close to the ABAQUS solution when Δ_0 is taken as the initial out-of-straightness of the compression flange. The out-of-straightness did not affect the elastic buckling load associated with very large lateral displacements.

5.3 Beams with Lateral Bracing

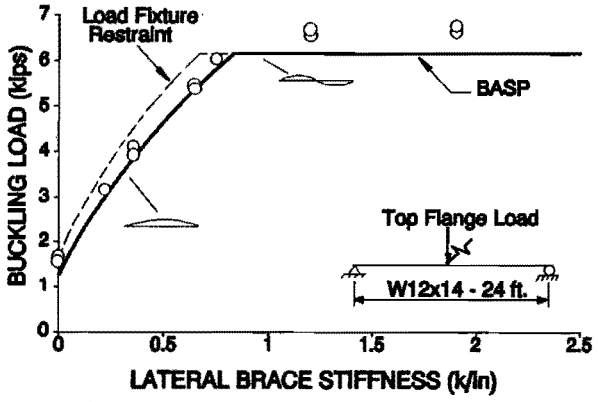

Figure 5.4 Lateral bracing tests.

A summary of the Series B lateral bracing tests is given in Figure 5.4. The test results show good agreement with the BASP theory. At brace stiffness below 0.8 k/in., the beams buckled in a single half sine curve as predicted. For brace stiffnesses greater than 0.8 k/in., full bracing is achieved and the test beams buckled into an S shape between brace points. The dashed line is the theoretical solution assuming that the gravity load simulator provides additional lateral restraint. The test results are closer to the theory neglecting this fixture restraint which indicates that the vibration motor was effective in reducing the friction.

The tests had initial top flange out-of-straightness between 0.15 in. and 0.36 in. but there was no apparent effect on the buckling loads. The experimental buckling loads obtained from Meck plots of the load-twist-lateral deflection data give the expected buckling

load if the beams would have been deformed beyond the 1 in. displacement limited in the experiments to control yielding of the beams.

A comparison of the test results with the continuous lateral bracing formulation, Equation 2.8, is shown in Figure 5.5 by the solid line. The figure shows that Equation 2.8 gives conservative results at brace stiffness near the ideal value, but in general the results are similar. As discussed in Chapter 2, the use of an equivalent continuous bracing formula for discrete braces produces the most error for the single brace at midspan. While Equation 2.8 was developed to handle all bracing arrangements and magnitude of brace stiffness, it may be simpler to adapt Winter's ideal bracing approach to the case of a concentrated load at midspan which controls design for most short span bridges.

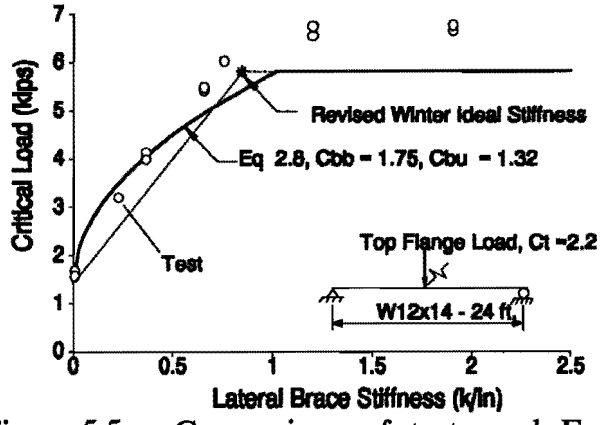

Figure 5.5 Comparison of tests and Eq. 2.1.

For beams under uniform moment the Winter brace lateral stiffness required to force buckling between the braces is $\beta_L^* = \#P_f / L_b$ as given in Table 1.1 where $P_f = \pi^2 EI_f / L_b^2$, I_f is the out-of-plane moment of inertia of the compression flange, $I_y / 2$, and # is a coefficient depending on the number of braces within the span. For other moment diagrams and top flange load, Winter's ideal bracing stiffness can be modified as follows,

$$\beta_L^* = \frac{\# P_f}{L_b} C_b C_t \qquad (5.7)$$

where C_b is the moment diagram modification factor given in by Eq. 1.2 for braced beams and C_t is defined by Equation 2.8. For the test beams braced only at midspan, # = 2, C_b = 1.75, C_t = 1 + 1.2 / 1 = 2.2, L_b = 144 in. and $P_f = \pi^2 (29000) (2.32 / 2) (144)^2 = 16.01$ kips, β_L^* = 0.856 k/in which is shown by the * in Figure 5.5. A linear response between zero bracing and ideal bracing is assumed and shown by the dashed line. Equation 5.7 compares very favorably with the test results and is a simpler alternative to the use of Equation 2.8.

The Series B tests with no stiffener, B9 and B10, gave approximately the same results when a 4 x 1/4 web stiffener was used in B8 and B7, respectively. The test results and theoretical studies indicate that web distortion is not an important factor when lateral bracing is attached to the top compression flange of a beam.

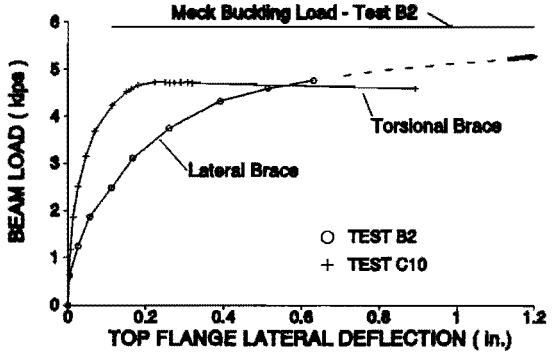

Figure 5.6 Typical test results

5.4 Beams with Torsional Bracing

The Series C torsional bracing tests were designed to study the influence of brace stiffness and the effect of cross section distortion. A typical load-lateral displacement response (Test C10) is shown in Figure 5.6. A peak load was reached at a displacement of approximately 0.2 in. which is taken as the buckling load. This behavior is very different from the typical response for the lateral bracing tests represented by Test B2 in Figure 5.6. For lateral bracing, no peak was reached in the experiment and the buckling load had to be determined by the Meck plotting technique. The Meck buckling load is the load that would be reached at large lateral displacement represented by the dash line. The difference between the two responses is caused by local distortion of the cross section at the points at which the torsional bracings are attached. Without distortion, the two flanges and the web should have the same angle of twist. The twist of the top flange and the bottom flange were measured near the brace at midspan in all experiments. The twist data show that at the brace there is no difference in the measured twist of each flange for lateral bracing but there was a significant difference for torsional bracing as the peak load was reached. In Test C10 at the peak load, the bottom flange twist of 1.23° was 2.3 times the top flange twist.

Cross-section distortion can be controlled by properly attached stiffeners. In Series C there were three general stiffener arrangements, namely, no stiffener, a stiffener in contact with the flange where the brace is attached which controls cross section distortion, and a web stiffener which does not touch either flange. This latter type of stiffener arrangement controls bending of the web but each flange is permitted to twist relative to the web. Figure 5.7 shows a comparison of the Series C tests with no stiffener and the buckling load predicted by BASP. In all of these tests, the beam buckled in a single half wave. No brace was sufficient to force the beam to buckle into an S-shape because of local distortion at the brace point. The test loads are significantly greater than the BASP solution assuming no lateral restraint by the loading fixture (heavy solid line). Two additional BASP solutions are shown which indicate that the effect of lateral restraint is very significant. The 0.026 k/in. for each beam is approximately 1/4 of the restraint calibrated in Figure 3.5 for no vibration motor and is a lower bound to the test data. The highest BASP solution corresponds to the full calibrated

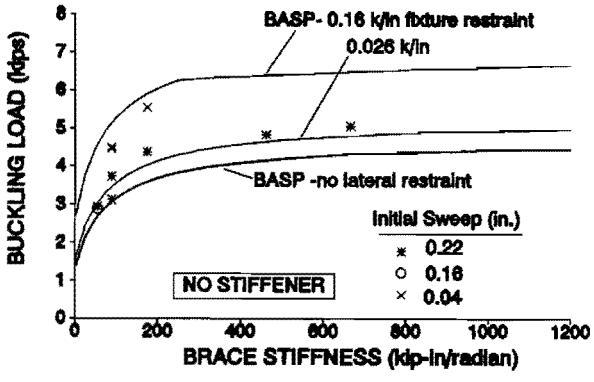

Figure 5.7 Torsional bracing - no stiffener.

lateral restraint by the gravity-load simulator. The test results fall within the bounds of the BASP solutions. In the lateral bracing tests, Series B, the effect of the fixture restraint was relatively minor, but this is not the case for torsional bracing. As indicated in Figure 2.8, the interaction of lateral and torsional bracing is very effective. For example, a lateral brace of 10 percent of the required lateral bracing reduces the torsional bracing requirement by 40 percent.

The data in Figure 5.7 indicates that the beams with the smallest initial sweep had the largest buckling loads. This was probably due to smaller lateral displacements and the likelihood that friction in the test fixture was not broken. The test results for initial sweep equal to 0.04 in. are very close to the BASP solution with full fixture restraint.

The Series C results for a stiffener in contact with the torsionally braced flange compare very well with the BASP results, as shown in Figure 5.8. These tests simulate the typical design situation of a stiffener welded to the compression flange and cut short of the tension flange. The effect of possible fixture restraint is not as important for this case where cross section distortion is prevented by the 4 x 1/4 stiffener at each brace location. The ideal brace stiffness is approximately 320 kip-in/radian. At the ideal stiffness, the buckled shape changes from a single half wave to the S-shape corresponding to full bracing at midspan. All the tests with bracing greater than 320 kip-in/radian buckled into an S shape.

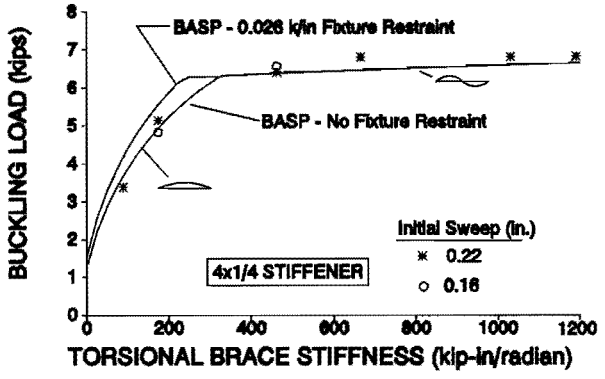

Figure 5.8 Torsional bracing tests - Full stiffener.

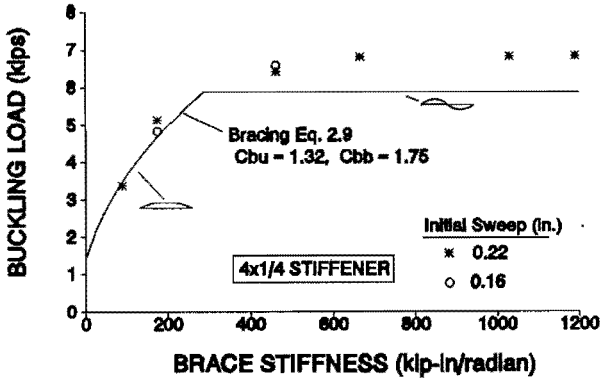

Figure 5.9 Eq. 2.9 - Full stiffener.

The torsional bracing formula, Equation 2.9, is compared to the test results for the stiffened and unstiffened cases in Figures 5.9 and 5.10, respectively. The difference between these two cases is caused by cross section distortion. In the torsional bracing formula, β_{scc} = 114 kip-in/radian for the unstiffened web and 11030 for a beam with a 4 x 1/4 stiffener at the brace points. As β_{scc} get smaller, the attached brace becomes less effective. An attached brace with a stiffness of 250 kip-in/radian is almost fully effective (247 kip-in/radian from Eqs. 2.5 and 2.6) but the same brace is effectively reduced to 119 kip-in/rad,

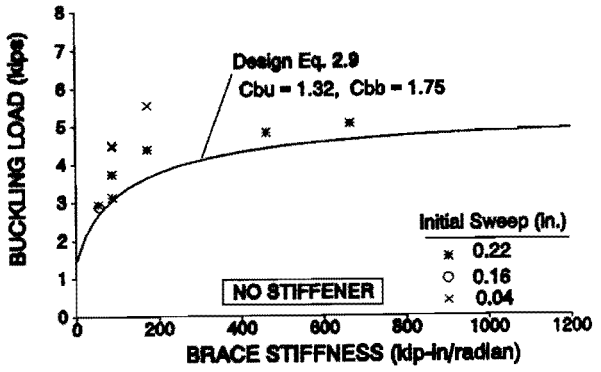

Figure 5.10 Eq. 2.9 - No stiffener.

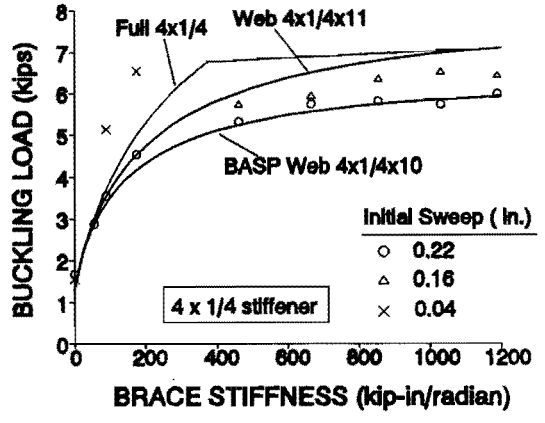

Figure 5.11 Web stiffened test results.

about a fifty percent reduction, if the web is unstiffened. The design equations follow the trend of the data very well.

When the stiffener is not welded or in contact with the braced flange, then the web can twist relative to the flange as illustrated in Figure 5.1(b). In such a case, the effectiveness of the stiffener in controlling distortion is reduced and Equation 2.9 is not applicable. Tests in which the 4 x 1/4 web stiffener did not touch the braced flange are summarized in Figure 5.11. The web was stiffened, not the flanges in these tests. The tests are similar for a 2 x 1/4 stiffener. The tests compare favorably with BASP solution in which the web stiffener is assumed to be 10 in. long or 11 in. long. The actual stiffener was an angle eleven inches long but it was bolted to the web and the distance between connectors was 9 in. Therefore it is questionable that the total length of the stiffener is effective. Stiffeners that do not contact the braced flange are not recommended and these tests illustrate the reduced strength when compared with the results in Figure 5.9.

5.5 Effect of Torsional Brace Location

Theoretically, the attachment height of a torsional brace should have no effect on the buckling load if the beam web does not distort. Figure 5.12 and 5.13 show values of critical load for tests with torsional bracing placed on the compression flange, tension flange or split evenly between the compression and tension flanges (combined bracing). Figures 5.12 and 5.13 show that the combined bracing produced a slightly higher critical load for beams with no stiffener, however, the beam with a 4x1/4-in. stiffener and a brace stiffness of 175 k-in/rad also showed an increase in critical load. Based on these tests, the brace location did not significantly affect the critical load regardless of the cross-section stiffness of the test beam.

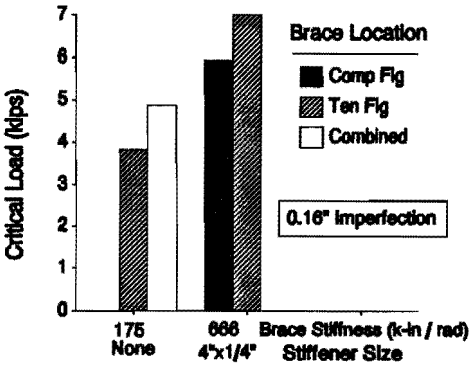

Figure 5.12 Effect of brace location.

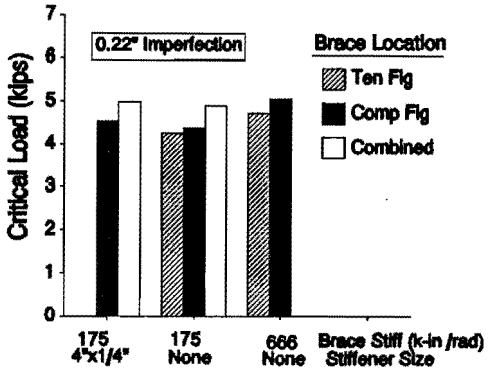

Figure 5.13 Forced 0.22-in. imperfection.

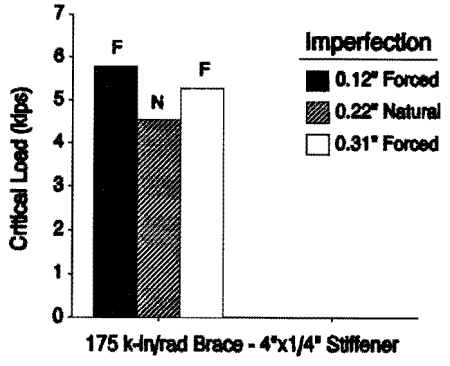

Figure 5.14 Forced initial imperfections.

5.6 Forced Imperfections

In the experiments, two types of imperfections were tested; natural imperfections and forced imperfections. Since a natural imperfection requires equilibrium of internal stresses and a forced imperfection requires equilibrium with an applied external reaction, there is no theoretical basis for assuming that both types of imperfection would have the same impact on the effective brace stiffness.

Based on Figure 5.14, a forced imperfection has an effect similar to a natural imperfection. Since lateral-torsional buckling involves both a twist and a lateral displacement, the magnitude of initial twist may also have an effect on the brace stiffness.

CHAPTER SIX

SUMMARY AND CONCLUSIONS

6.1 Summary of the Investigation

The purpose of the investigation was to evaluate the effects of intermediate lateral and torsional bracing on the lateral-torsional buckling of steel beams. Bracing equations were developed to determine the critical load for beams braced by lateral and/or torsional bracing.

The effects of brace stiffness, brace location, and stiffener size were studied experimentally and also analytically using the program BASP. The effects of imperfections were studied mainly with the experimental program. The bracing formulas, Eqs. 2.8 and 2.9, are presented and compared to finite element solutions for straight beams in Chapter 2 and are compared to experimental results in Chapter 5.

6.2 Conclusions

The analytical and experimental study indicated that cross section distortion has a significant effect on the torsional bracing requirements. Published formulations, which do not account for the distortion, should not be used for design. Equations 2.5, 2.6. and 2.9 directly account for the distortion. They can also be used to design adequate stiffeners to make the attached bracing more effective. The distortion effect is mainly related to the web thickness.

Lateral bracing at the top flange of simply supported beams was very effective and was not affected by cross section distortion (stiffeners are not necessary). The shape of the moment diagram and top flange loading have significant effect on the bracing requirements and the bracing formulas were developed to account for these two effects.

The BASP program and bracing equations developed from the analytical studies showed good correlation with the test results. The tests verified that cross section distortion is very important for torsional bracing. The W12X14 test beams could not reach the load level corresponding to buckling between braces unless web stiffeners in contact with the braced flange were used. Torsional bracing at the bottom tension flange was just as effective as bracing on the compression.

The Meck technique for obtaining experimental buckling loads worked very well for lateral bracing, but was not useful for torsional bracing because of the effect of local cross section distortion. In the torsional bracing experiments, the results were sensitive to the slight lateral restraint provided by the test fixture especially for very straight beams.

Combined lateral and torsional bracing is very effective in controlling lateral buckling of slender beams.

The initial sweep of the beam did not affect the buckling load of laterally braced beams, but did influence the results in the torsional buckling experiments. The experimental buckling were all larger than the BASP prediction regardless of the level of initial imperfection, so the apparent out-of-straightness effect was related to lateral fixture restraint.

6.3 Recommendations for Design

Equations 2.8 and 2.9 should not be used directly for design. While they show very good agreement with the theoretical and experimental results, they need to be adjusted to keep brace forces low as described in Section 5.2. Beams with initial out-of-straightness (sweep) deflect laterally under any loading. The lateral displacement and twist get very large as the buckling load is approached which introduces large forces into the braces. These lateral deflections can be controlled by over-designing the braces. If a brace with twice the stiffness required by Eqs. 2.8 or 2.9 is used, then the additional lateral deflection will be no greater than the magnitude of the initial sweep itself when the load reaches the buckling load. Thus, a doubling of the theoretical brace stiffeners reduces the lateral displacement of the brace point from infinity to Δ_0 at the buckling load. The resulting brace forces will then be limited to 0.008 of the compression force in the flanges for an initial sweep of L/500.

The recommendations for design are given in Appendix B. They are the same as Eqs. 2.8, 2.9 and 5.7, with the brace stiffness divided by a factor of two. Eqs. 2.8 and 2.9 give the buckling load for any magnitude of bracing. Eq. 5.7 is a simpler expression which can be used to determine the lateral bracing stiffness to force the beam to buckle between braces.

APPENDIX A
LOAD - DEFLECTION CURVES

TEST A1.001

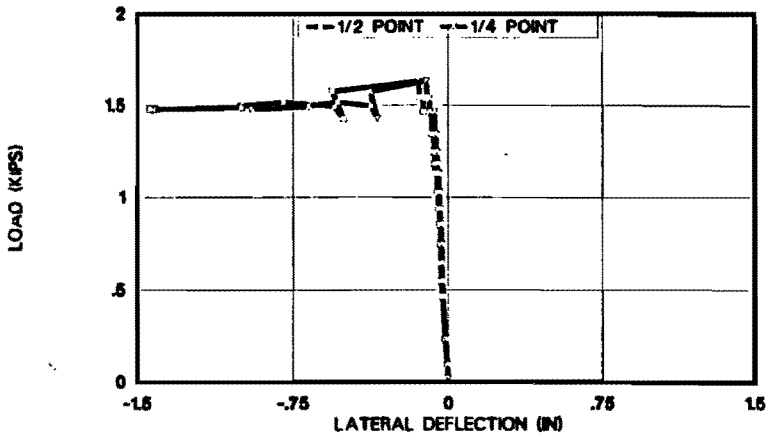

TEST A2.001

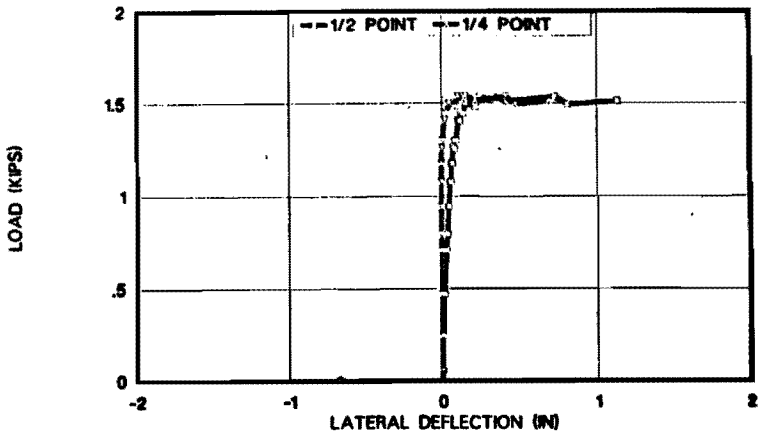

TEST A3.001

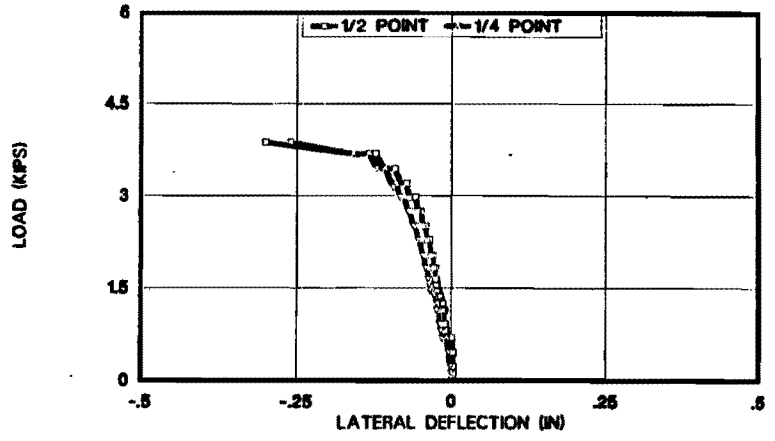

TEST A4.001

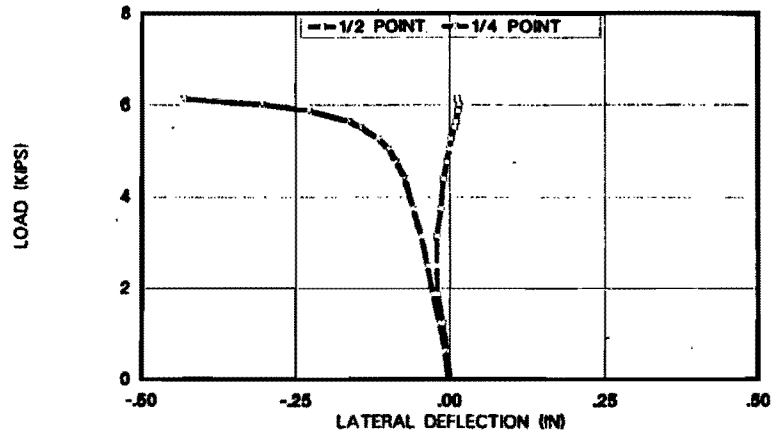

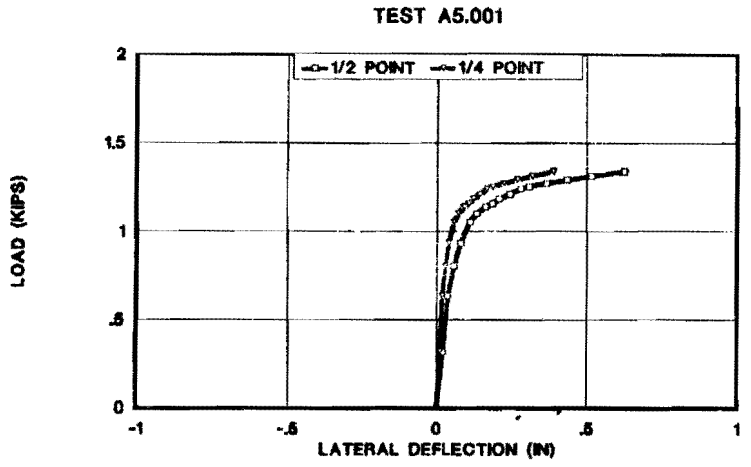
TEST A5.001
1/2 POINT
1/4 POINT
LOAD (KIPS)
2
1.5
1
.5
0
-1
-.5
0
.5
1
LATERAL DEFLECTION (IN)

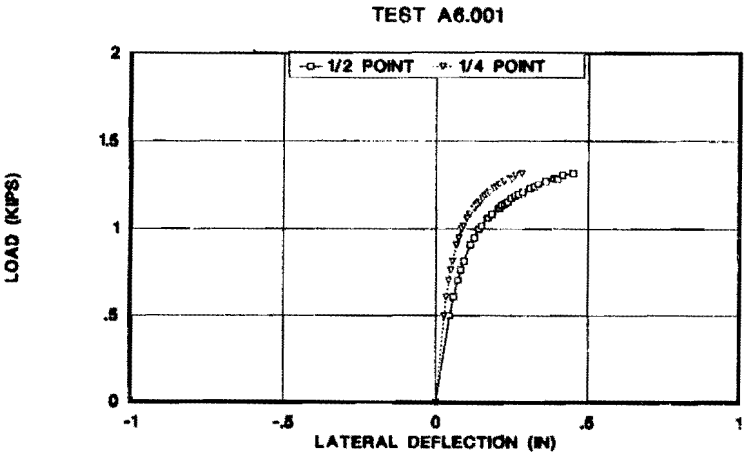
TEST A6.001
1/2 POINT
1/4 POINT
LOAD (KIPS)
2
1.5
1
.5
0
-1
-.5
0
.5
1
LATERAL DEFLECTION (IN)

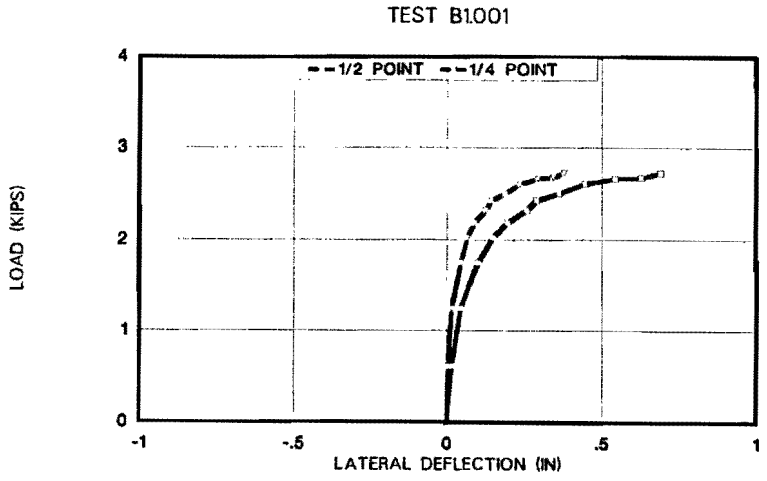
TEST B1.001
1/2 POINT
1/4 POINT
LOAD (KIPS)
4
3
2
1
0
-1
-.5
0
.5
1
LATERAL DEFLECTION (IN)

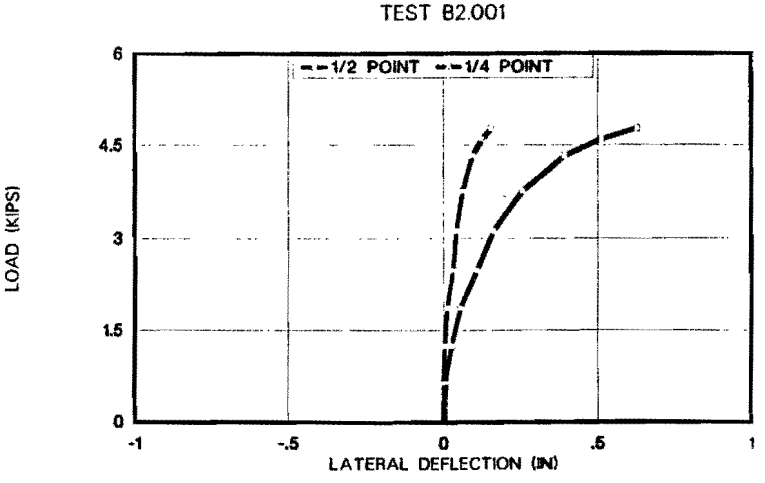
TEST B2.001
1/2 POINT
1/4 POINT
LOAD (KIPS)
6
4.5
3
1.5
0
-1
-.5
0
.5
1
LATERAL DEFLECTION (IN)

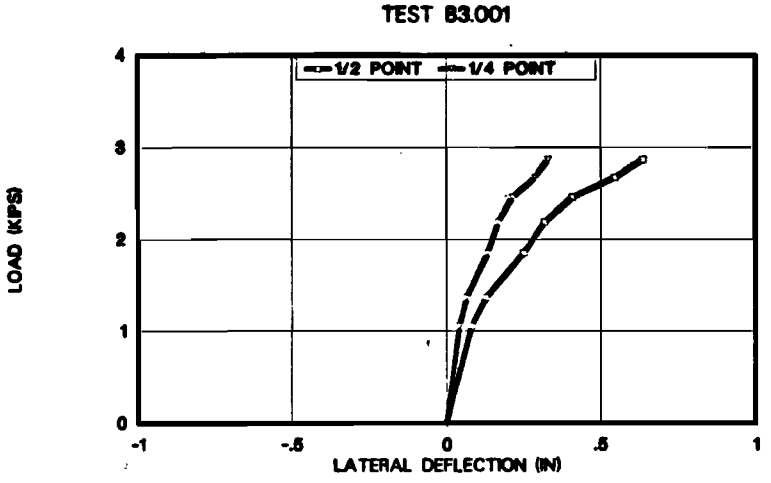
TEST B3.001
1/2 POINT
1/4 POINT
LOAD (KIPS)
LATERAL DEFLECTION (IN)
0
1
2
3
4
-1
-.5
0
.5
1

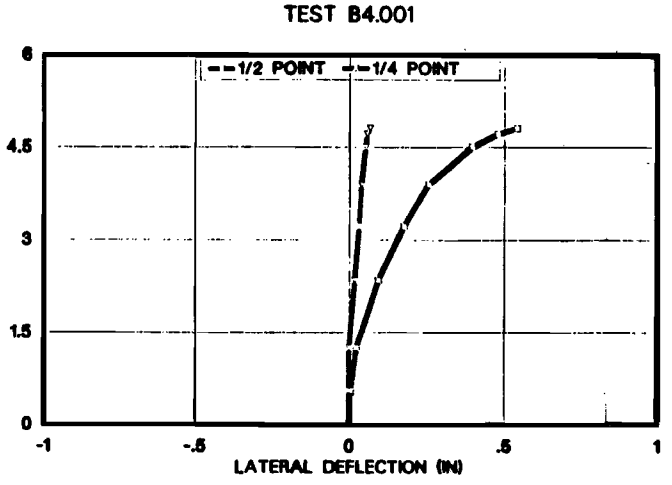
TEST B4.001
1/2 POINT
1/4 POINT
LOAD (KIPS)
LATERAL DEFLECTION (IN)
0
1.5
3
4.5
6
-1
-.5
0
.5
1

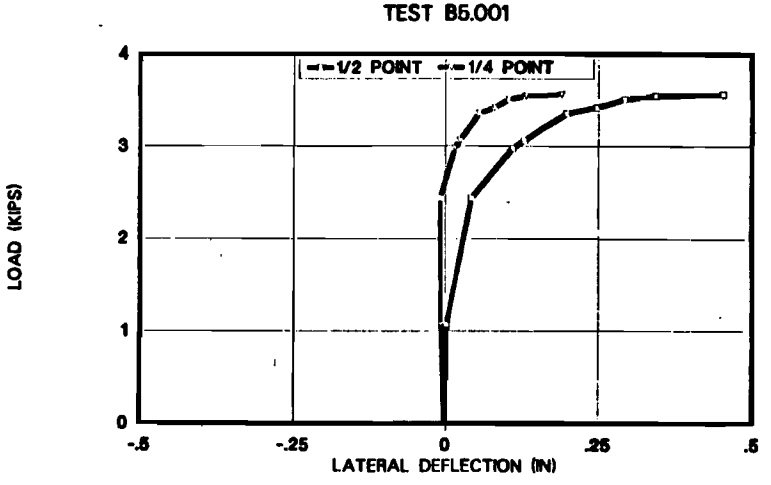
TEST B5.001
1/2 POINT
1/4 POINT
LOAD (KIPS)
LATERAL DEFLECTION (IN)
0
1
2
3
4
-.5
-.25
0
.25
.5

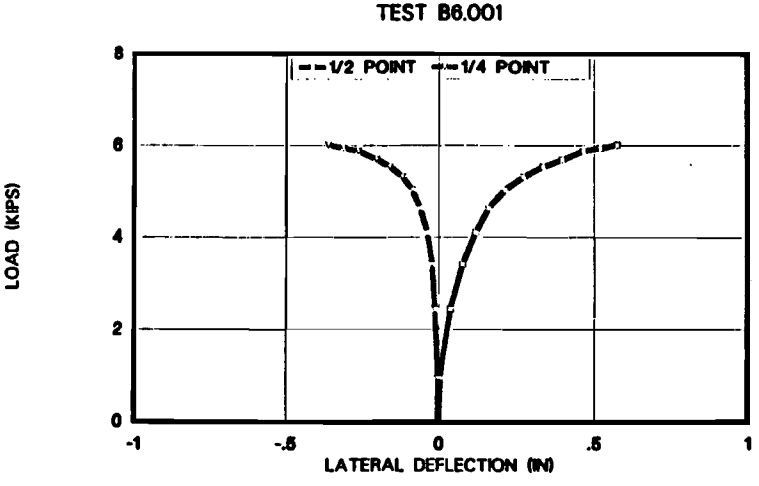
TEST B6.001
1/2 POINT
1/4 POINT
LOAD (KIPS)
LATERAL DEFLECTION (IN)
0
2
4
6
8
-1
-.5
0
.5
1

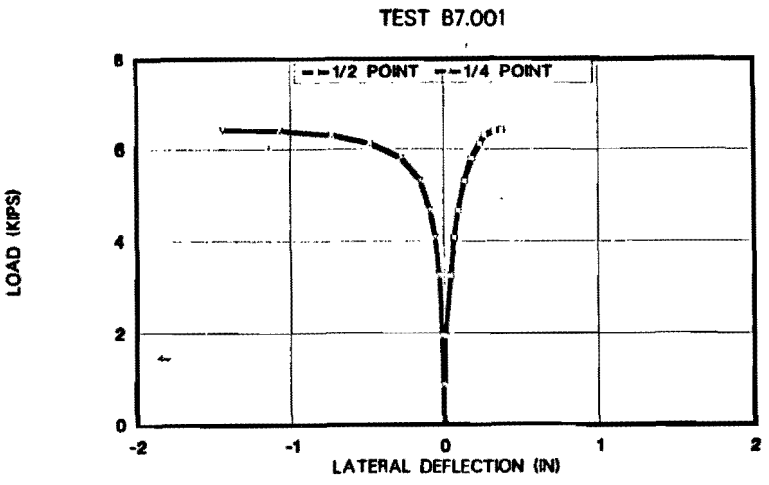
TEST B7.001
1/2 POINT
1/4 POINT
LOAD (KIPS)
LATERAL DEFLECTION (IN)
0
2
4
6
-2
-1
0
1
2

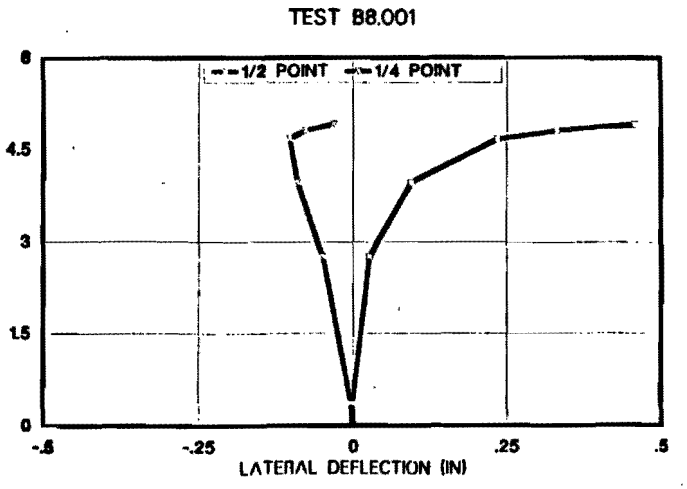
TEST B8.001
1/2 POINT
1/4 POINT
LOAD (KIPS)
LATERAL DEFLECTION (IN)
0
1.5
3
4.5
6
-.5
-.25
0
.25
.5

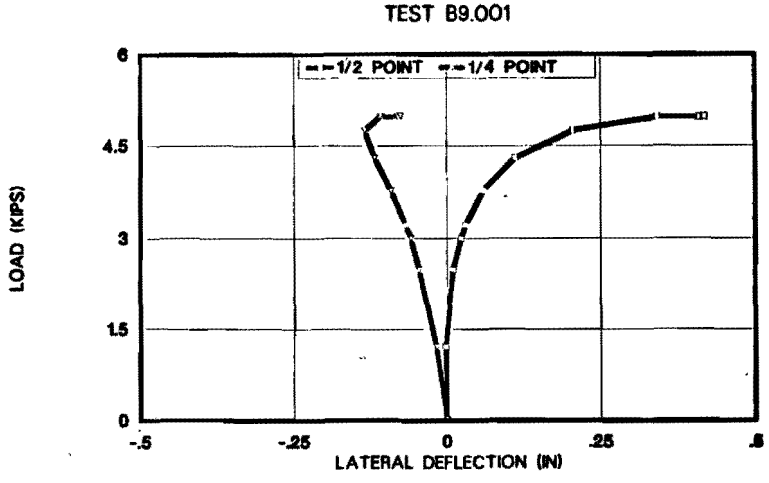
TEST B9.001
1/2 POINT
1/4 POINT
LOAD (KIPS)
LATERAL DEFLECTION (IN)
0
1.5
3
4.5
6
-.5
-.25
0
.25
.5

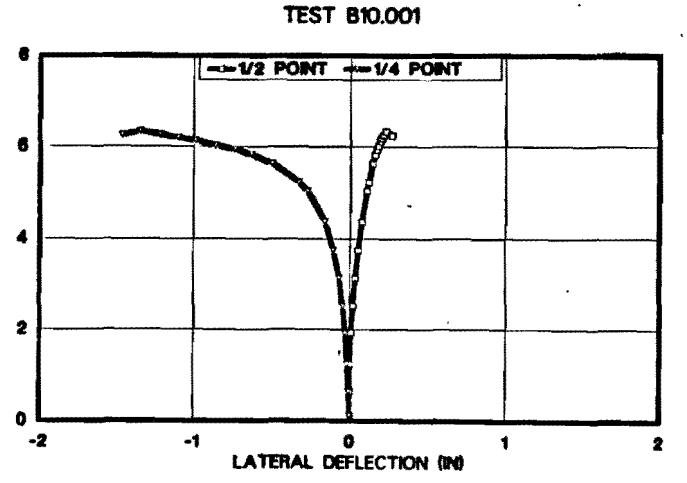
TEST B10.001
1/2 POINT
1/4 POINT
LOAD (KIPS)
LATERAL DEFLECTION (IN)
0
2
4
6
-2
-1
0
1
2

TEST C1.001

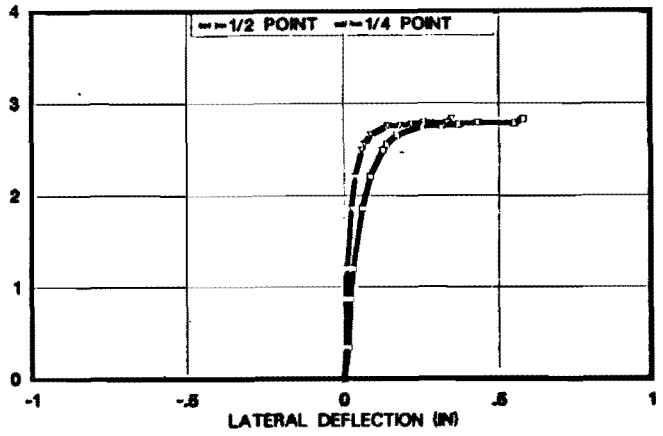

TEST C2.001

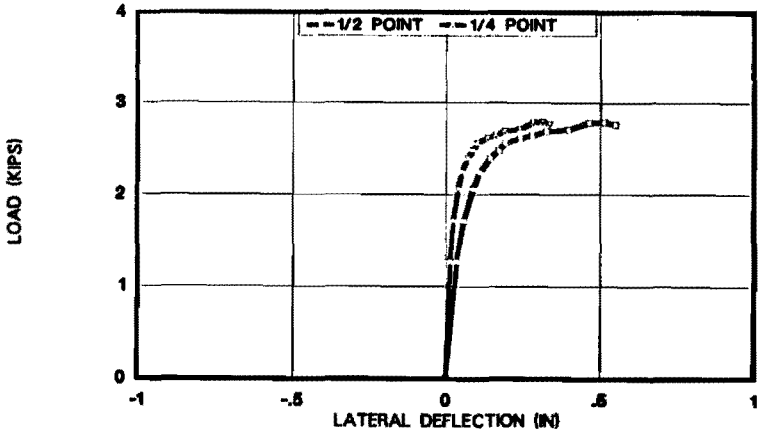

TEST C3.001

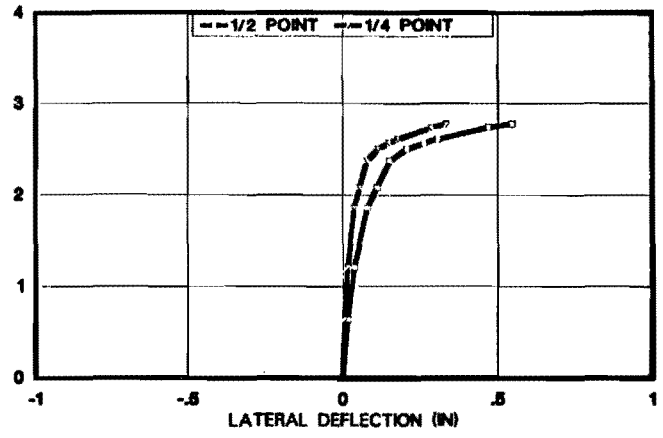

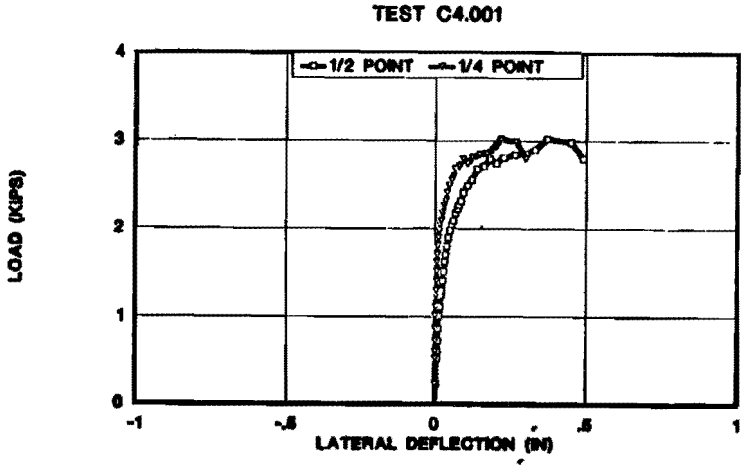
TEST C4.001
1/2 POINT
1/4 POINT
LOAD (KIPS)
LATERAL DEFLECTION (IN)
0
1
2
3
4
-1
-.5
0
.5
1

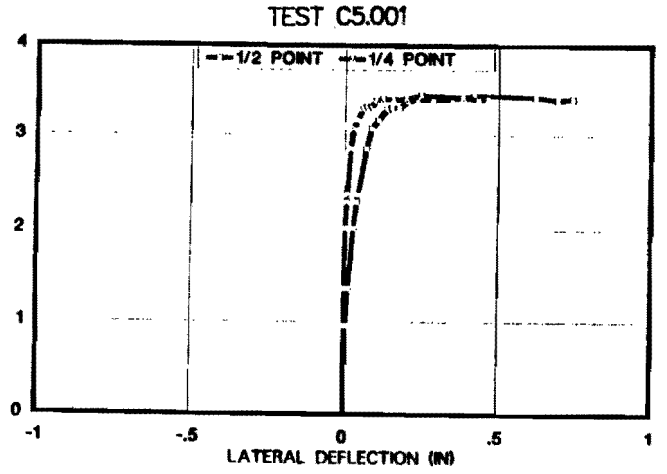
TEST C5.001
1/2 POINT
1/4 POINT
LOAD (KIPS)
LATERAL DEFLECTION (IN)
0
1
2
3
4
-1
-.5
0
.5
1

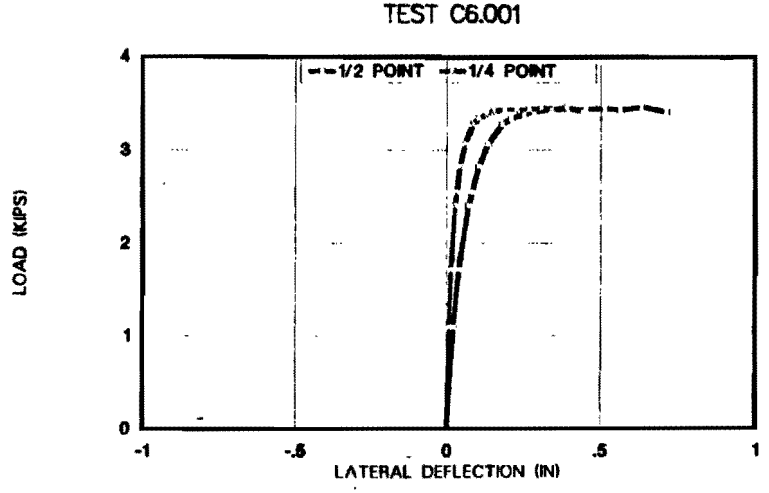
TEST C6.001
1/2 POINT
1/4 POINT
LOAD (KIPS)
LATERAL DEFLECTION (IN)
0
1
2
3
4
-1
-.5
0
.5
1

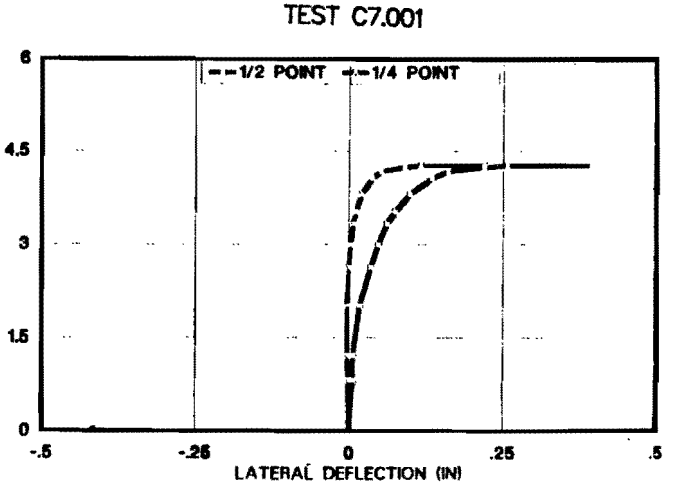
TEST C7.001
1/2 POINT
1/4 POINT
LOAD (KIPS)
LATERAL DEFLECTION (IN)
0
1.5
3
4.5
6
-.5
-.25
0
.25
.5

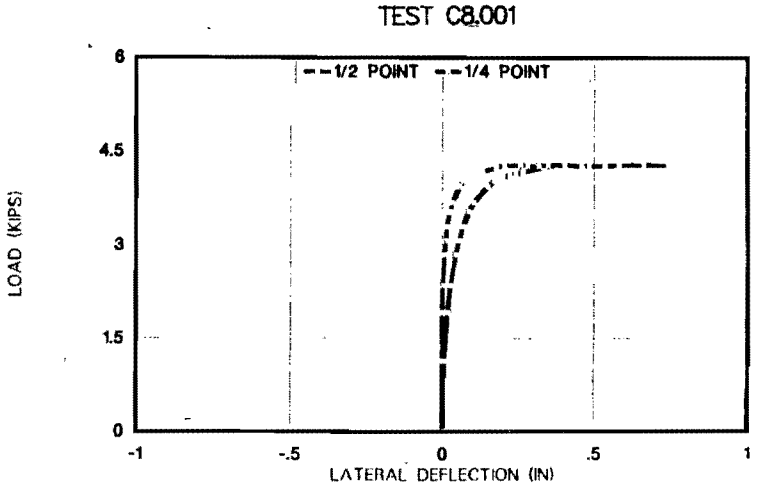
TEST C8.001
--1/2 POINT --1/4 POINT
LOAD (KIPS)
6
4.5
3
1.5
0
-1
-.5
0
.5
1
LATERAL DEFLECTION (IN)

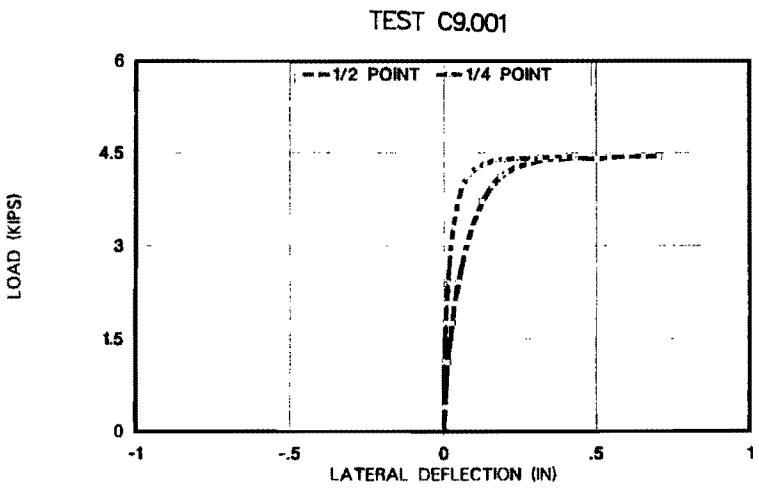
TEST C9.001
--1/2 POINT --1/4 POINT
LOAD (KIPS)
6
4.5
3
1.5
0
-1
-.5
0
.5
1
LATERAL DEFLECTION (IN)

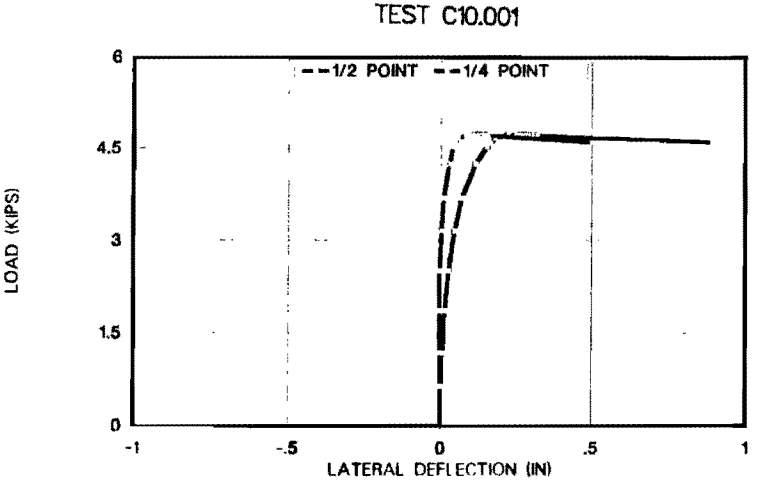
TEST C10.001
--1/2 POINT --1/4 POINT
LOAD (KIPS)
6
4.5
3
1.5
0
-1
-.5
0
.5
1
LATERAL DEFLECTION (IN)

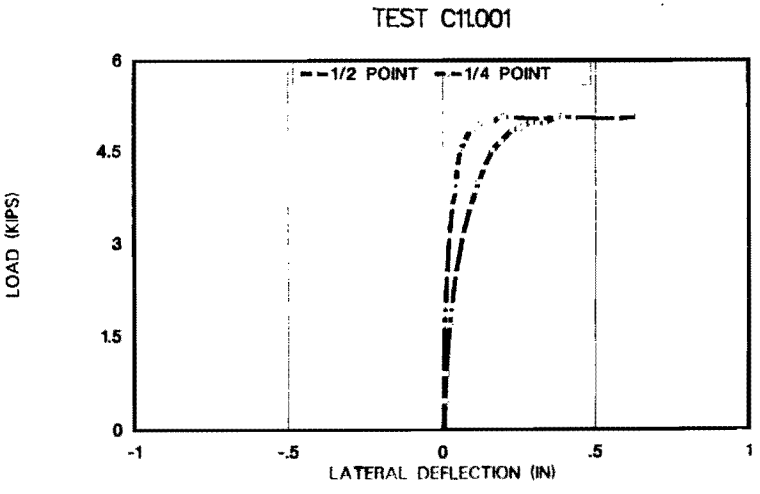
TEST C11.001
--1/2 POINT --1/4 POINT
LOAD (KIPS)
6
4.5
3
1.5
0
-1
-.5
0
.5
1
LATERAL DEFLECTION (IN)

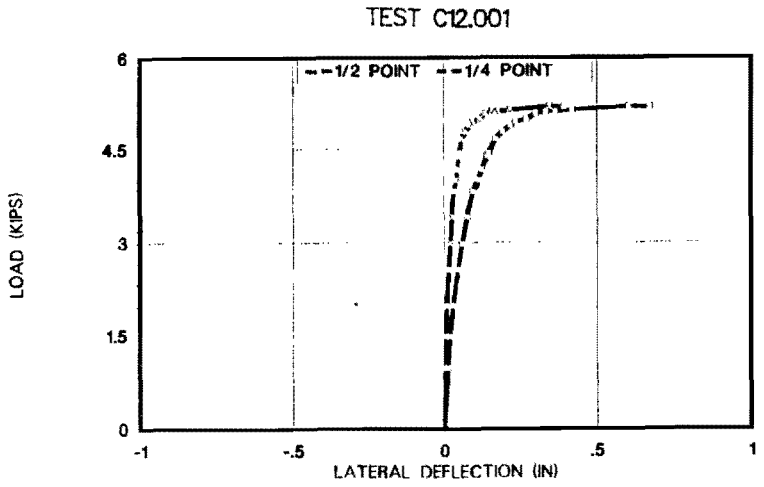
TEST C12.001
--1/2 POINT --1/4 POINT
LOAD (KIPS)
6
4.5
3
1.5
0
-1
-.5
0
.5
1
LATERAL DEFLECTION (IN)

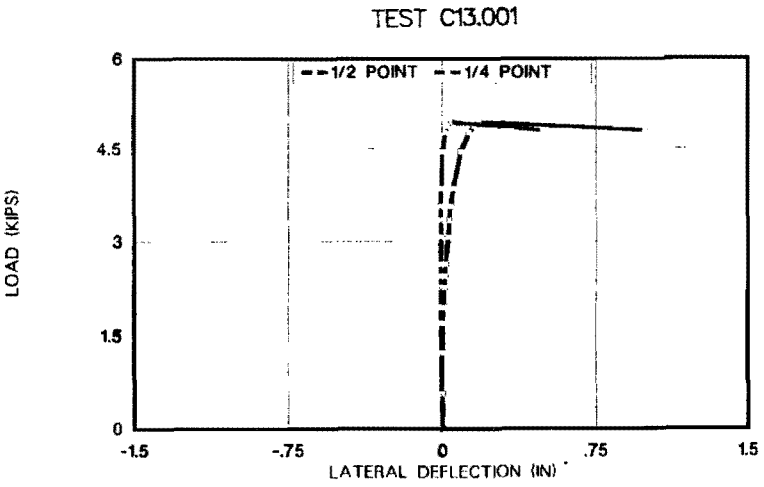
TEST C13.001
--1/2 POINT --1/4 POINT
LOAD (KIPS)
6
4.5
3
1.5
0
-1.5
-.75
0
.75
1.5
LATERAL DEFLECTION (IN)

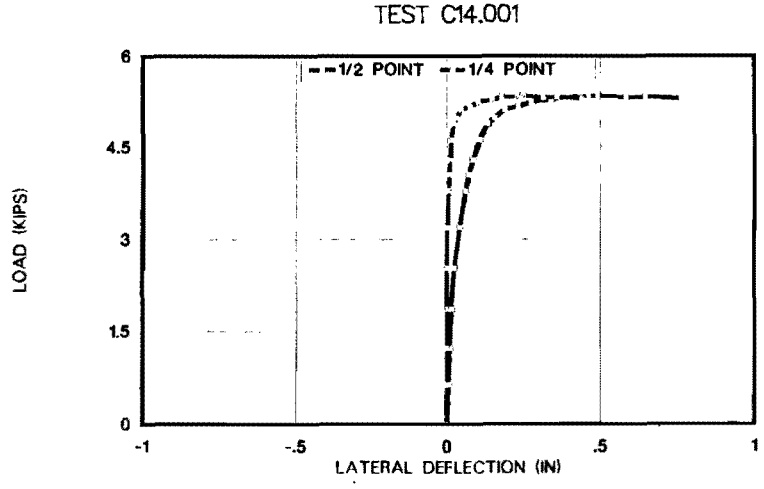
TEST C14.001
--1/2 POINT --1/4 POINT
LOAD (KIPS)
6
4.5
3
1.5
0
-1
-.5
0
.5
1
LATERAL DEFLECTION (IN)

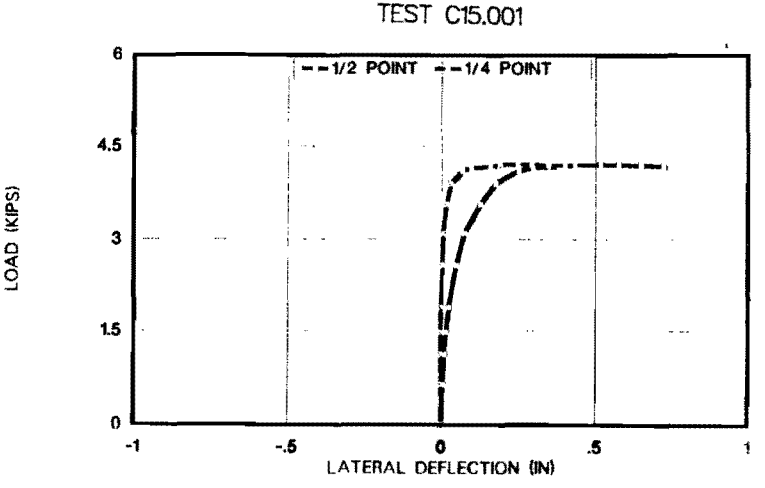
TEST C15.001
--1/2 POINT --1/4 POINT
LOAD (KIPS)
6
4.5
3
1.5
0
-1
-.5
0
.5
1
LATERAL DEFLECTION (IN)

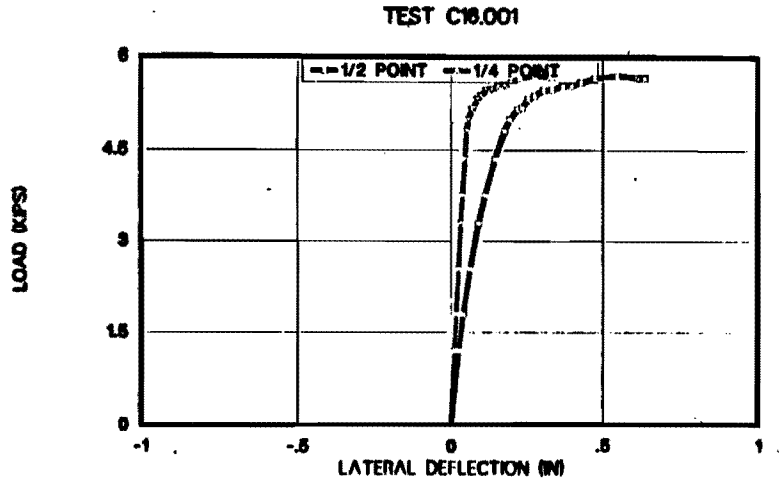
TEST C16.001
1/2 POINT
1/4 POINT
LOAD (KIPS)
LATERAL DEFLECTION (IN)
0
1.5
3
4.5
6
-1
-.5
0
.5
1

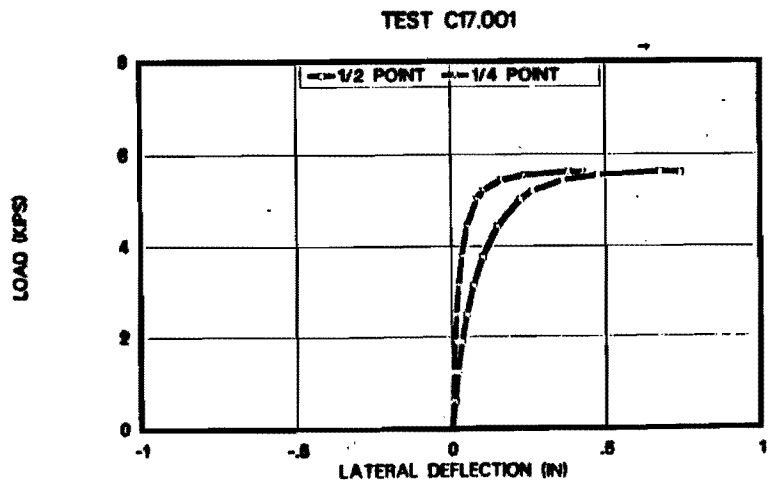
TEST C17.001
1/2 POINT
1/4 POINT
LOAD (KIPS)
LATERAL DEFLECTION (IN)
0
2
4
6
8
-1
-.5
0
.5
1

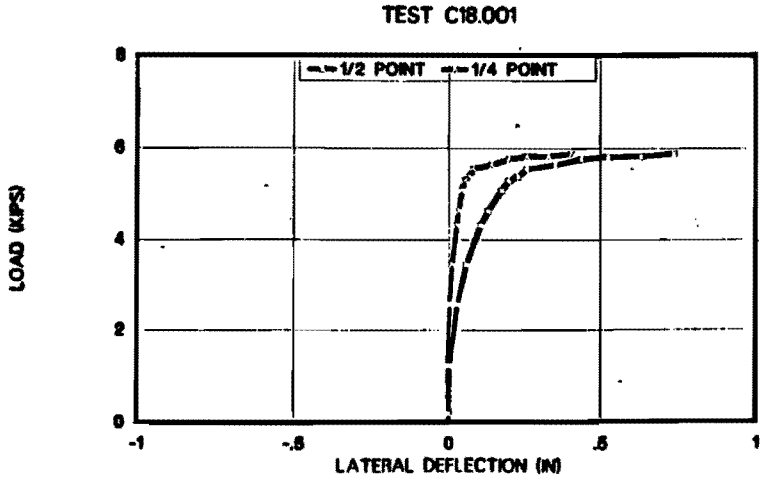
TEST C18.001
1/2 POINT
1/4 POINT
LOAD (KIPS)
LATERAL DEFLECTION (IN)
0
2
4
6
8
-1
-.5
0
.5
1

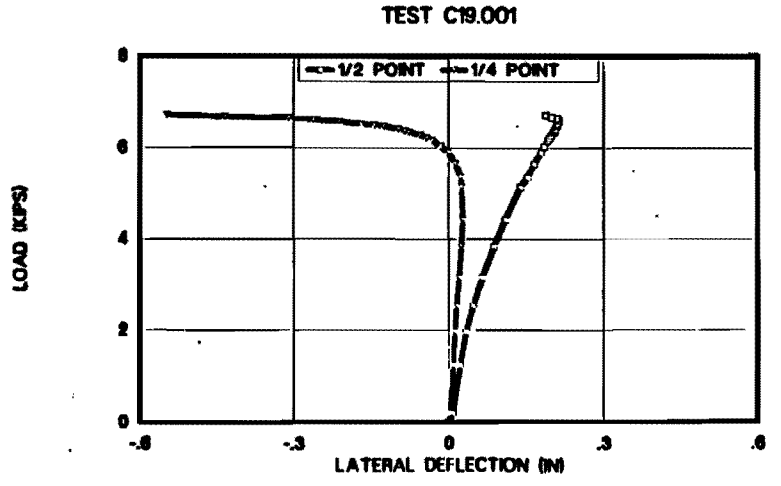
TEST C19.001
1/2 POINT
1/4 POINT
LOAD (KIPS)
LATERAL DEFLECTION (IN)
0
2
4
6
8
-.6
-.3
0
.3
.6

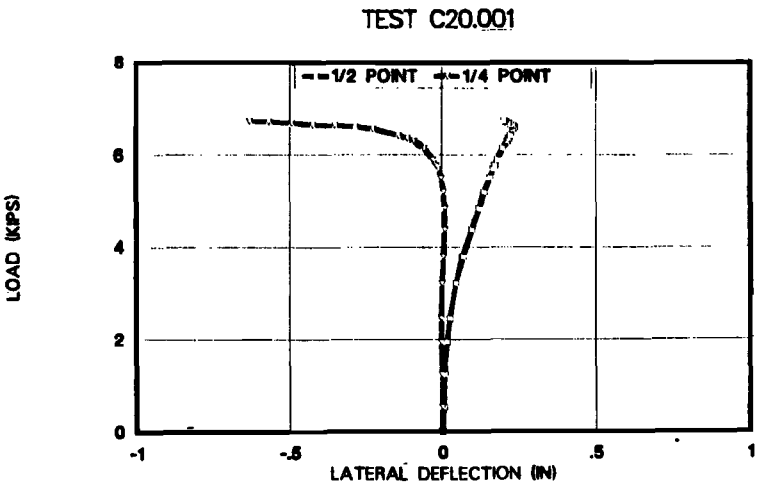
TEST C20.001
1/2 POINT
1/4 POINT
LOAD (KIPS)
LATERAL DEFLECTION (IN)

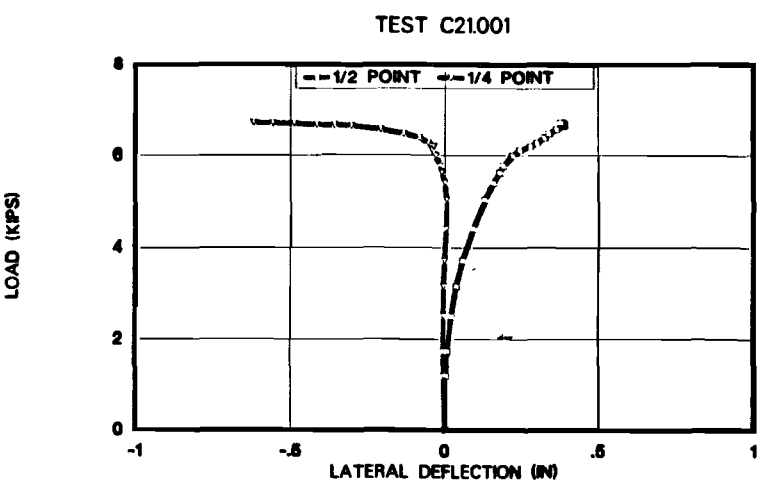
TEST C21.001
1/2 POINT
1/4 POINT
LOAD (KIPS)
LATERAL DEFLECTION (IN)

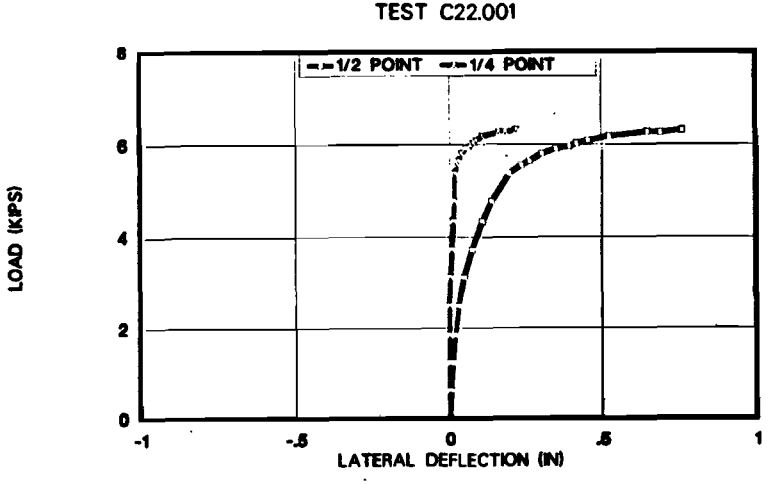
TEST C22.001
1/2 POINT
1/4 POINT
LOAD (KIPS)
LATERAL DEFLECTION (IN)

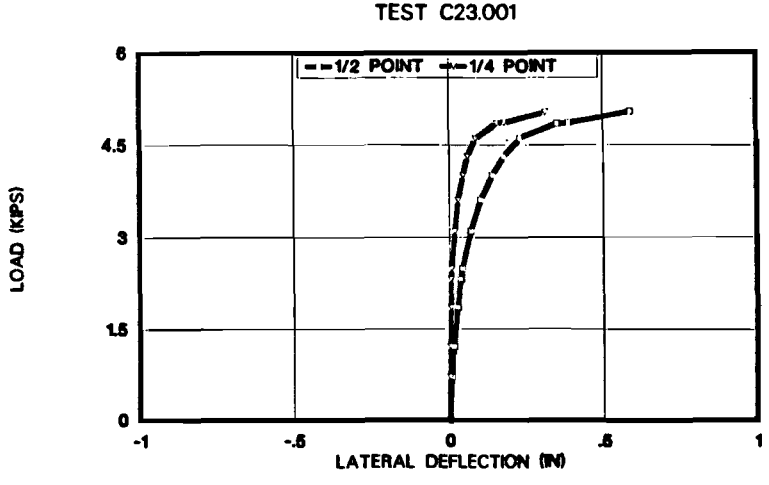
TEST C23.001
1/2 POINT
1/4 POINT
LOAD (KIPS)
LATERAL DEFLECTION (IN)

TEST C24.001

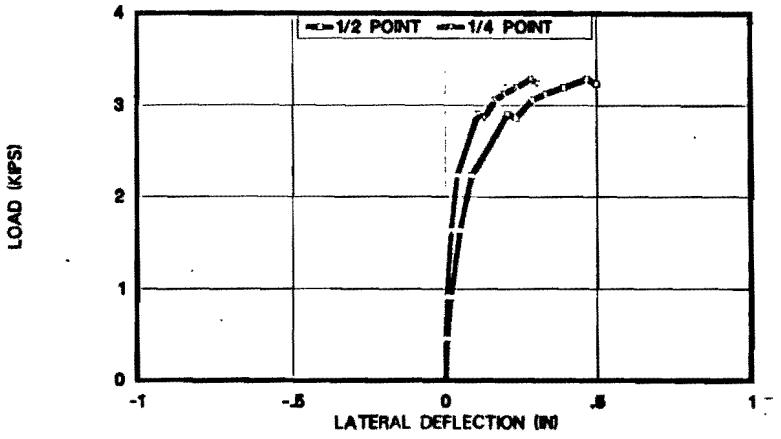

TEST C26.001

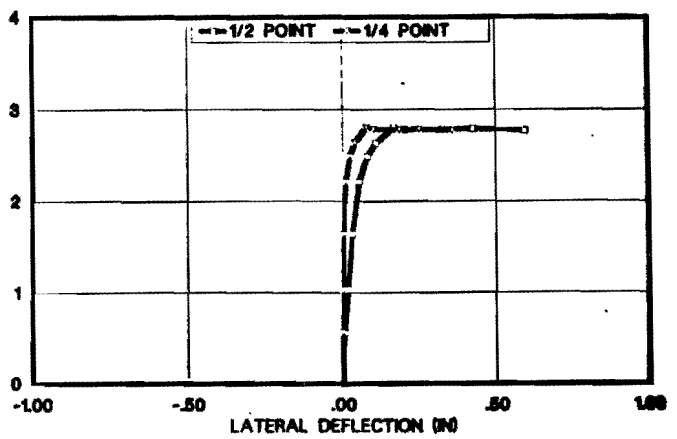

TEST C26.001

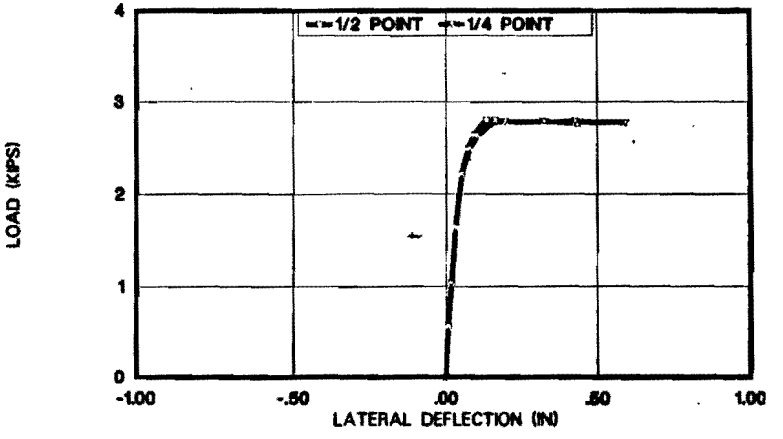

TEST C27.001

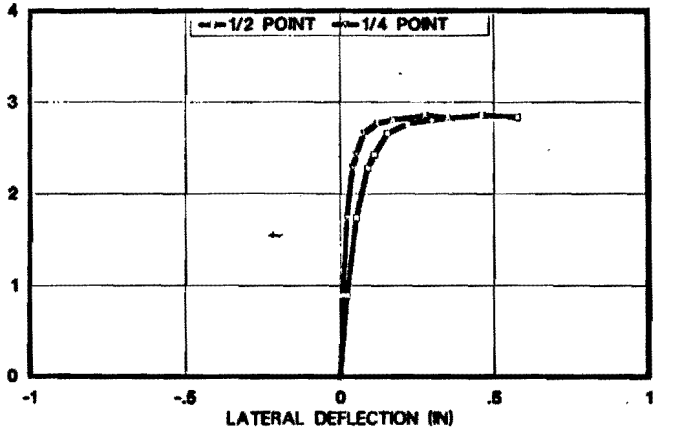

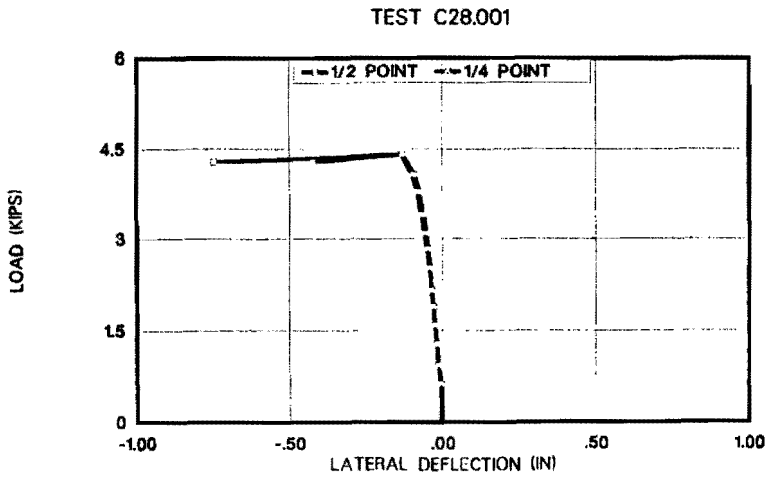
TEST C28.001
1/2 POINT
1/4 POINT
LOAD (KIPS)
6
4.5
3
1.5
0
-1.00
-.50
.00
.50
1.00
LATERAL DEFLECTION (IN)

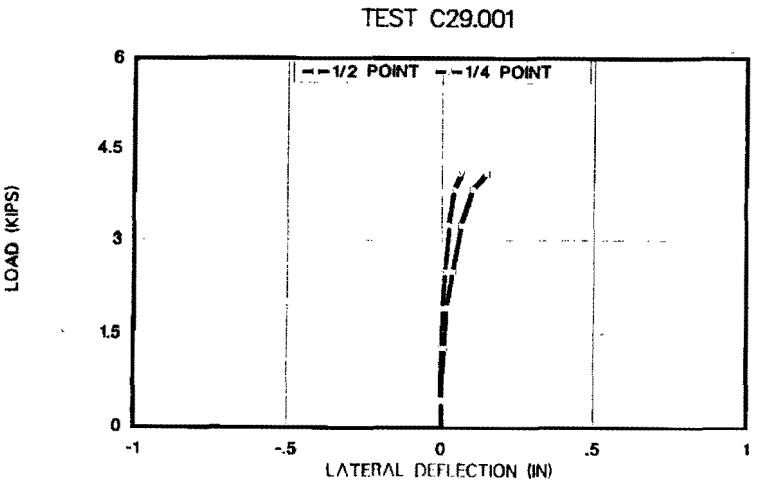
TEST C29.001
1/2 POINT
1/4 POINT
LOAD (KIPS)
6
4.5
3
1.5
0
-1
-.5
0
.5
1
LATERAL DEFLECTION (IN)

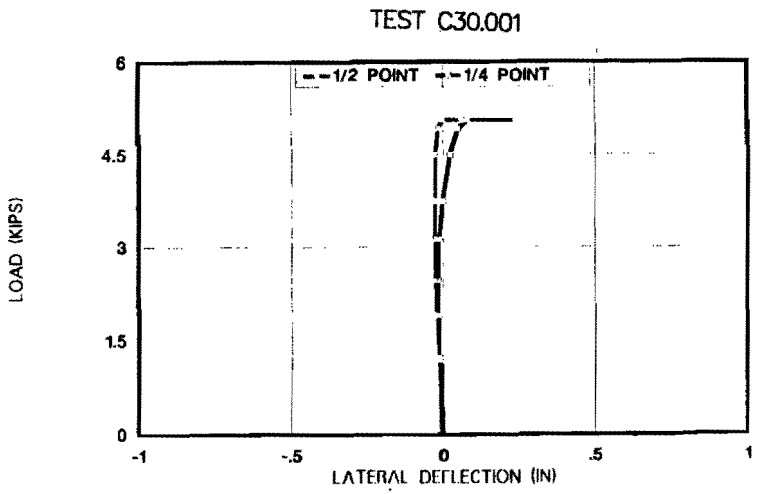
TEST C30.001
1/2 POINT
1/4 POINT
LOAD (KIPS)
6
4.5
3
1.5
0
-1
-.5
0
.5
1
LATERAL DEFLECTION (IN)

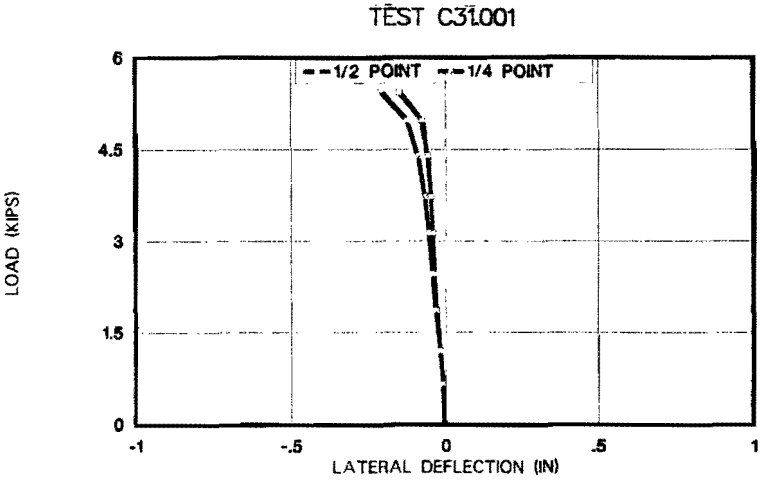
TEST C31.001
1/2 POINT
1/4 POINT
LOAD (KIPS)
6
4.5
3
1.5
0
-1
-.5
0
.5
1
LATERAL DEFLECTION (IN)

TEST C32.001

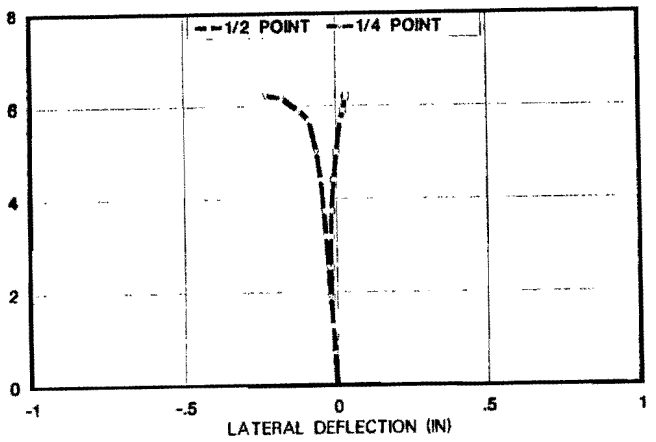

TEST C33.001

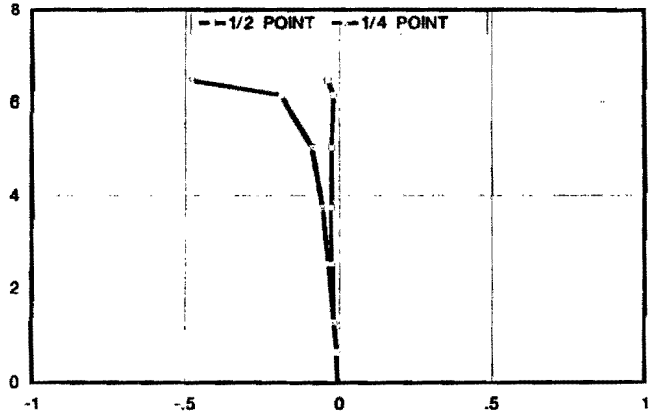

TEST C34.001

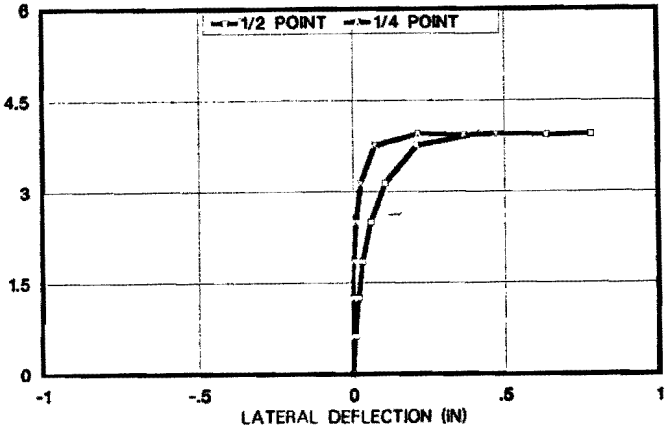

TEST C35.001

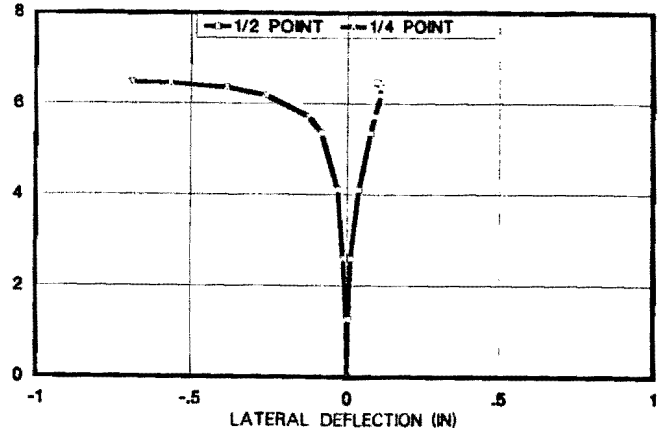

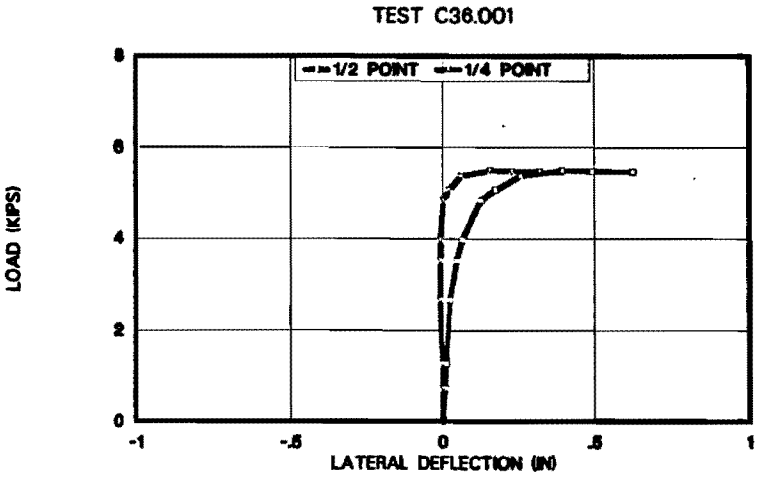
TEST C36.001
1/2 POINT
1/4 POINT
LOAD (KIPS)
LATERAL DEFLECTION (IN)
0
2
4
6
8
-1
-.5
0
.5
1

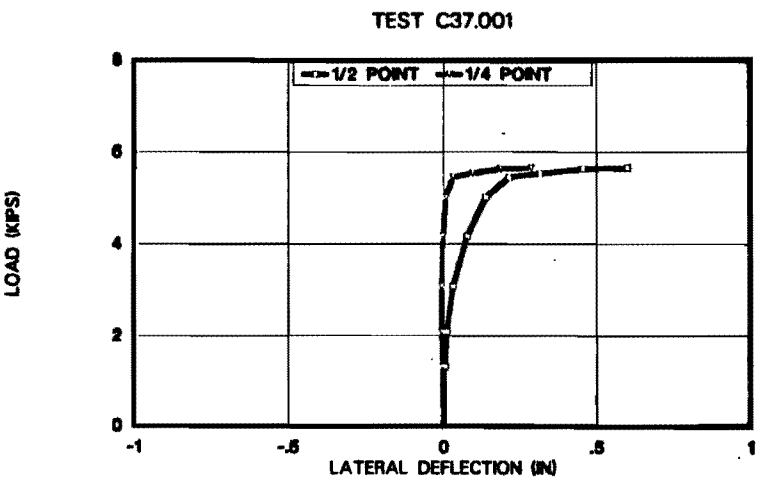
TEST C37.001
1/2 POINT
1/4 POINT
LOAD (KIPS)
LATERAL DEFLECTION (IN)
0
2
4
6
8
-1
-.5
0
.5
1

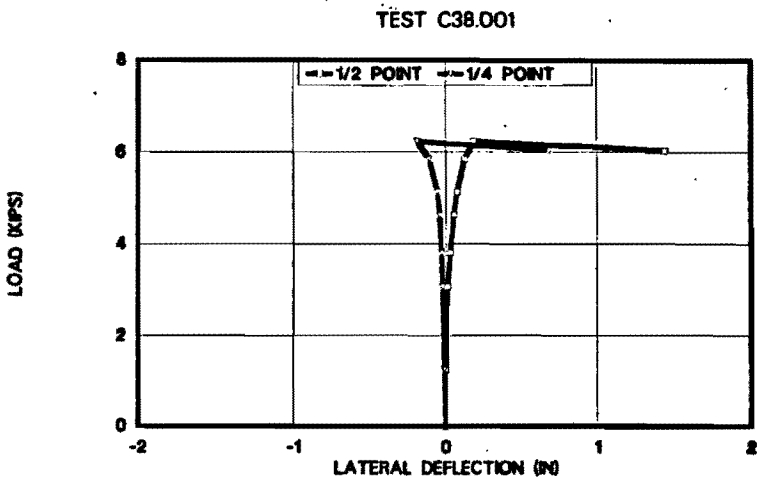
TEST C38.001
1/2 POINT
1/4 POINT
LOAD (KIPS)
LATERAL DEFLECTION (IN)
0
2
4
6
8
-2
-1
0
1
2

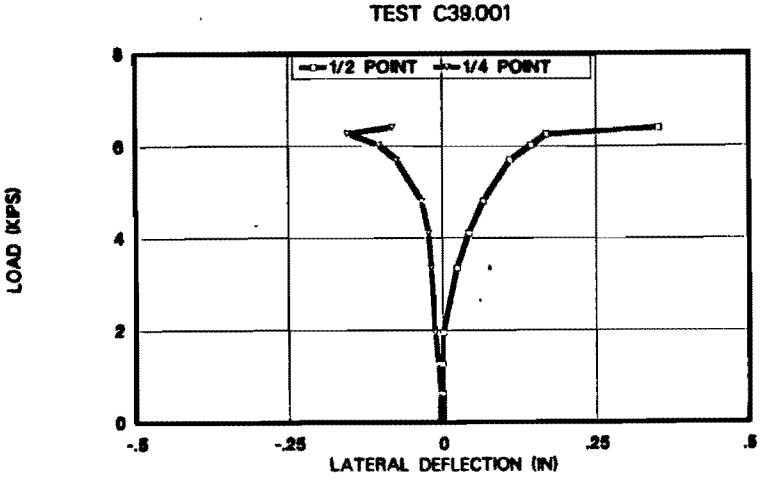
TEST C39.001
1/2 POINT
1/4 POINT
LOAD (KIPS)
LATERAL DEFLECTION (IN)
0
2
4
6
8
-.5
-.25
0
.25
.5

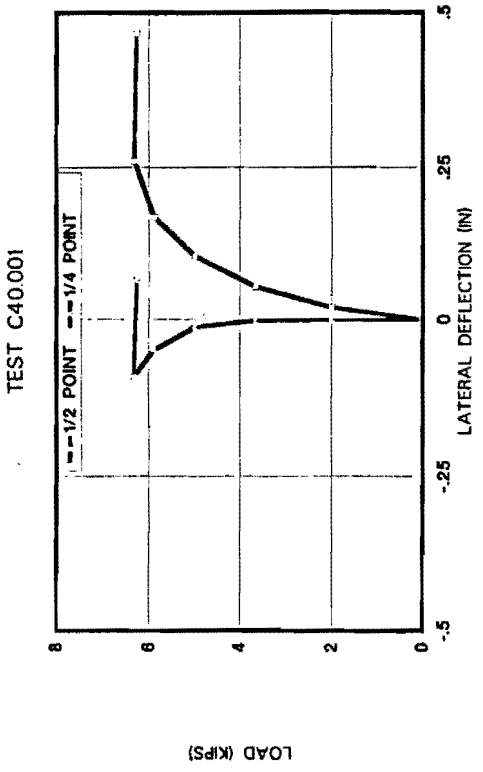
TEST C40.001
1/2 POINT
1/4 POINT
LOAD (KIPS)
LATERAL DEFLECTION (IN)
8
6
4
2
0
-.5
-.25
0
.25
.5

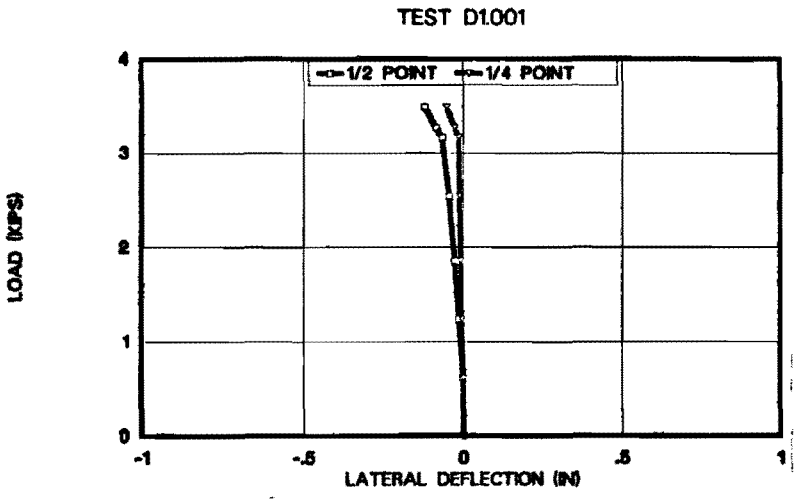
TEST D1.001
1/2 POINT
1/4 POINT
LOAD (KIPS)
LATERAL DEFLECTION (IN)
0
1
2
3
4
-1
-.5
0
.5
1

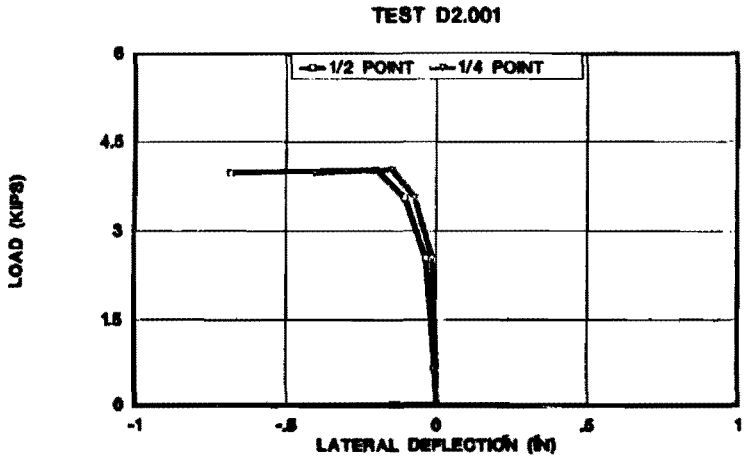
TEST D2.001
1/2 POINT
1/4 POINT
LOAD (KIPS)
LATERAL DEFLECTION (IN)
0
1.5
3
4.5
6
-1
-.5
0
.5
1

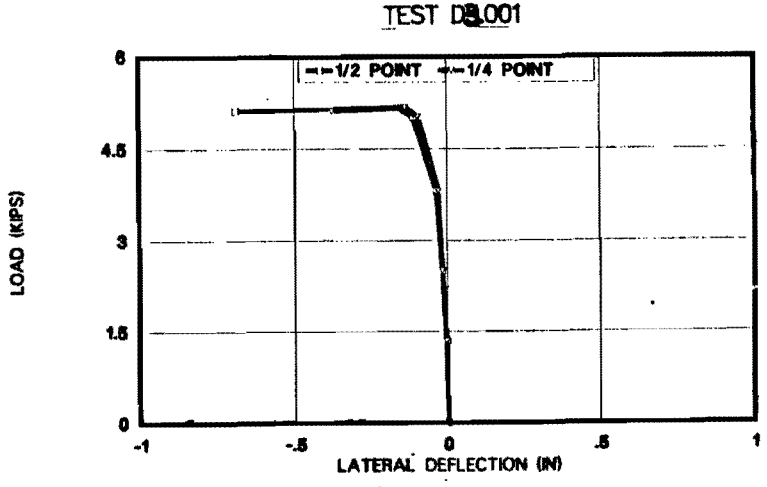
TEST D3.001
1/2 POINT
1/4 POINT
LOAD (KIPS)
LATERAL DEFLECTION (IN)
0
1.5
3
4.5
6
-1
-.5
0
.5
1

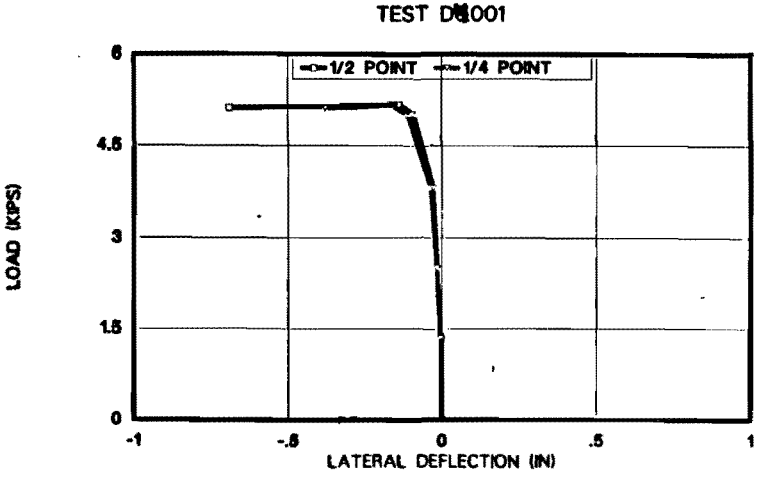
TEST D4.001
1/2 POINT
1/4 POINT
LOAD (KIPS)
LATERAL DEFLECTION (IN)
0
1.5
3
4.5
6
-1
-.5
0
.5
1

TEST E1.001

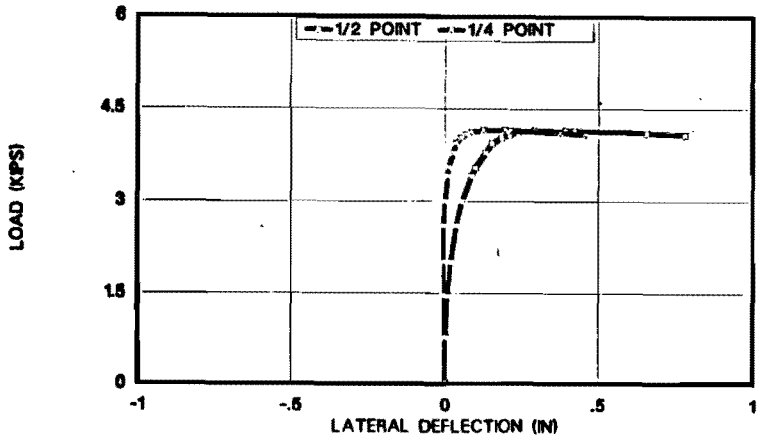

TEST E2.001

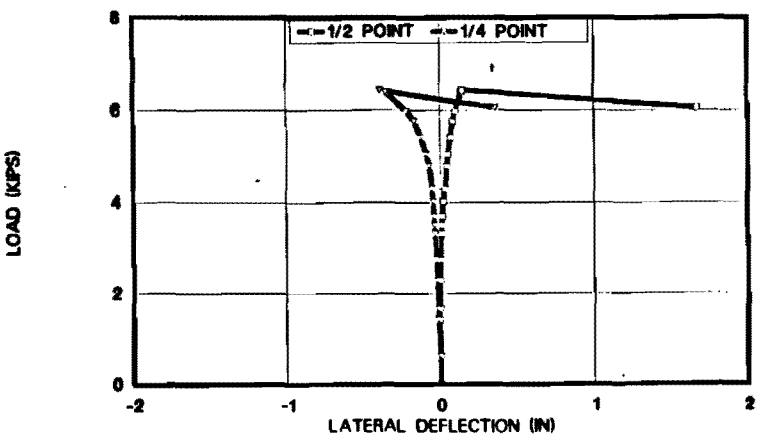

TEST E3.001

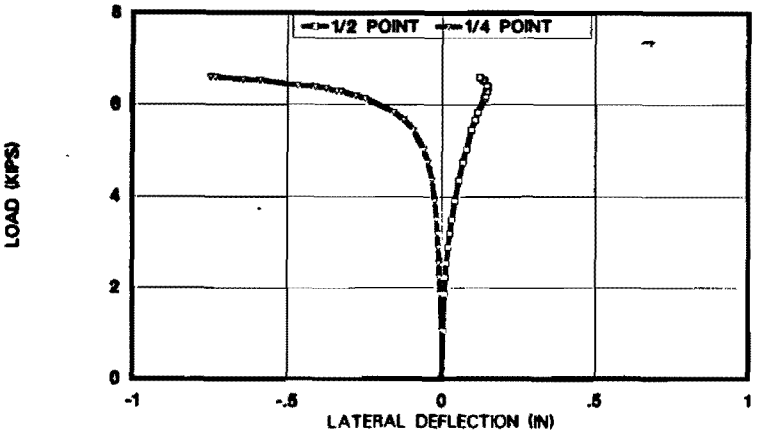

TEST E4.001

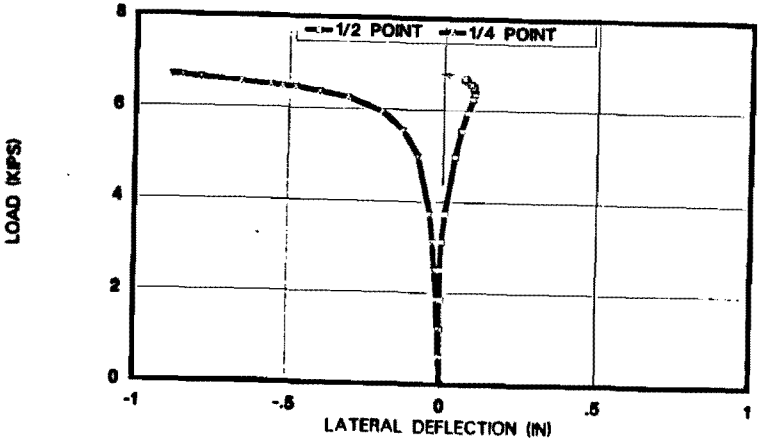

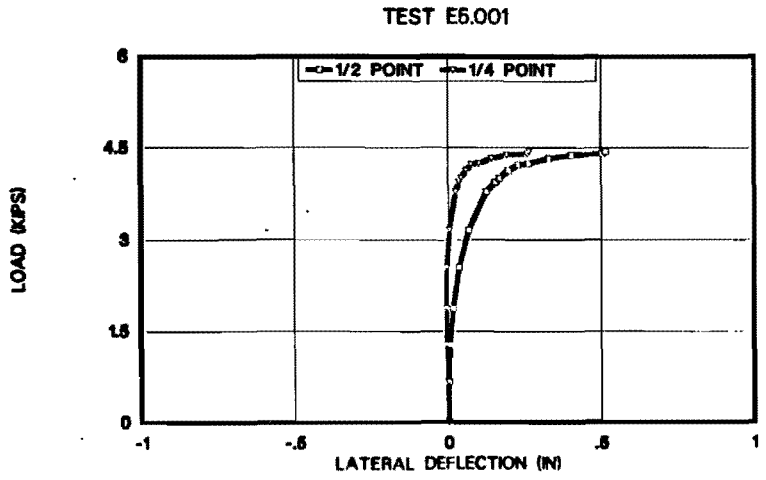
TEST E5.001
1/2 POINT
1/4 POINT
LOAD (KIPS)
6
4.5
3
1.5
0
-1
-.5
0
.5
1
LATERAL DEFLECTION (IN)

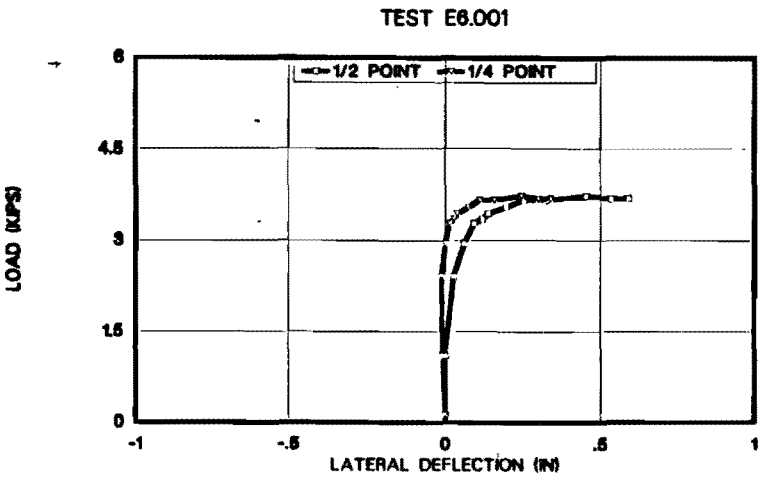
TEST E6.001
1/2 POINT
1/4 POINT
LOAD (KIPS)
6
4.5
3
1.5
0
-1
-.5
0
.5
1
LATERAL DEFLECTION (IN)

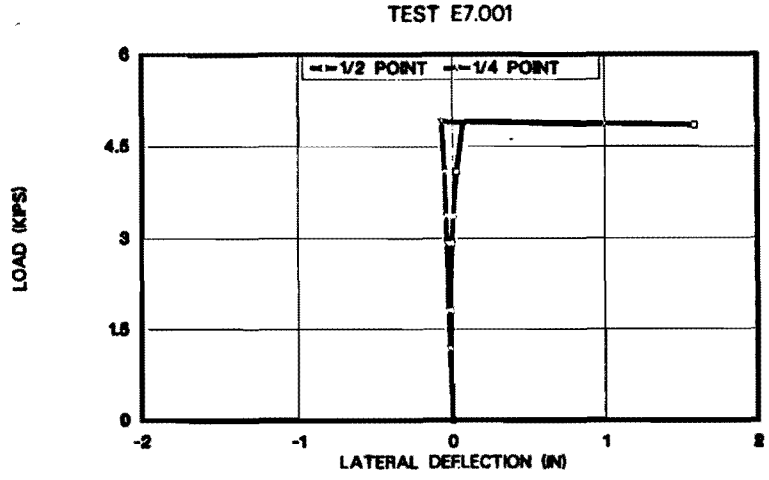
TEST E7.001
1/2 POINT
1/4 POINT
LOAD (KIPS)
6
4.5
3
1.5
0
-2
-1
0
1
2
LATERAL DEFLECTION (IN)

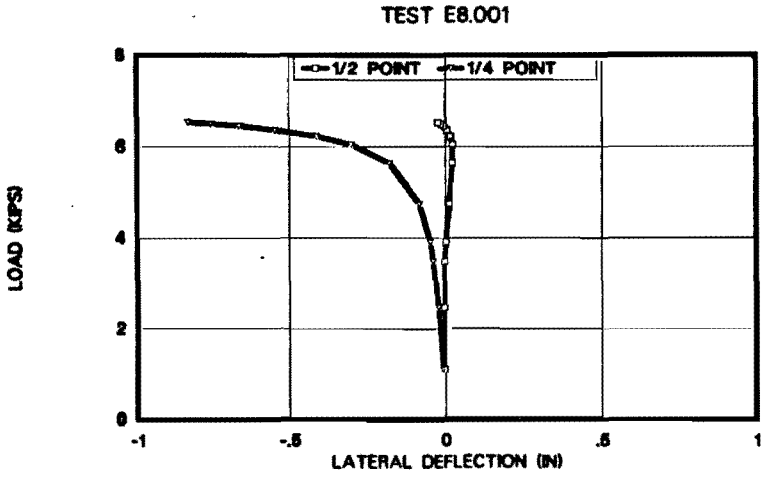
TEST E8.001
1/2 POINT
1/4 POINT
LOAD (KIPS)
8
6
4
2
0
-1
-.5
0
.5
1
LATERAL DEFLECTION (IN)

TEST E9.001

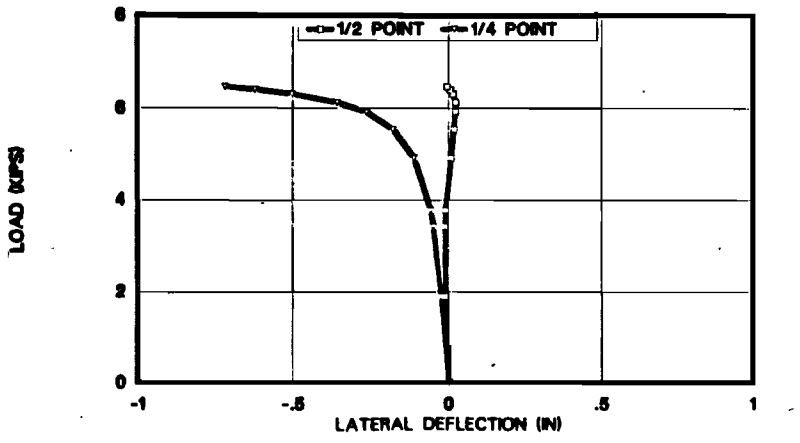

TEST E10.001

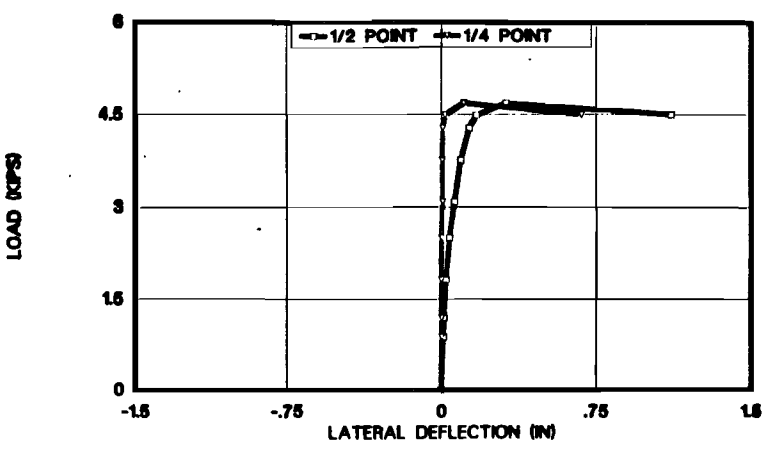

TEST F1.001

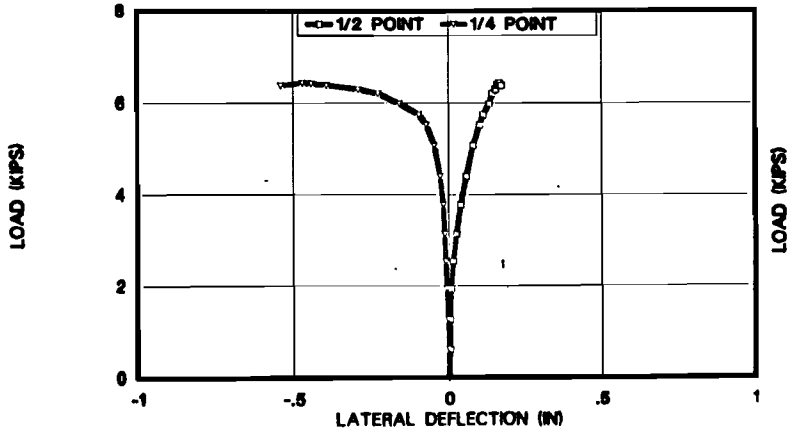

TEST F2.001

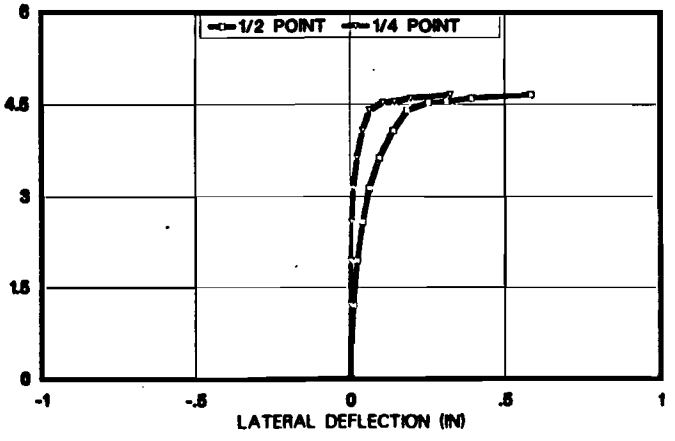

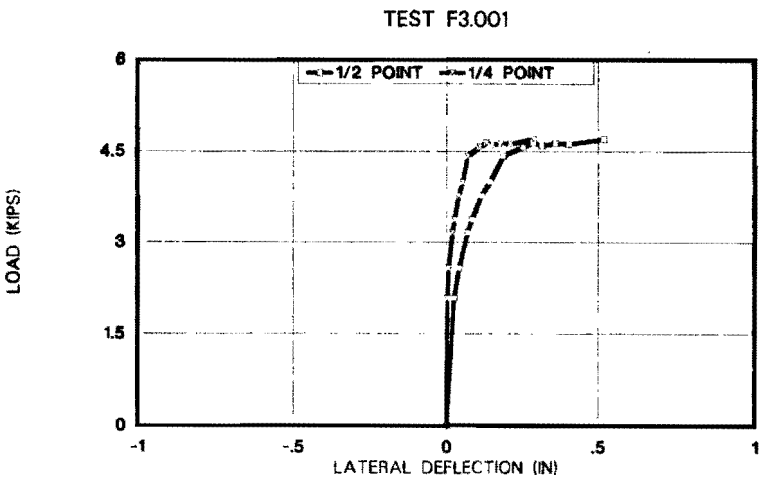
TEST F3.001
1/2 POINT
1/4 POINT
LOAD (KIPS)
6
4.5
3
1.5
0
-1
-.5
0
.5
1
LATERAL DEFLECTION (IN)

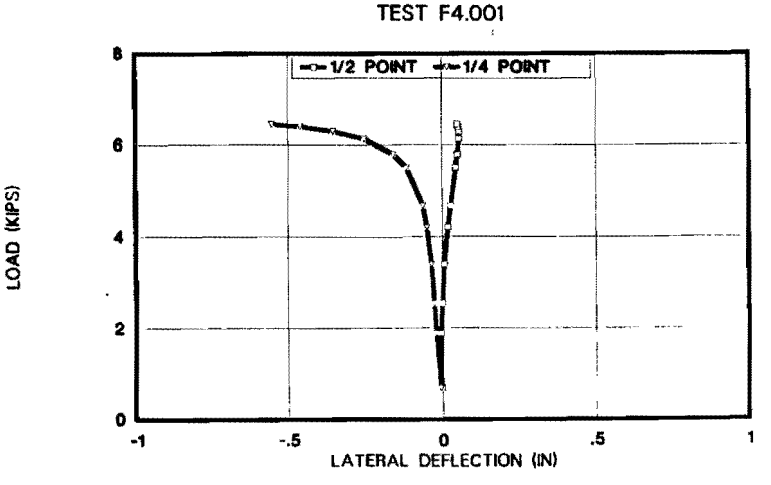
TEST F4.001
1/2 POINT
1/4 POINT
LOAD (KIPS)
6
4
2
0
-1
-.5
0
.5
1
LATERAL DEFLECTION (IN)

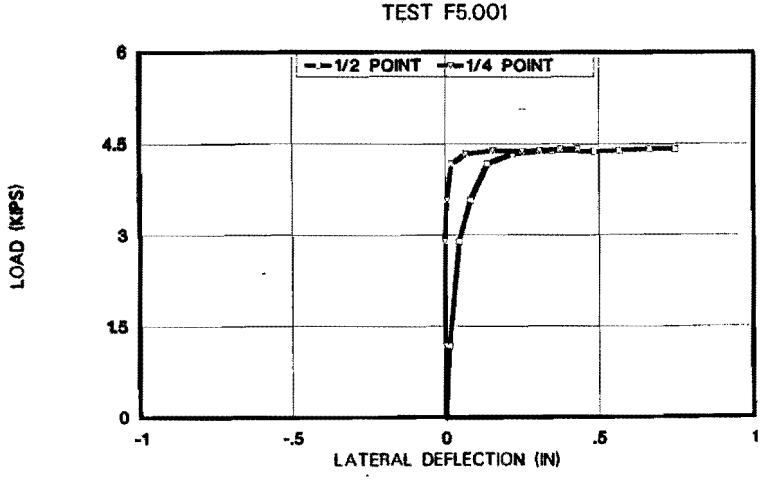
TEST F5.001
1/2 POINT
1/4 POINT
LOAD (KIPS)
6
4.5
3
1.5
0
-1
-.5
0
.5
1
LATERAL DEFLECTION (IN)

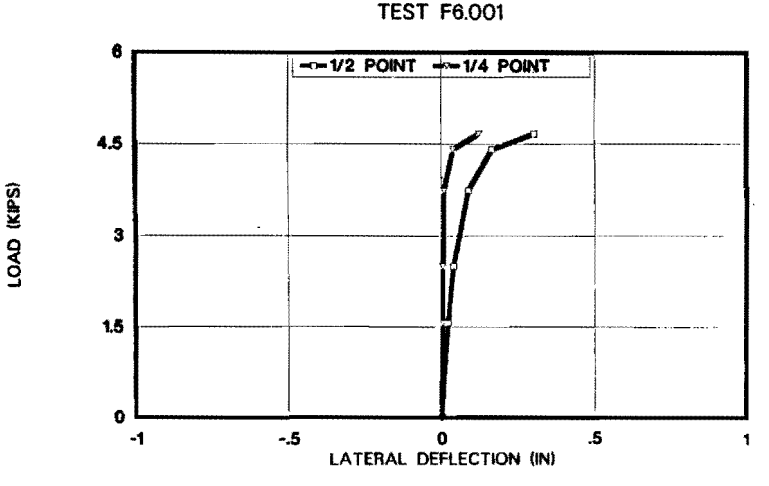
TEST F6.001
1/2 POINT
1/4 POINT
LOAD (KIPS)
6
4.5
3
1.5
0
-1
-.5
0
.5
1
LATERAL DEFLECTION (IN)

APPENDIX B
BRACING EQUATIONS FOR DESIGN

LATERAL BRACING - Load Factor Design

Brace Stiffness - discrete or continuous bracing

$$M_{cr} = \sqrt{\left[\left(C_{bu} M_o\right)^2 + \left(C_{bb} P_{yc} h\right)^2 A_d\right]\left(1 + A_d\right)} \leq M_y \text{ or } M_s \tag{B1}$$

where

$$P_{yc} = \frac{\pi^2 E I_{yc}}{L^2} \tag{B2}$$

$$A_d = L\sqrt{\frac{.17\beta_L}{C_L P_{yc}}} \tag{B3}$$

$$C_L = 1 + \frac{1.2}{n} \tag{B4}$$

(top flange load)

= 1.0 (centroid or moment loading)

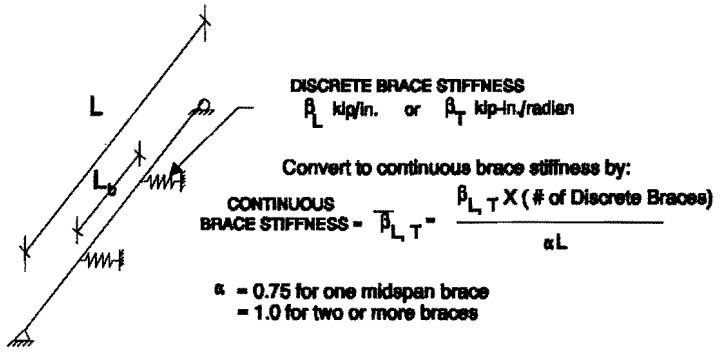

Figure B1. Equivalent continuous bracing.

$$M_o \text{ (lb-in. units)} = 91 \times 10^6 \frac{I_{yc}}{L}\sqrt{0.772\frac{J}{I_{yc}} + \left(\frac{\pi d}{L}\right)^2} \tag{B5}$$

For top flange loading adjust Eq. (B5) as given in the SSRC Guide (Galambos, 1988) or omit the second term under the square root. In the equations above

M_o = buckling strength assuming the beam is laterally unbraced along the span
M_s = buckling strength between braces; Eq. (B5) with L_b instead of L and C_{bb} (same as M_r in AASHTO)
C_L = top flange loading factor
C_{bu} = the C_b factor assuming the beam is unbraced
C_{bb} = the C_b factor assuming the beam braces are fully effective

and

n	=	number of discrete braces	G	=	shear modulus (E/2.6 for steel)
L	=	span length	J	=	St. Venant torsion constant
L_b	=	distance between braces	h	=	distance between flange centroids

I_{yc}	=	weak axis moment of inertia of compression flange	M_y	=	yield moment
E	=	modulus of elasticity	d	=	beam depth

Full Bracing Stiffness Requirement - Discrete or Relative Bracing

$$\beta_L^* = 2\,\#P_f\,C_{bb}\,C_L/L_b \tag{B6}$$

where # ≈ 4 - (2/n) or the coefficient in Table 2.1 for discrete bracing
= 1.0 for relative bracing
$P_f = \pi^2 E I_{yc}/L_b^2$

Strength Requirement

Discrete bracing: $F_{br} = 0.008\,M_f / h$ (B7)
Relative bracing: $F_{br} = 0.004\,M_f / h$ (B8)
where M_f is the maximum beam moment at factored load

LATERAL BRACING
Allowable Stress Design

Stiffness: $M_{allow} = 0.55\,M_{cr} \le 0.55\,M_y$ or $0.55\,M_s$
See Eq. (B1-B5)

Full Bracing Stiffness:
Use Eq. (B6) - no change

Strength:
Discrete bracing: $F_{br} = 0.008\,M/h$
Relative Bracing: $F_{br} = 0.004\,M/h$

where M is the maximum beam moment at service load.

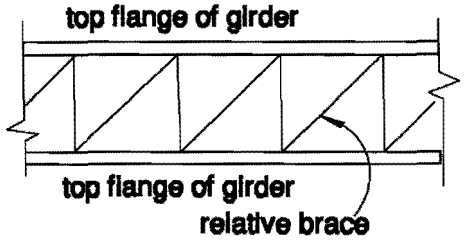

Figure B.2

TORSIONAL BRACING - Load Factor Design

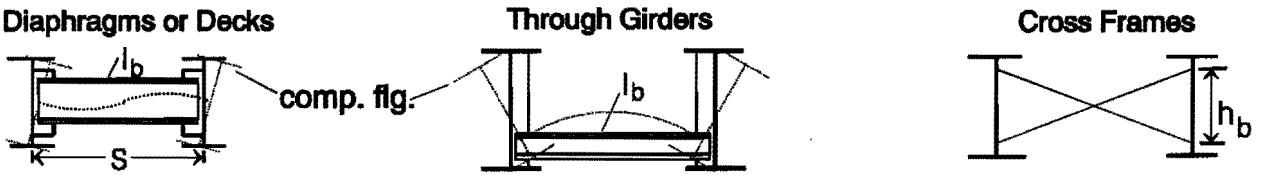

through girder

$$\beta_b = \frac{2 E I_b}{S} \qquad \beta_b = \frac{6 E I_b}{S} \qquad \beta_b \text{ (see Fig. 5.10)}$$

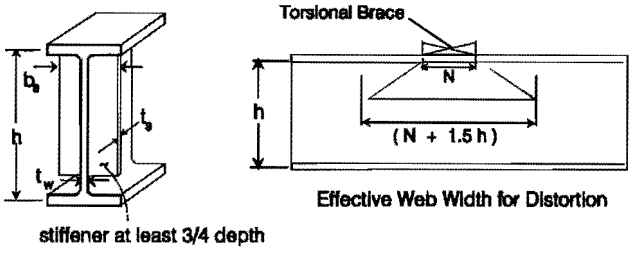

β_T = effective torsional brace
β_b = stiffness of attached brace
β_{sec} = accounts for cross section distortion

$$\beta_{sec} = \frac{3.3 E}{h}\left(\frac{t_w^3}{12}(N + 1.5h) + \frac{t_s b_s^3}{12}\right)$$

use 1 in. for continuous bracing

and $$\frac{1}{\beta_T} = \frac{1}{\beta_b} + \frac{1}{\beta_{sec}} \qquad \text{(B9)}$$

Brace Stiffness - discrete or continuous bracing

$$M_{cr} = \sqrt{c_{bu}^2 M_o^2 + \frac{C_{bb}^2 E I_{yc} \beta_T}{C_T}} \leq M_y \text{ or } M_s \qquad \text{(B10)}$$

where C_T = 1.2 for top flange loading
= 1.0 for other loading

Brace Strength

$$M_{br} = F_{br} h_b = \frac{0.02 L M^2}{n E I_{yc} C_{bb}^2} \qquad \text{(B.11)}$$

where M = maximum factored moment

TORSIONAL BRACING - Allowable Stress Design

Stiffness: $M_{allow} = 0.55 M_{cr} \leq 0.55 M_y$ or $0.55 M_s$ (See Eq. (B.9 - B.10)

Strength: Same as B.11 but with M as the maximum moment at service load

BIBLIOGRAPHY

Akay, H.U., Johnson, C.P., and Will, K.M., 1977, "Lateral and Local Buckling of Beams and Frames," *Journal of the Structural Division*, ASCE, ST9, September, pp. 1821-1832.

Linder, J., Schmidt, J.S., 1982, "Biegedrillknicken von I-Trägern unter Berücksichtigung wirklichkeitsnaher Lasteinleitung," *Der Stahlbau*, 51, H.9, S. 257-263.

Bleich, 1978, *Buckling Strength of Metal Structures, New York.*

Choo, K.M., 1987, Thesis presented to The University of Texas at Austin, May, "Buckling Program BASP for Use on a Microcomputer."

Fischer, M., 1970 and 1973, "Das stabilitätsproblem des in Höhe des oberen Flansches wirklichkeitsnah belasteten I-Trägers. *Der Stahlbau*, 39, H.9, S. 267-275 und 42, H.5, S. 129-138.

Flint, A.R., 1951a, "The Stability of Beams Loaded through Secondary Members," *Civil Engineering and Public Works Review*, Vol. 46, No. 537-8, pp. 175-177, 259-260.

Flint, A.R., 1951b, "The Influence of Restraint on the Stability of Beams," *The Structural Engineer*, September 1951, pp. 235-246.

Galambos, T.V., Ed., 1988, Structural Stability Research Council, *Guide to Stability Design Criteria for Metal Structures*, 4th Edition, New York: John Wiley & Sons, Inc.

Gedies, R.W., 1983, Thesis presented to The University of Texas at Austin, December, "Beam Buckling Tests with Various Brace Stiffnesses."

Kirby, P.A. and Nethercot, D.A., 1979, *Design for Structural Stability*, Wiley.

Kissane, R.J., 1985, "Lateral Restraint of Non-Composite Beams," Research Report 123, New York State Department of Transportation, August.

Meck, H.R., 1977, "Experimental Evaluation of Lateral Buckling Loads," *Journal of the Engineering Mechanics Division*, ASCE, EM2, April, pp. 331-337.

Milner, H.R. and Rao, S.N., 1978, "Strength and Stiffness of Moment Resisting Beam - Purlin Connections," *Civil Engineering Transactions, Institute of Engineers, Australia*, CE 20(1), pp. 37-42.

Mutton, B.R. and Trahair, N.S., 1973, "Stiffness Requirements for Lateral Bracing," *Journal of the Structural Division*, ASCE, ST10, October, pp. 2167-2181.

Nethercot, D.A. and Rockey, K.C., 1972, "The Lateral Buckling of Beams Having Discrete Intermediate Restraints," *The Structural Engineer*, October, No. 10, Vol. 50S.

Nethercot, D.A., 1973, "Buckling of Laterally or Torsionally Restrained Beams," *Journal of the Engineering Mechanics Division*, August, pp. 773-790.

Southwell, R.V., 1932, "On the Analysis of Experimental Observations in the Problems of Elastic Stability," Proceedings of the Royal Philosophical Society of London, Series A, Vol. 135, April, p. 601.

Taylor, A.C. and Ojalvo, M., 1966, "Torsional Restraint of Lateral Buckling," *Journal of the Structural Division*, ASCE, ST2, April, pp. 115-129.

Timoshenko, S. and Gere, J., 1961, *Theory of Elastic Stability*, New York: McGraw-Hill Book Company.

Tong, G.S. and Chen, S.H., 1988, "Buckling of Laterally and Torsionally Braced Beams," *Construction Steel Research.*

Trahair, N.S., 1966, "Elastic Stability of I-Beam Elements in Rigid-Jointed Structures," *The Journal of The Institution of Engineers, Australia*, July.

Trahair, N.S., 1969, "Deformations of Geometrically Imperfect Beams," *Journal of the Structural Division*, ASCE, ST7, July, p. 1475.

Trahair, N.S. and Nethercot, D.A., 1982, "Bracing Requirements in Thin-Walled Structures," Chapter 3, *Developments in Thin-Walled Structures - Vol. 2*, Rhodes and Walker - Ed., Elsevier Applied Science Publishers, pp. 93-129.

Winter, G., 1958, "Lateral Bracing of Columns and Beams," *Journal of the Structural Division*, ASCE, ST2, March, pp. 1561-1565.

Winter, G., 1960, "Lateral Bracing," *ASCE Transactions*, pp. 809-825.

Wong-Chung, A.D., and Kitipornchai, S., 1986, "Partially Braced Inelastic Beam Buckling Experiments," Research Report No. CE 72, University of Queensland, June.

Yarimci, E., Yura, J.A., and Lu, L.W., 1967, "Techniques for Testing Structures Permitted to Sway," *Experimental Mechanics*, Journal of the Society for Experimental Stress Analysis, Vol. 7, No. 8, August.

Yura, J.A., 1971, "Design of Bracing for Columns, Beams and Frames," *AISC National Engineering Conference*, Cleveland.

Yura, J.A., 1990, Class Notes.